An assessment of the use of a Carbon Fiber Heating Element in Thermoplastic Resistance Welding for PEEK and PEI Thermoplastic Composite

May/2023

Developed under Cooperative Agreement: 80NSSC22PB269 (NIAR) (NASA)

Authors: Waruna Seneviratne (NIAR), Upul Palliyaguru (NIAR), Mark Walthers (NIAR), and Andrew Bleything (NIAR)

Scope

This document outlines an assessment of the quality and performance of thermoplastic composite welded single lap shear joints, double lap shear joints, mode one joints, and mode two joints. The technique of resistance welding PEEK and PEI thermoplastic composite with a carbon fiber heating element was used in this research.

Table of Contents

List of Figures

List of Tables

1.0 APPLICABLE DOCUMENTS

The latest issue of the publications shall apply. If a referenced document has been canceled and no superseding document has been specified, the last published issue of that document shall apply.

1.1 ASTM Publications

ASTM D3418-21	Standard Test Method for Transition Temperatures and Enthalpies of Fusion and Crystallization of Polymers by Differential Scanning Calorimetry
ASTM D3528-96	Standard Test Method for Strength Properties of Double Lap Shear Adhesive Joints by Tension Loading
ASTM D5868-01	Standard Test Method for Lap Shear Adhesion for Fiber Reinforced Plastic (FRP) Bonding
ASTM D5528-01	Standard Test Method for Mode I Interlaminar Fracture Toughness of Unidirectional Fiber-Reinforced Polymer Matrix Composites
ASTM D7905	Standard Test Method for Determination of the Mode II Interlaminar Fracture Toughness of Unidirectional Fiber-Reinforced Polymer Matrix Composites

1.2 Abbreviations and Acronyms

ASTM	American Society for Testing and Materials
DSC	Differential Scanning Calorimetry
DLS	Double Lap Shear
FOD	Foreign Object Debris
G_{IC}	Mode I Fracture Toughness
G_{IIC}	Mode II Fracture Toughness
IM	Intermediate Modulus
IPA	Isopropyl Alcohol
NASA	The National Aeronautics and Space Administration
NDI	Non-Destructive Inspection
NIAR	National Institute for Aviation Research
PEEK	Polyetheretherketone
PEI	Polyetherimide
RW	Resistance Weld

SLS	Single Lap Shear
SM	Standard Modulus
TPC	Thermoplastic Composite
ΔH_f°	Theoretical maximum heat of fusion for a fully crystalline sample

2.0 Requested Test Matrix

The requested test matrix from NASA is shown below in Table 1. Two material systems were compared in this research – TC1000 PEI AS4 and TC1200 PEEK AS4. Both of these material systems were supplied by Toray. Four main test methods were utilized in this study as well as three different layups. DSC coupons and photomicrograph coupons were extracted from each type of joint (A-J) for weld quality inspection. The letter abbreviation "K" is a hybrid joint in the fact that it is two different materials being welded together. There were three single lap shear coupons tested with this joint type but no DSC or photomicrograph coupons were extracted.

Table 1 – NASA Requested Test Matrix

NASA Resistance Welding with a Carbon Fiber Heating Element Finalized Test Matrix							
Substrate Material	**Letter Abbreviation**	**ASTM Standard**	**Layup**	**Size (0° X 90°)**	**Coupons Tested**	**DSC Coupons**	**Photomicrographs**
TC1000 PEI AS4	A	D3528	$[45/0/-45/90]_{ns}$	Type A - 8.0" X 1.0" (1.0" Overlap)	6	1	1
	B	D5868		7.0" X 1.0" (1.0" Overlap)	6	1	1
	C		$[0/-45/90/45]_{ns}$		6	1	1
	D	D5528	$[0]_n$	10" X 1.0"	6	1	1
	E	D7905	$[0]_n$	7.0" X 1.0"	6	1	1
TC1200 PEEK AS4	F1	D3528	$[45/0/-45/90]_{ns}$	Type A - 8.0" X 1.0" (1.0" Overlap)	6	1	1
	G	D5868		7.0" X 1.0" (1.0" Overlap)	6	1	1
	H		$[0/-45/90/45]_{ns}$		6	1	1
	I	D5528	$[0]_n$	10" X 1.0"	6	1	1
	J	D7905	$[0]_n$	7.0" X 1.0"	6	1	1
TC1000 PEI AS4/ TC1200 PEEK AS4	K	D5868	$[0/-45/90/45]_{ns}$	7.0" X 1.0" (1.0" Overlap)	3	0	0

3.0 Definition of Welding Process

3.1 Single Lap Shear/Double Lap Shear Manufacturing

Materials must be prepared for the welding process. For the single lap shear and double lap shear configurations two substrates (16 ply), two resin films (compatible with substrate, 60µm), and one carbon fiber heating element (Thickness = 0.012") must be acquired as seen below in Figure 1.

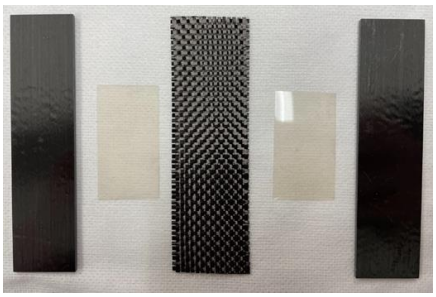

Figure 1 – SLS/DLS Material Example

After materials are prepped, the transverse fibers in the carbon fiber heating element must be removed as seen below in Figure 2. It's important to keep the same number of longitudinal fibers so that the resistance value stays consistent. Only remove the transverse fibers that will be in the weld area or in this case the middle inch of the heating element.

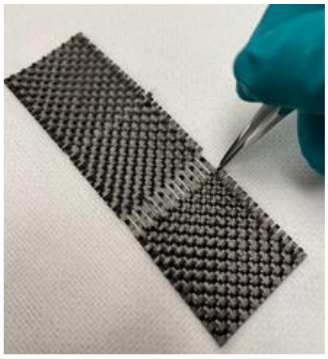

Figure 2 – Removing Transverse Fibers from CFHE

After the heating element is prepared, wipe down both substrates and resin films in order to reduce the risk of FOD at the weld line. Ensure the IPA has dried before placing any shims onto the substrate.

Figure 3 – Degreasing Substrate and Resin

After degreasing the welding materials with IPA, locate the appropriate metal shims for the weld joint. These shims are stainless steel wrapped in high-temperature Kapton tape. The overall thickness of each shim is around 0.02". Measure out 1" from the substrate edge as seen in Figure 4. Attach shims with high temperature Kapton tape.

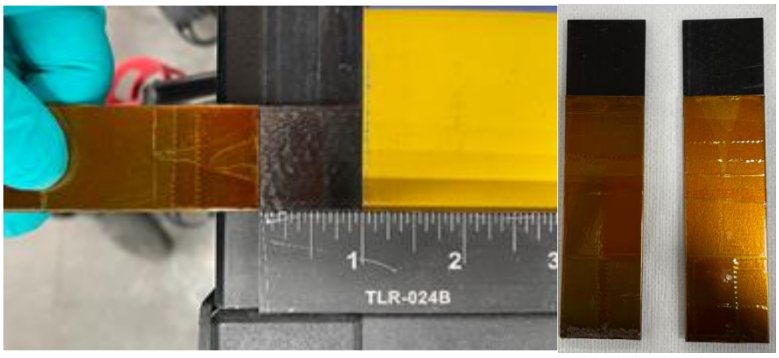

Figure 4 – Attaching Metal Shims

After the shims have been attached to the substrates, place the first substrate into the welding fixture ensuring the edges are flush with the copper terminals as seen below in Figure 5. Use tension clamps to secure the first substrate into place.

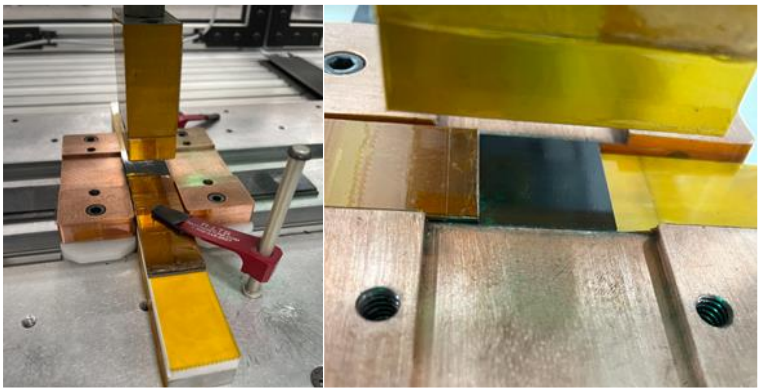

Figure 5 - First Substrate Placement

Place the resin films and carbon fiber heating element into the copper terminals as shown in Figure 6. Make sure the longitudinal fibers in the heating element are undisturbed as this can vary the resistance value.

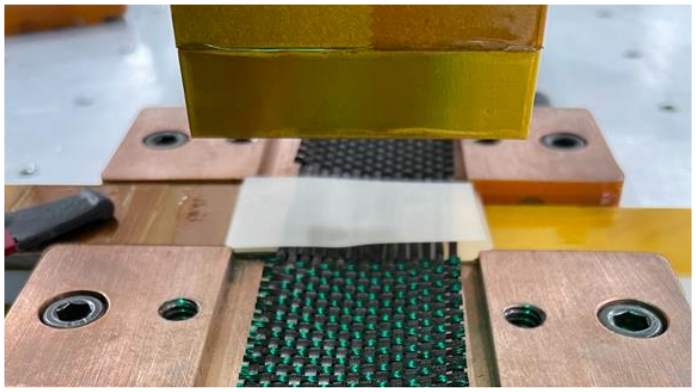

Figure 6 – Weld Stack

Tighten the copper terminals and place the second substrate on top of the weld stack and secure it with the secondary tension clamp as seen in Figure 7.

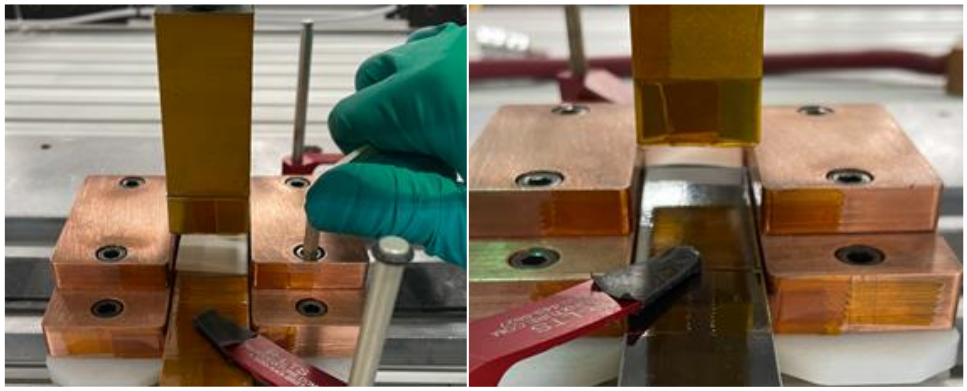

Figure 7 – Second Substrate Placement

Place the ceramic block and silicone block on top of the secondary substrate and attach the welding leads as seen in Figure 8.

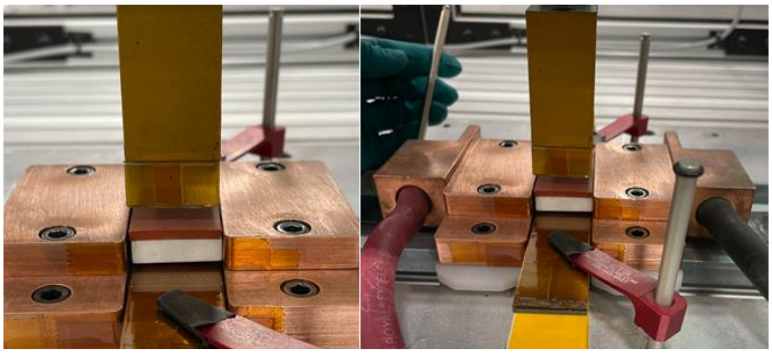

Figure 8. Pressure Block Placement and Welding Leads

Apply pressure with the appropriate actuator as seen in Figure 9. Select the proper weld cycle and run the weld program. Once the welding is complete, take the pressure off and take the specimen out of the weld fixturing.

Figure 9 – Pressure Application

3.2 Mode I / Mode II Manufacturing

Materials must be prepared for the welding process. For the mode I and mode II configurations two substrates, two resin films (compatible with substrate), and one carbon fiber heating element must be acquired as seen below in Figure 10.

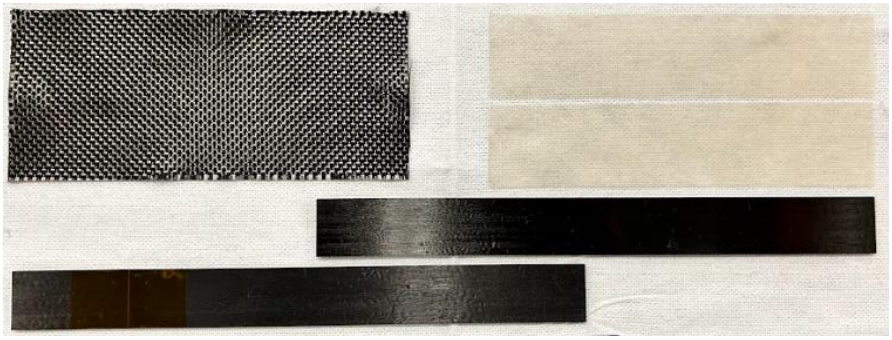

Figure 10 – Mode I / Mode II Materials

After materials are prepped, the transverse fibers in the carbon fiber heating element must be removed as seen below in Figure 11. It's important to keep the same number of longitudinal fibers so that the resistance value stays consistent. Only remove the transverse fibers that will be in the weld area or in this case the middle inch of the heating element. After the heating element is prepared wipe down the substrates and resin films with IPA to mitigate any FOD at the weld line.

Figure 11 – Mode I / Mode II CFHE

For Mode I and Mode II a thermoplastic composite base was used in order to place the materials more concisely. Two shims were used on either side of the coupon in order to create a zero-level entry for the heating element. Fiberglass insulation was attached on top of the shim in order for the heating element to not react with the shim as shown in Figure 12.

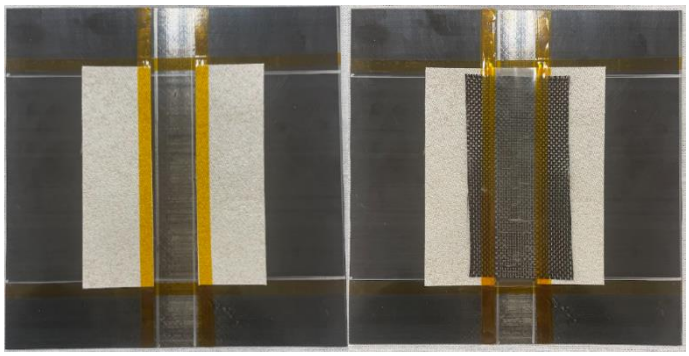

Figure 12 – Mode I / Mode II Material Placement

After all of the materials are secured into place, the entire base is moved under the appropriate actuator and pressure is applied in the same way as the single lap shear setup as shown in Figure 13. The welding leads are then tied into each section and each weld section is completed until the whole specimen is welded together.

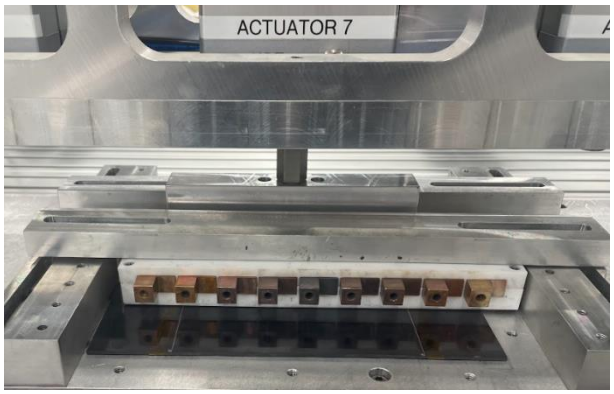

Figure 13 – DCB Manufacturing Setup

4.0 Weld Processing Data

4.1 Process Development Data

In the resistance welding process there are multiple data points recorded for every weld. These include pressure, resistance, voltage, current, and weld time. In process developments, K-Type micro-thermocouples are placed at the weld line and interface temperature is recorded. The utilized processing temperatures for these materials came from a recommendation from the material supplier. There were four main process developments for each material type. The primary weld in the single lap shear coupon and double lap shear coupon, the secondary weld in the double lap shear coupon, the edge welds in the mode I / mode II coupons and the middle welds in the mode I / mode II coupons. The process development thermocouple locations for the different configurations are shown below in Figure 14.

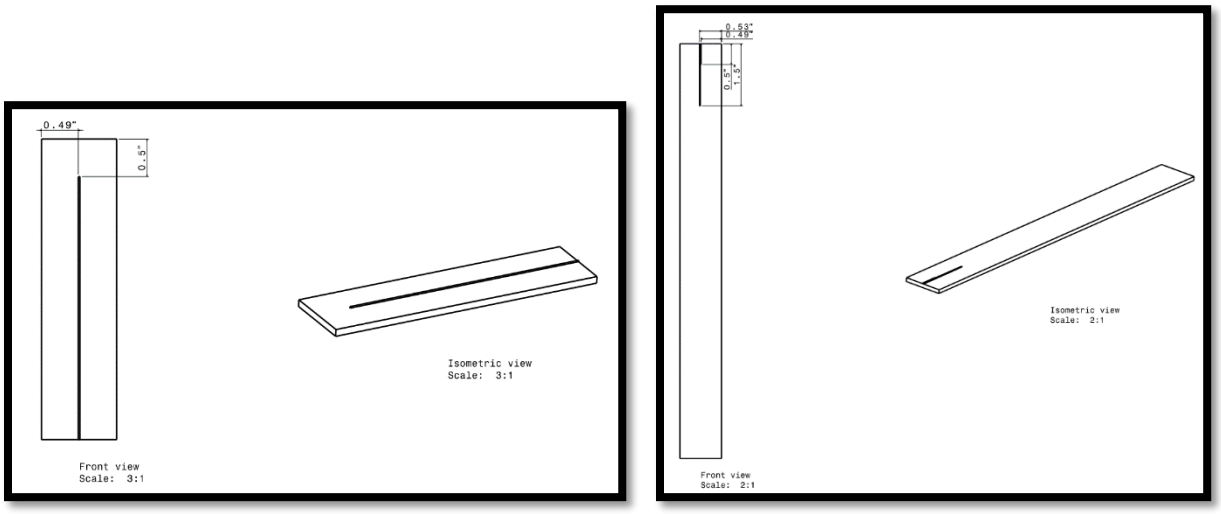

Figure 14 – SLS/DLS and Mode I / Mode II Thermocouple Locations

The first chart shows the initial temperature control run. This data shows what power is needed in order to achieve the desired temperature. This is done by controlling a PID loop and automatically adjusting the power supply level.

Once this data is acquired, a power curve optimization or derivation is done to produce a power control curve in the welding software. The power curve is then ran while still monitoring the temperature at the interface. Multiple iterations may be needed in order to achieve the desired temperature response but once the temperature response is acceptable, the process development is now completed. The last check is making sure the temperature control resistance and power control resistance is similar just to ensure a defect was not developed in the heating element during process development. The process developments for processes A-K are shown below.

4.1.1 Process Development A1 (Primary Weld in Double Lap Shear), B, & C

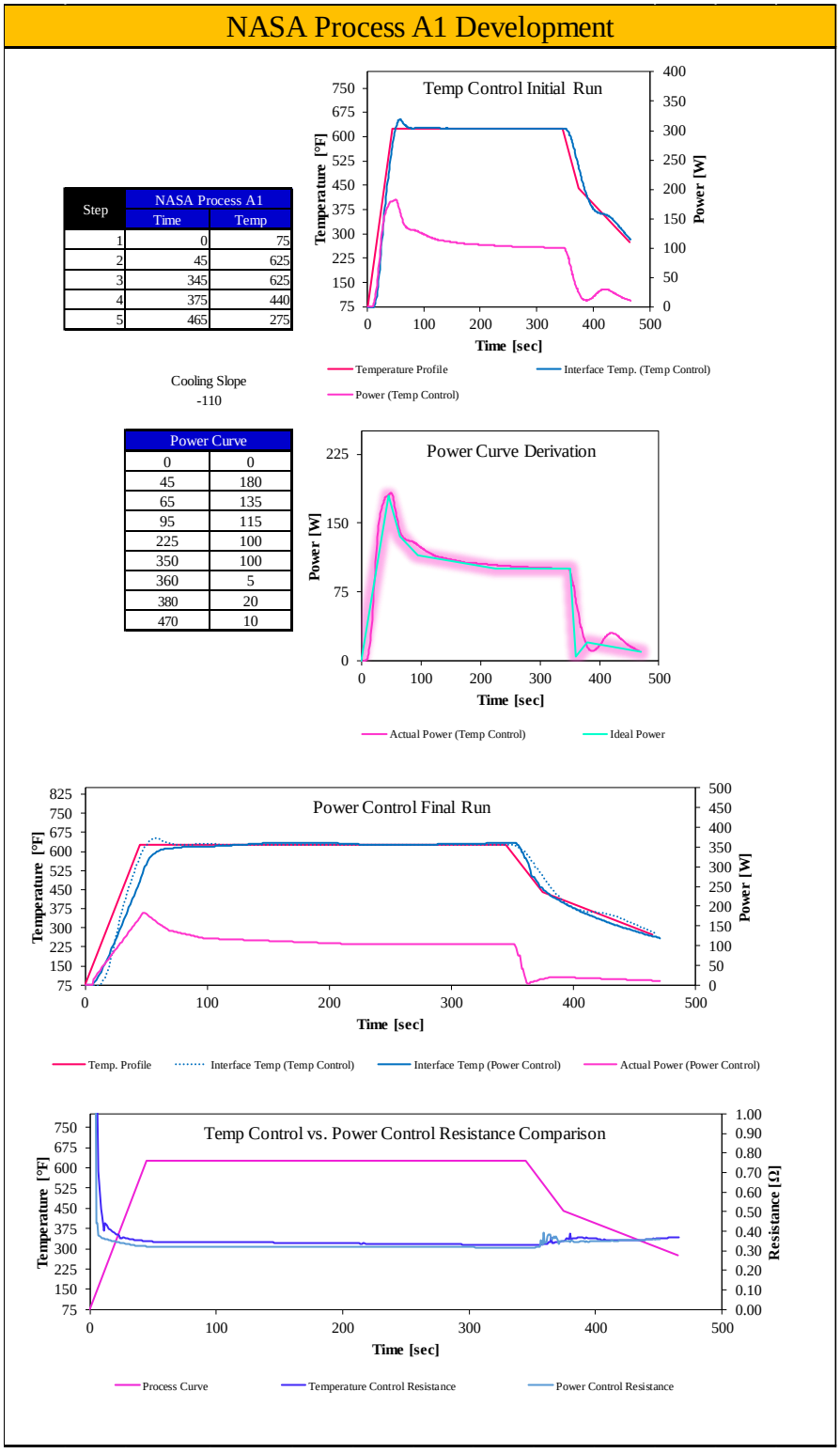

Step	NASA Process A1	
	Time	Temp
1	0	75
2	45	625
3	345	625
4	375	440
5	465	275

Power Curve	
0	0
45	180
65	135
95	115
225	100
350	100
360	5
380	20
470	10

Figure 15 – Process A1 Development

4.1.2 Process Development A2 (Secondary Weld in Double Lap Shear)

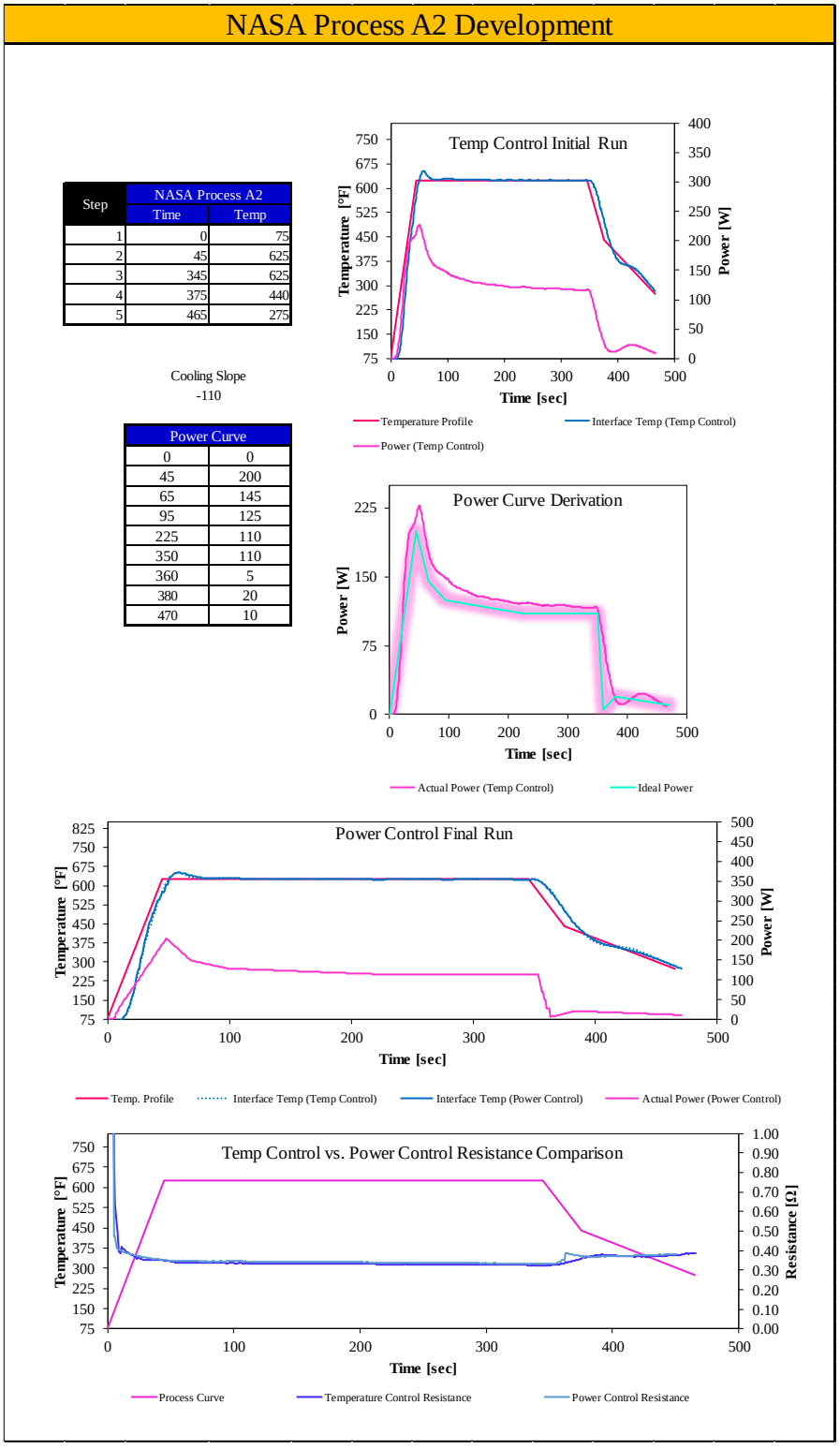

Figure 16 – Process A2 Development

4.1.3 Process Development D & E (Middle Sections)

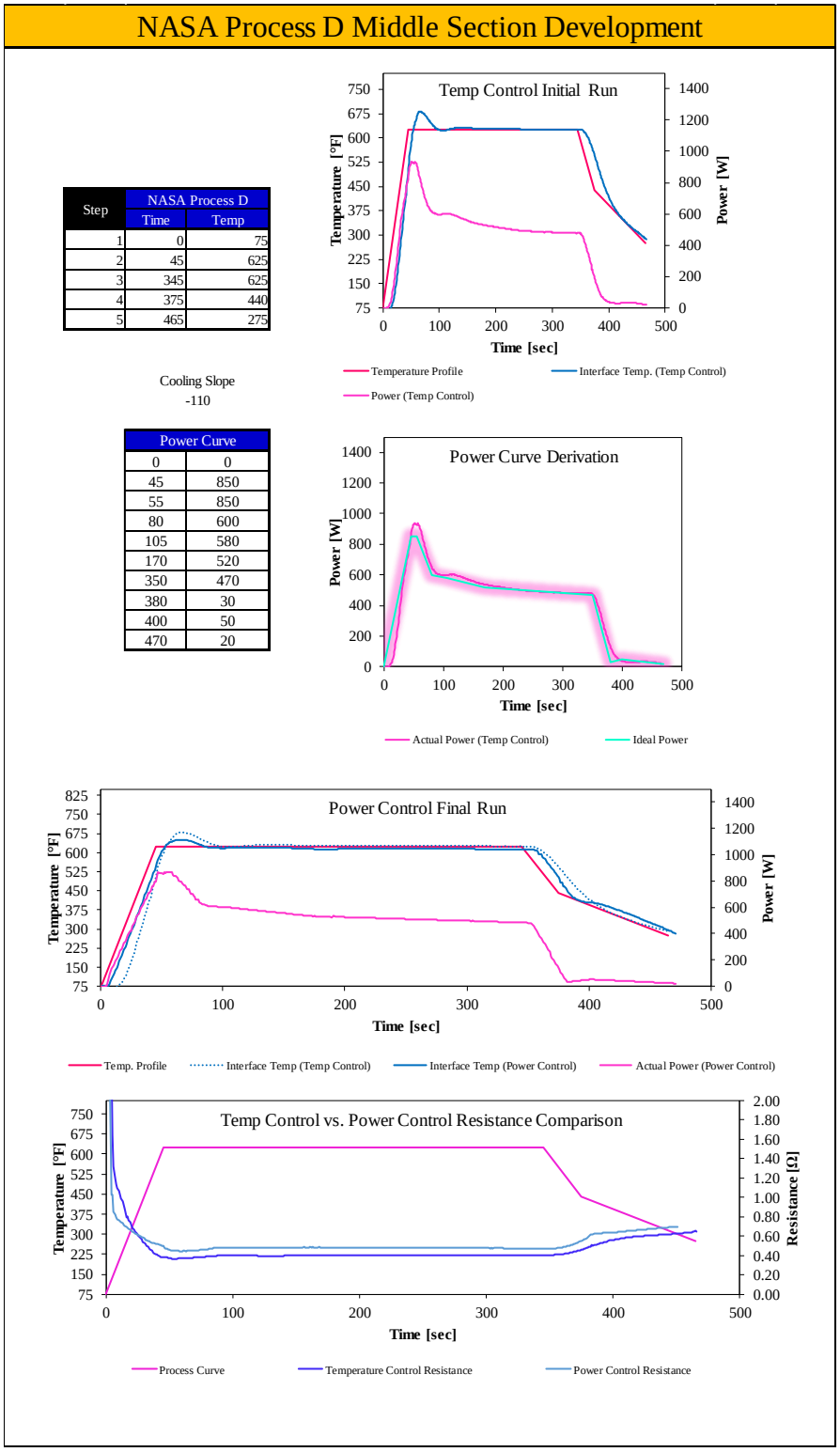

Step	NASA Process D	
	Time	Temp
1	0	75
2	45	625
3	345	625
4	375	440
5	465	275

Power Curve	
0	0
45	850
55	850
80	600
105	580
170	520
350	470
380	30
400	50
470	20

Figure 17 – Process D & E Middle Section Development

4.1.4 Process Development D & E (End Sections)

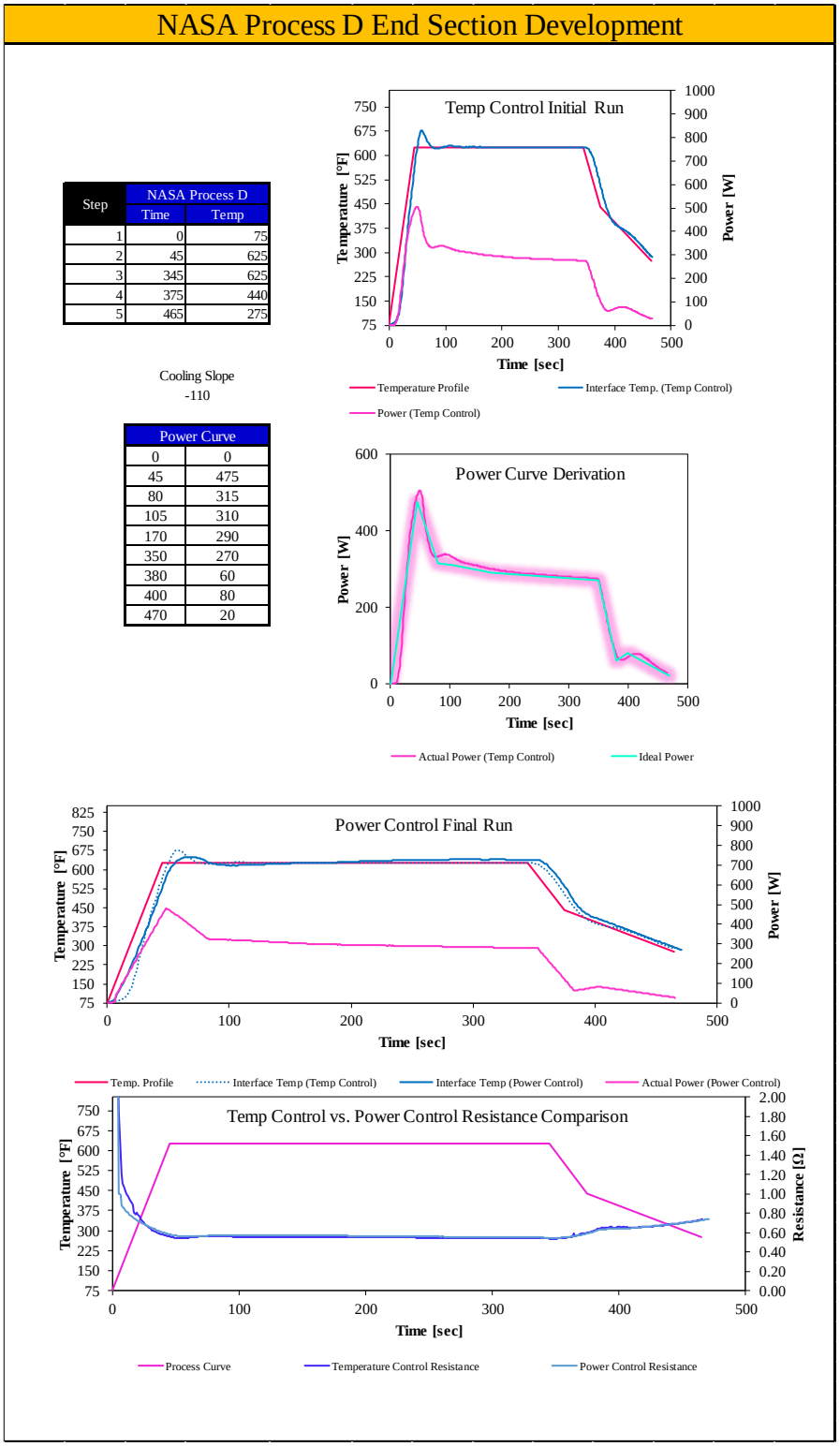

Figure 18 – Process D & E End Section Development

4.1.5 Process Development F1 (Primary Weld in Double Lap Shear), G, H, & K

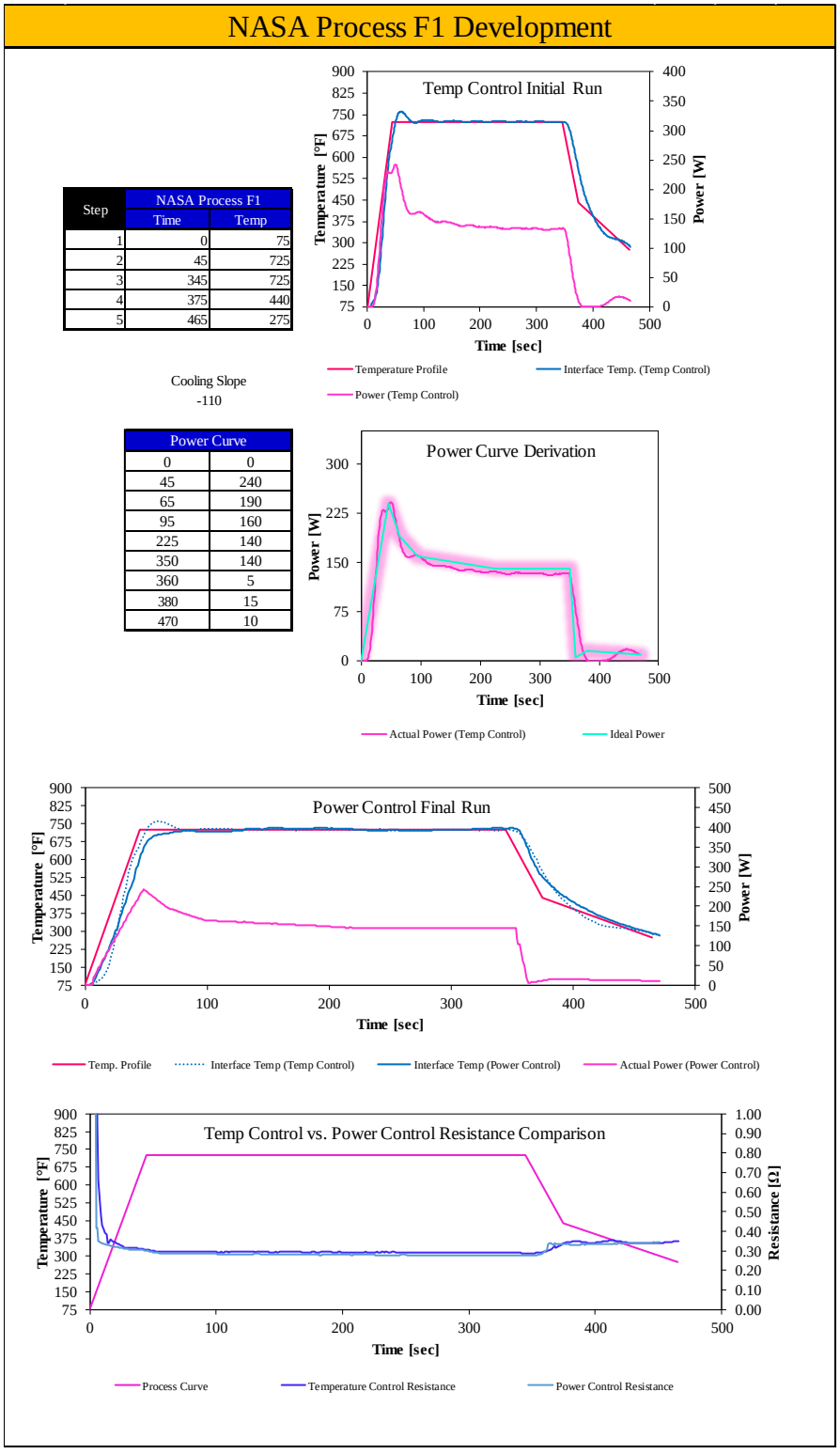

Step	NASA Process F1	
	Time	Temp
1	0	75
2	45	725
3	345	725
4	375	440
5	465	275

Power Curve	
0	0
45	240
65	190
95	160
225	140
350	140
360	5
380	15
470	10

Figure 19 – Process F1 Development

4.1.6 Process Development F2 (Secondary Weld in Double Lap Shear)

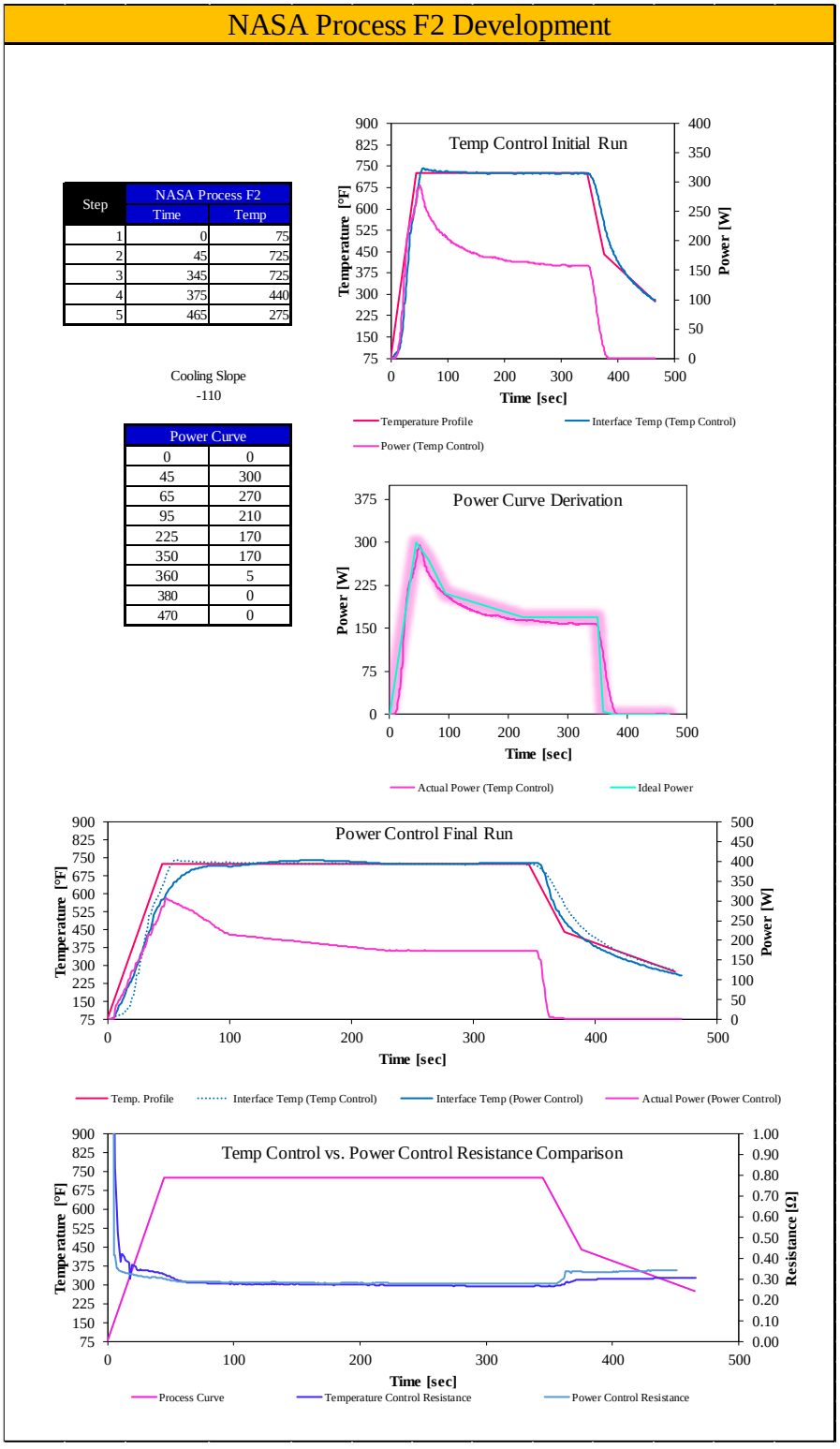

Step	NASA Process F2	
	Time	Temp
1	0	75
2	45	725
3	345	725
4	375	440
5	465	275

Cooling Slope
-110

Power Curve	
0	0
45	300
65	270
95	210
225	170
350	170
360	5
380	0
470	0

Figure 20 – Process F2 Development

4.1.7 Process Development I & J (Middle Sections)

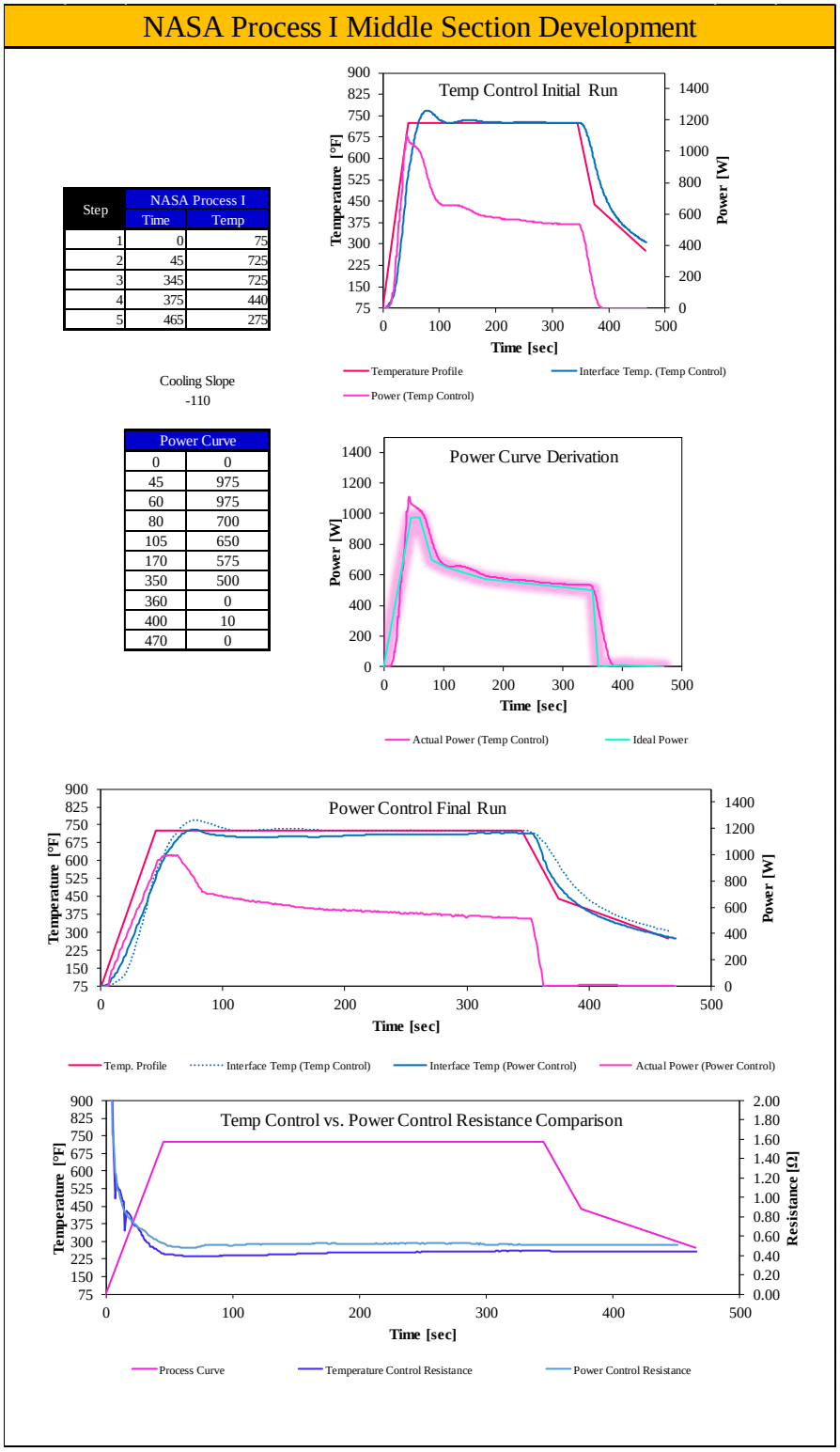

Step	NASA Process I	
	Time	Temp
1	0	75
2	45	725
3	345	725
4	375	440
5	465	275

Power Curve	
0	0
45	975
60	975
80	700
105	650
170	575
350	500
360	0
400	10
470	0

Figure 21 – Process I & J Middle Section Development

4.1.8 Process Development I & J (End Sections)

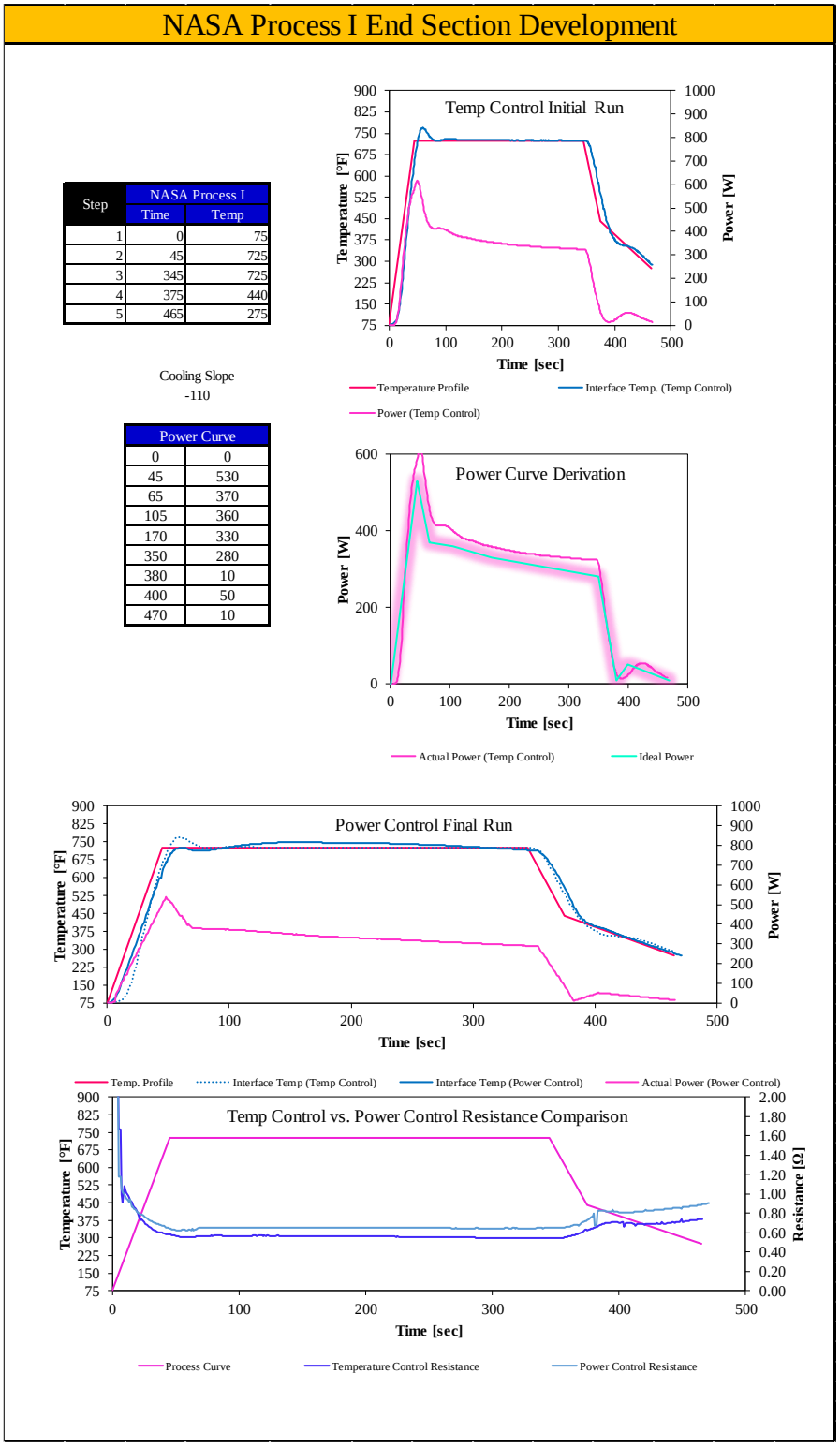

Figure 22 – Process I & J End Section Development

4.2 Welding Metrics

For each weld, resistance data and power data was captured. For single lap shear there was one weld per specimen, for double lap shear there were two welds per specimen, for Mode I there were seven welds per specimen, and for Mode II there were five welds per specimen. The summaries for the welding metrics for processes A-K can be seen in this section.

4.2.1 Process A Welding Metric Summary

It can be seen in this summary that NASA-RW-A3-1 experienced a higher resistance. This could be due to a few reasons; a defect in the heating element, oxidation of the heating element, or current leakage. This instance was most likely due to a defect in the heating element, which could have happened in the placement of the welding stack. This change in resistance will lead to a difference in welding temperature and overall weld strength.

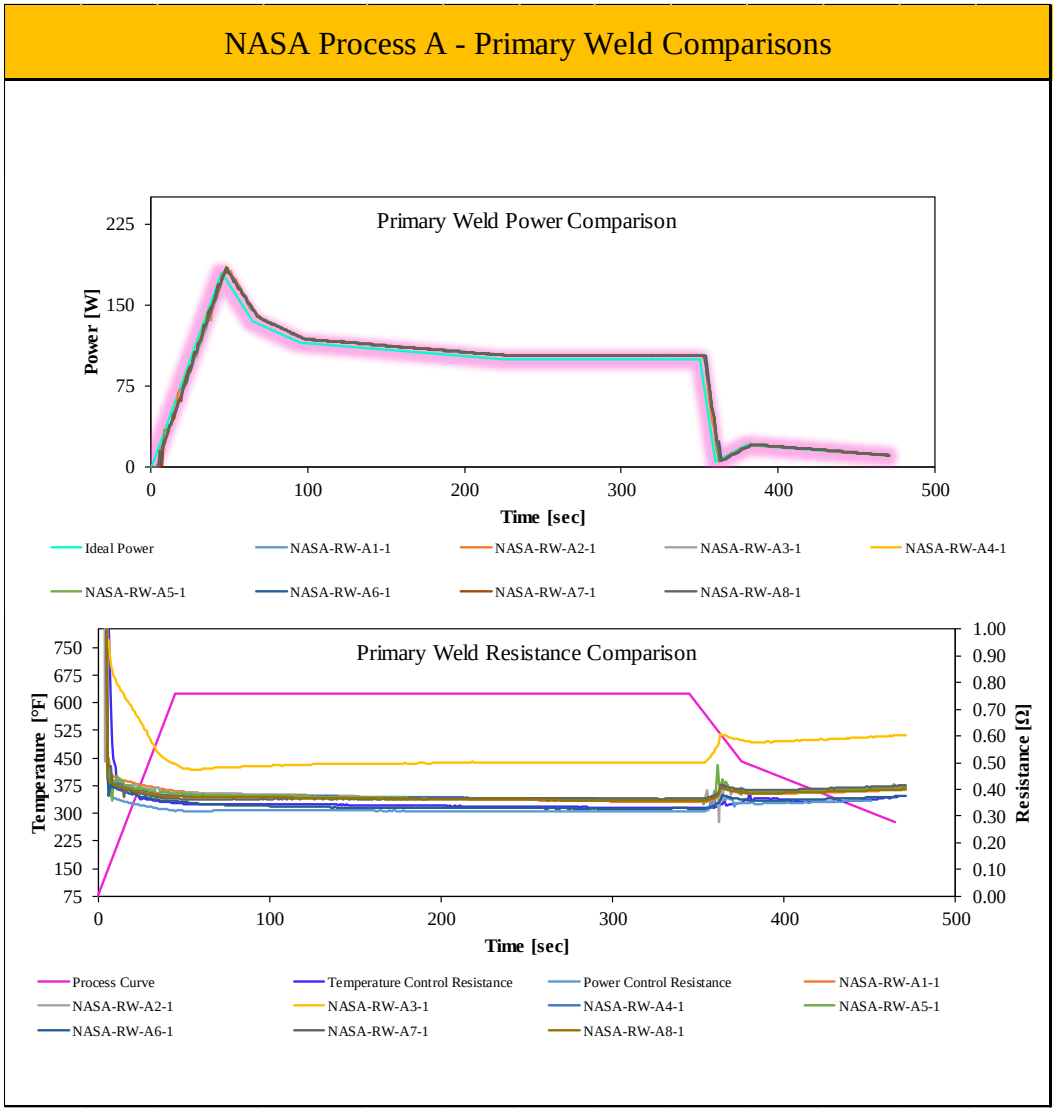

Figure 23 – Process A1 Weld Summary

The only anomaly seen in the data below is that NASA-RW-A4-2 experiences a spike in resistance as soon as the temperature starts to decrease. This is to be expected as the resistance value is volatile during this welding period as the temperature is changing fairly rapidly. This same occurrence can be seen in other weld processes as well. This does not affect the integrity of the weld since the power is so low during the spike in resistance.

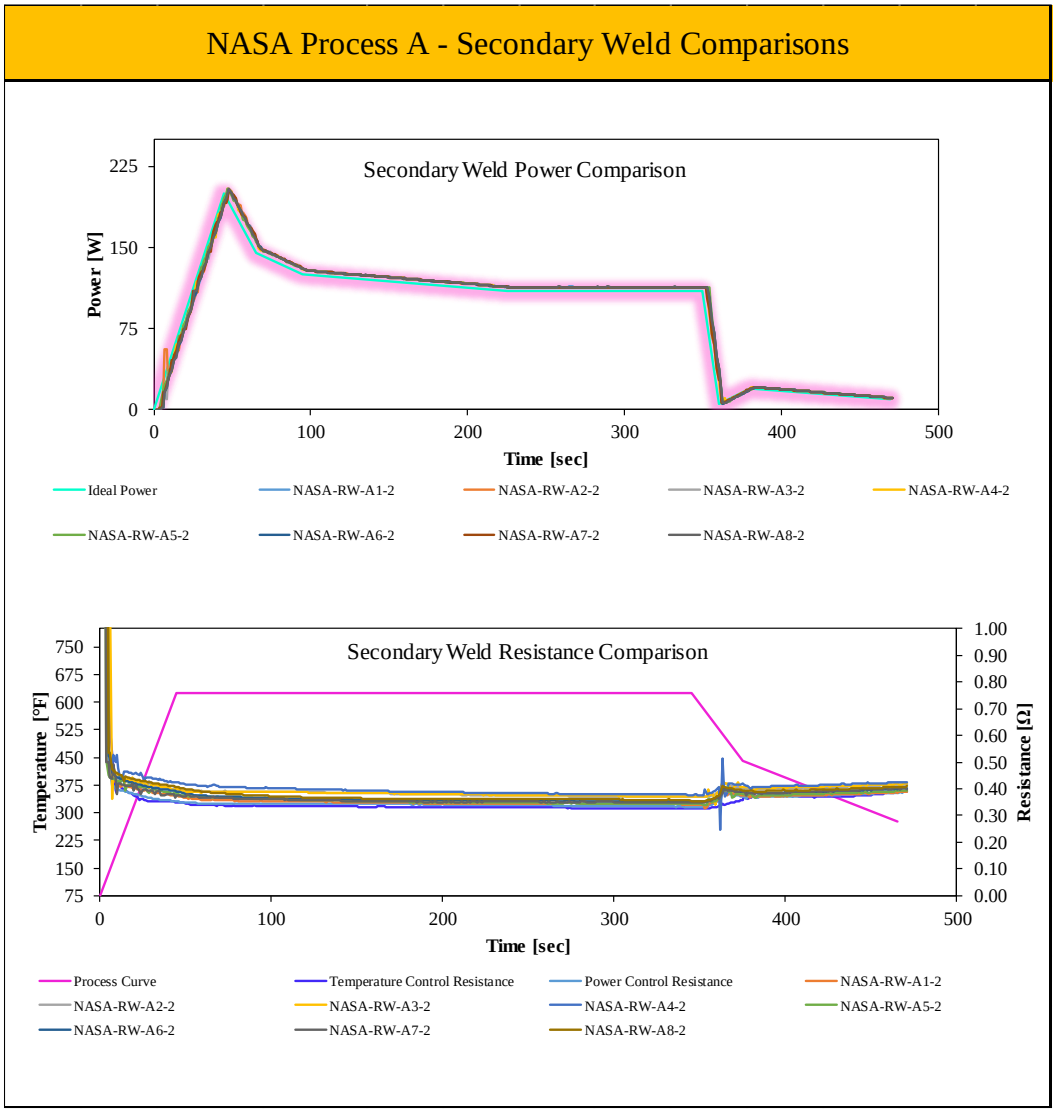

Figure 24 – Process A2 Weld Summary

4.2.2 Process B Welding Metric Summary

This data summary shows uniform power and resistance across all welded specimens which then should result in a low COV when it comes to strength testing, assuming all other metrics are as expected (uniform pressure, no defects in substrate or FOD).

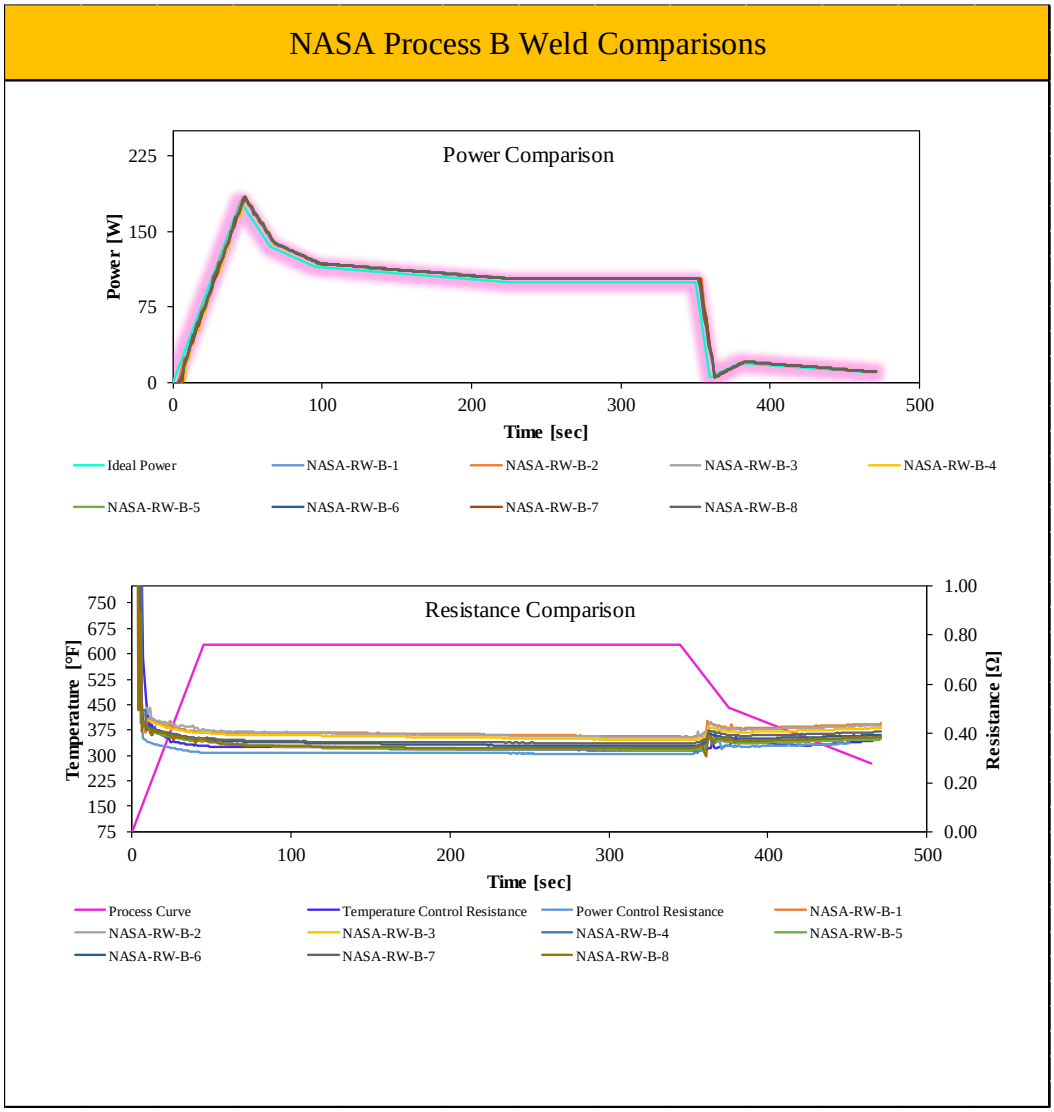

Figure 25 – Process B Weld Summary

4.2.3 Process C Welding Metric Summary

As in the process B welding metric summary this data shows uniform power and resistance which shows an acceptable welding temperature was reached in each specimen. The same process development was used across processes A1, B and C as the joint geometry was the same, the only difference was fiber orientation at the interface (45° vs. 0°). Which in resistance welding has a minimal effect on temperature as all of the heat is generated from the heating element, not the substrate.

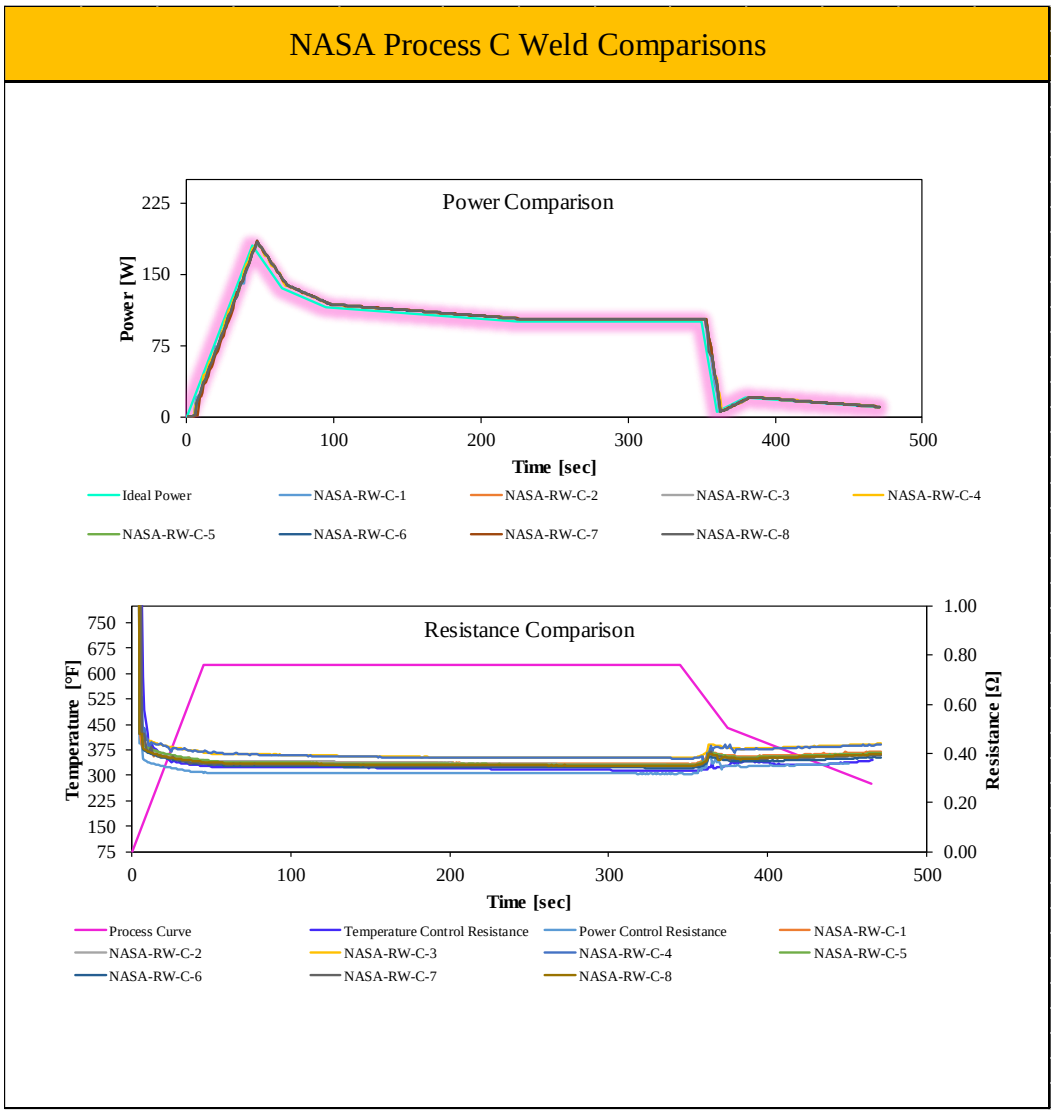

Figure 26 – Process C Weld Summary

4.2.4 Process D Welding Metric Summary

Summaries of the 1st and 2nd welds will be shown for Processes D & E as there are seven and five total welds respectively. Summaries of all welds can be seen in Appendix I – Welding Metrics. All mode I and mode II specimen welds require a significantly higher power as the heating element that is used is much bigger in size (3" X 5-7" vs. 1" X 4"). Even though only 1" is welded at a time, power is lost to other areas of the heating element. This effect is what causes the requirement for a higher power. This higher power also causes a larger difference in resistance values when in the cooling stage of the welding process seen below in Figure 27.

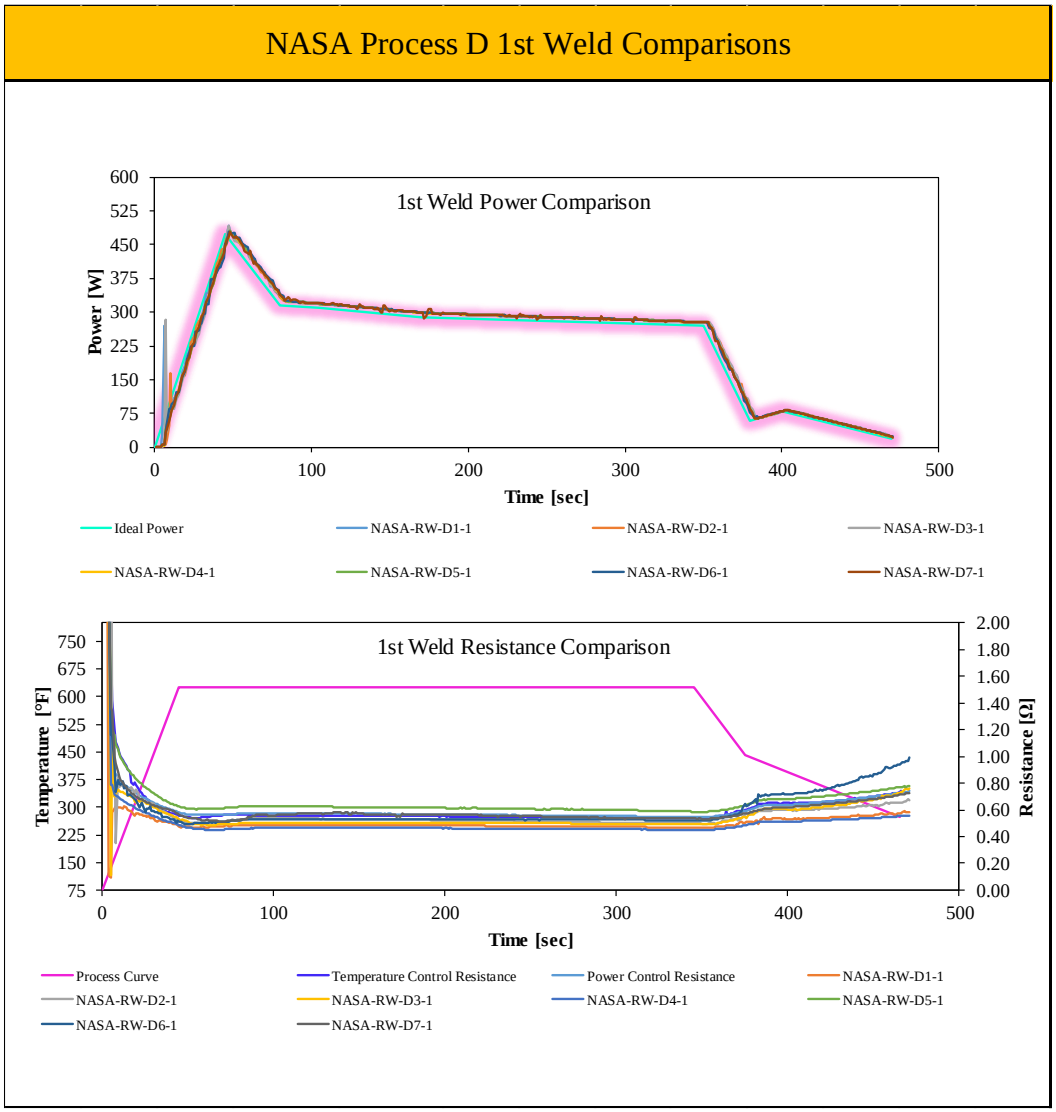

Figure 27 – Process D 1st Weld Summary

In the second weld comparison it can be seen below in Figure 28 that NASA-RW-D2-2 experienced a lower power at the peak of the weld process. This would lead to a lower welding temperature depending on if the resistance was similar to the power control resistance which is true in this case.

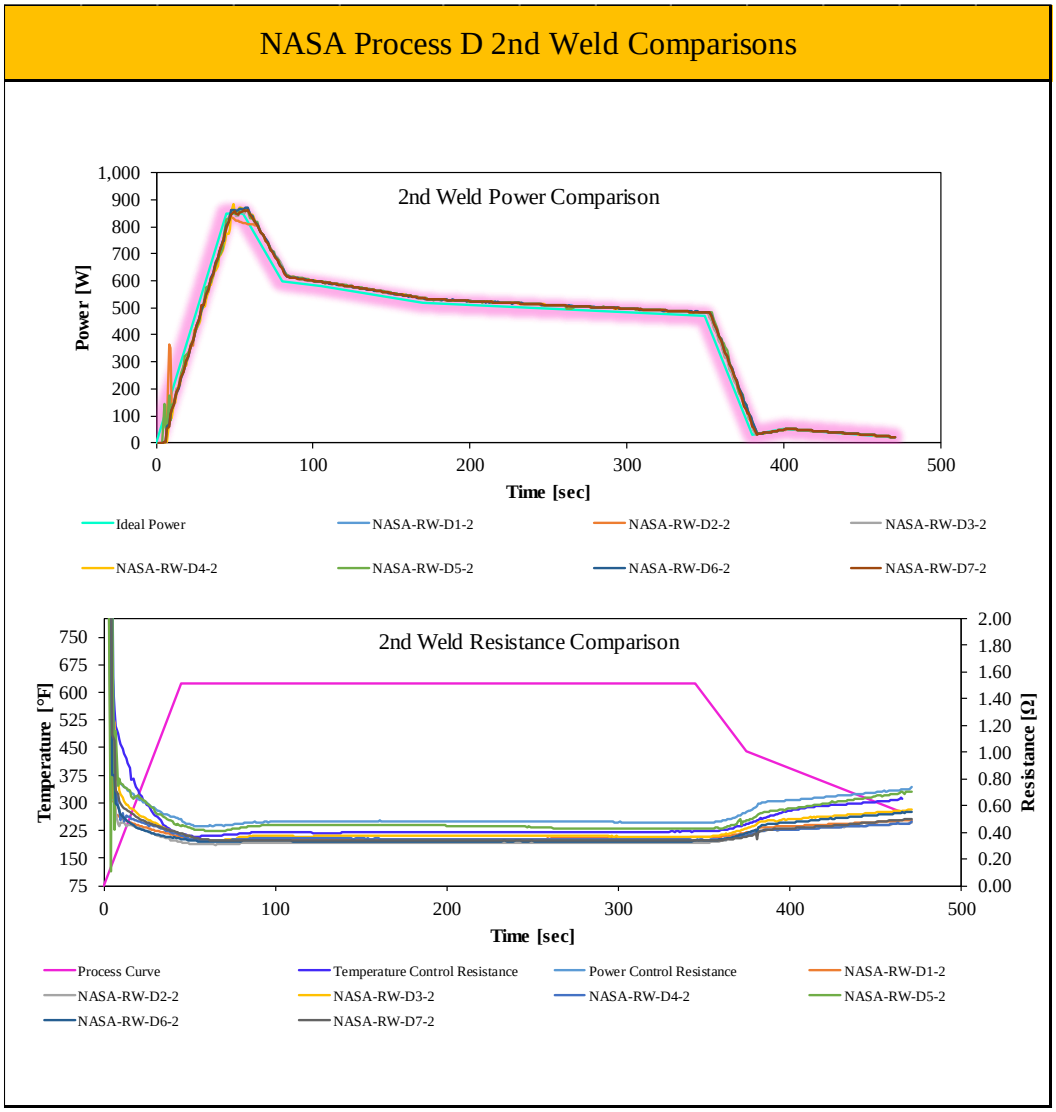

Figure 28 – Process D 2nd Weld Summary

4.2.5 Process E Welding Metric Summary

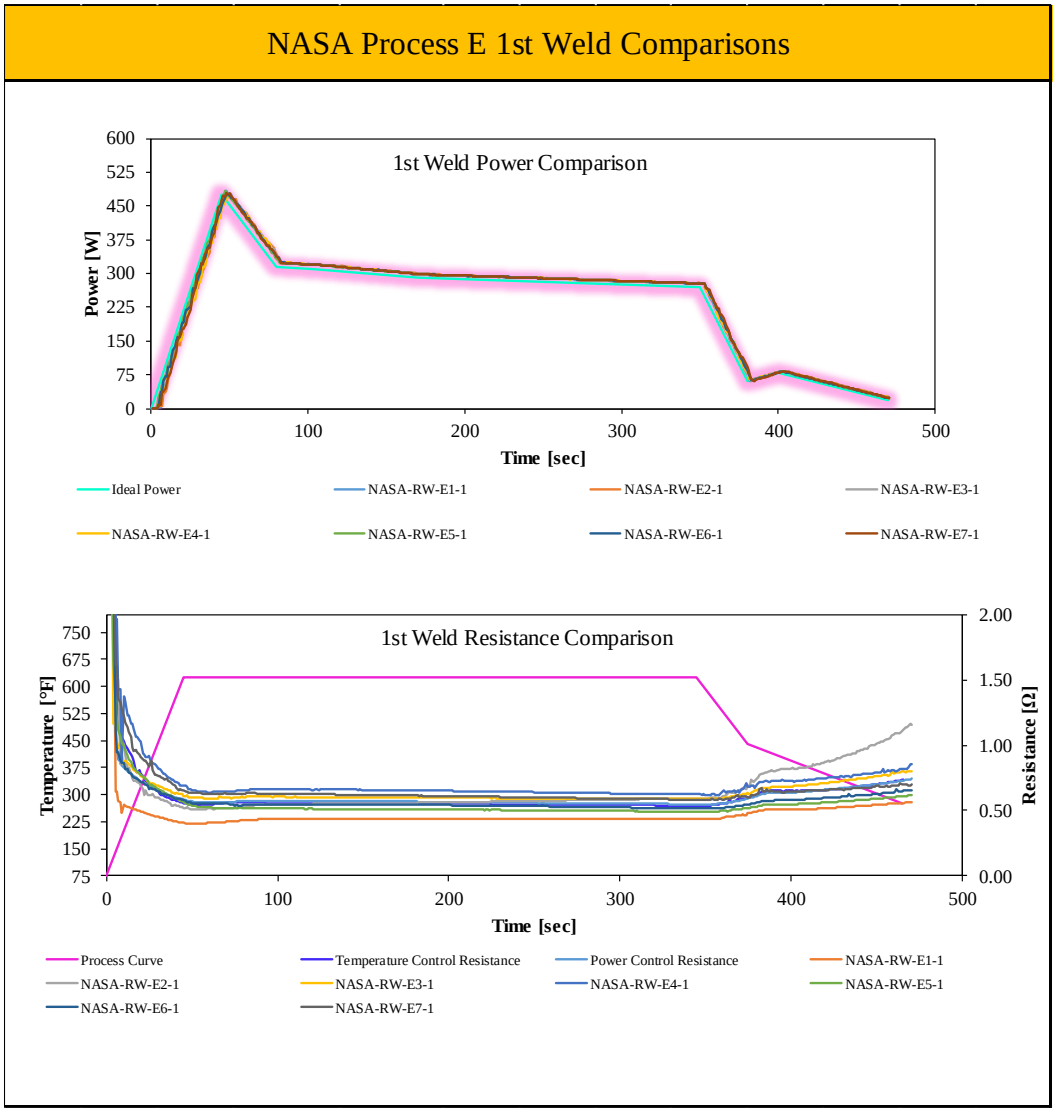

Figure 29 - Process E 1st Weld Summary

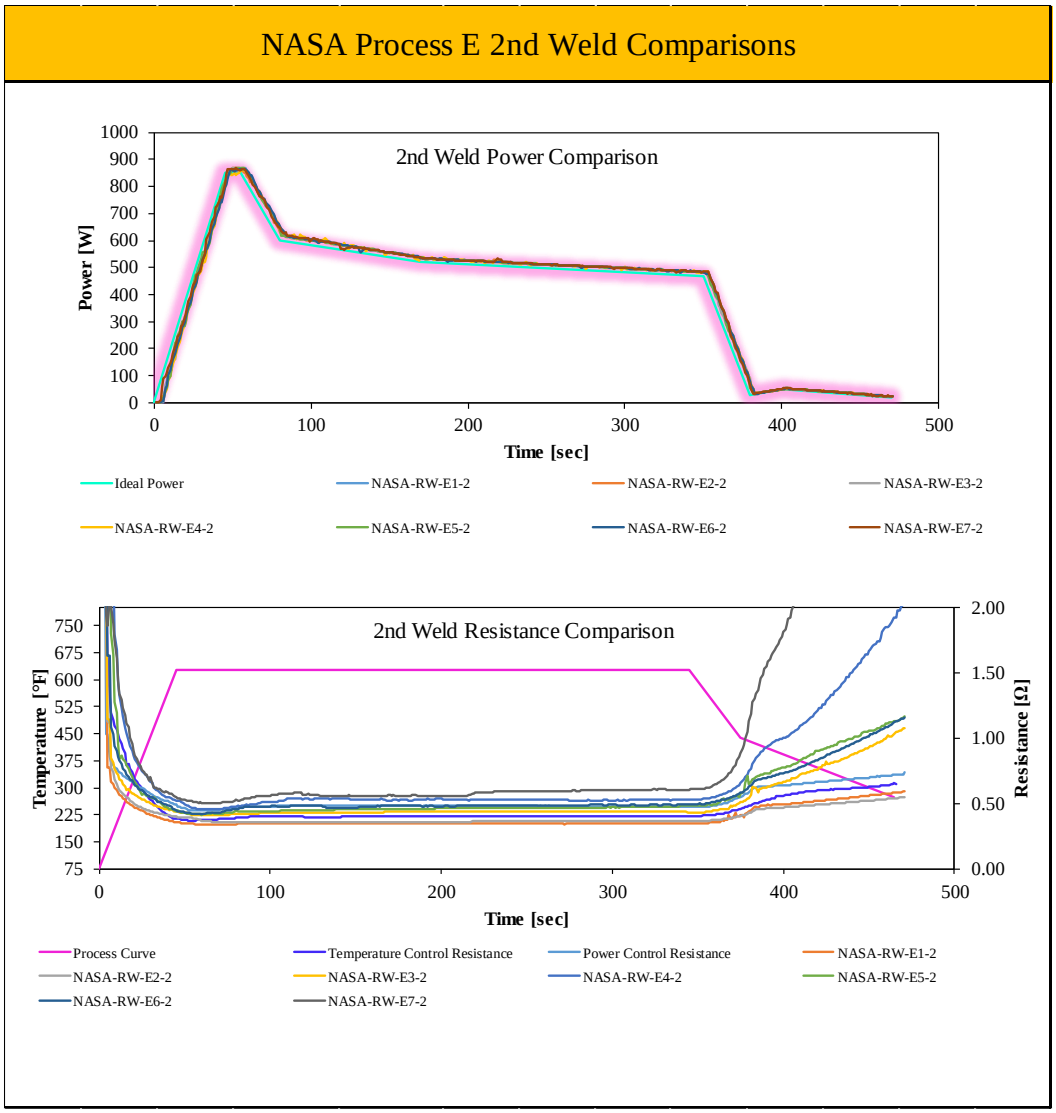

Figure 30 - Process E 2nd Weld Summary

4.2.6 Process F Welding Metric Summary

In this data summary NASA-RW-F3-1 and NASA-RW-F4-1 show a slightly higher average resistance than the other specimens which will lead to a change in weld temperature and may show a lower strength during single lap shear testing.

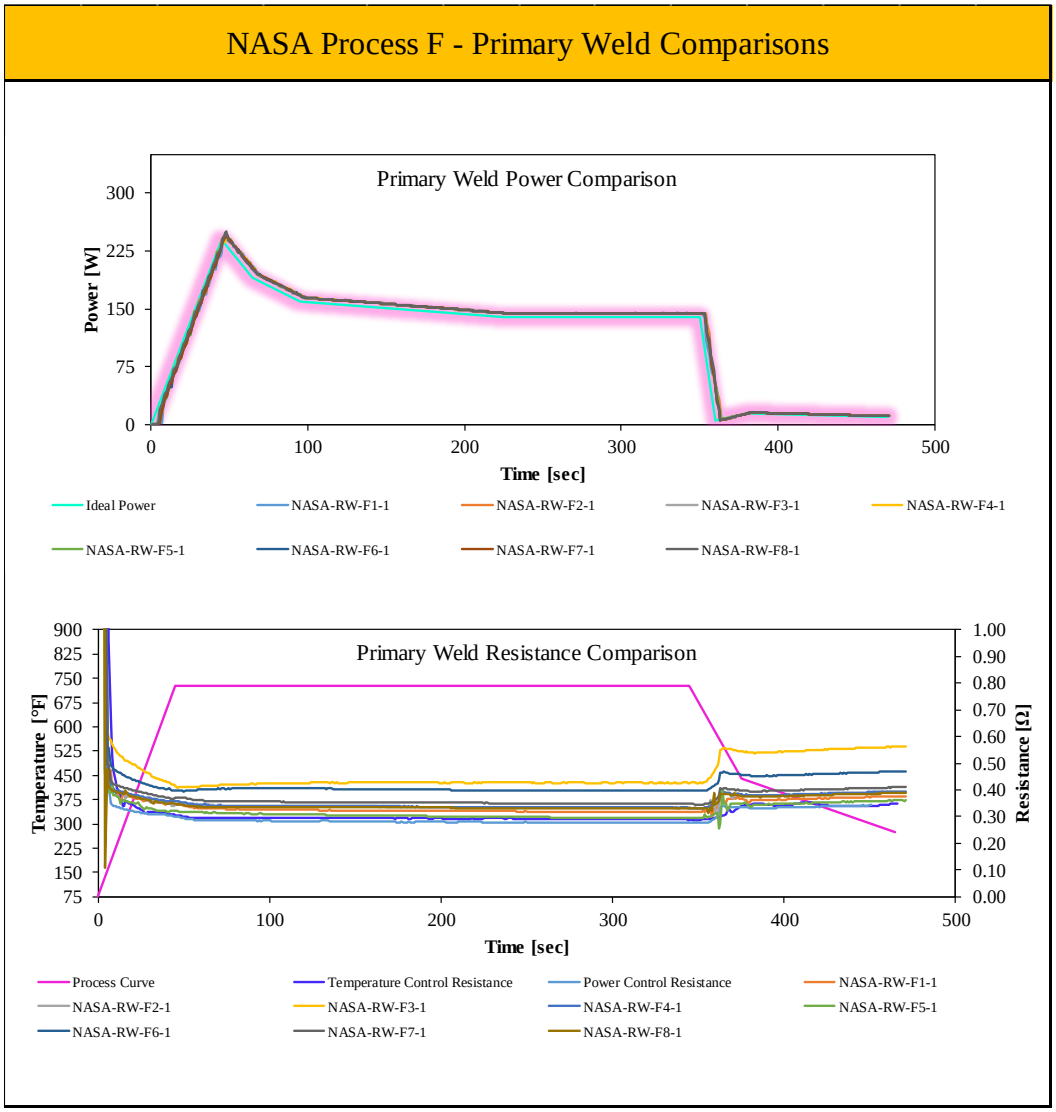

Figure 31 – Process F1 Weld Summary

The process F2 weld summary shows an anomaly that happens when extremely low power is put into the weld cycle. In this case, a command of 0 watts is used resulting in the resistance response wavering. This is due to the fact that the system needs a higher power input in order to read a consistent resistance. NASA-RW-F6-2 also is exhibiting a higher resistance which can then yield a lower weld temperature and a weaker overall joint.

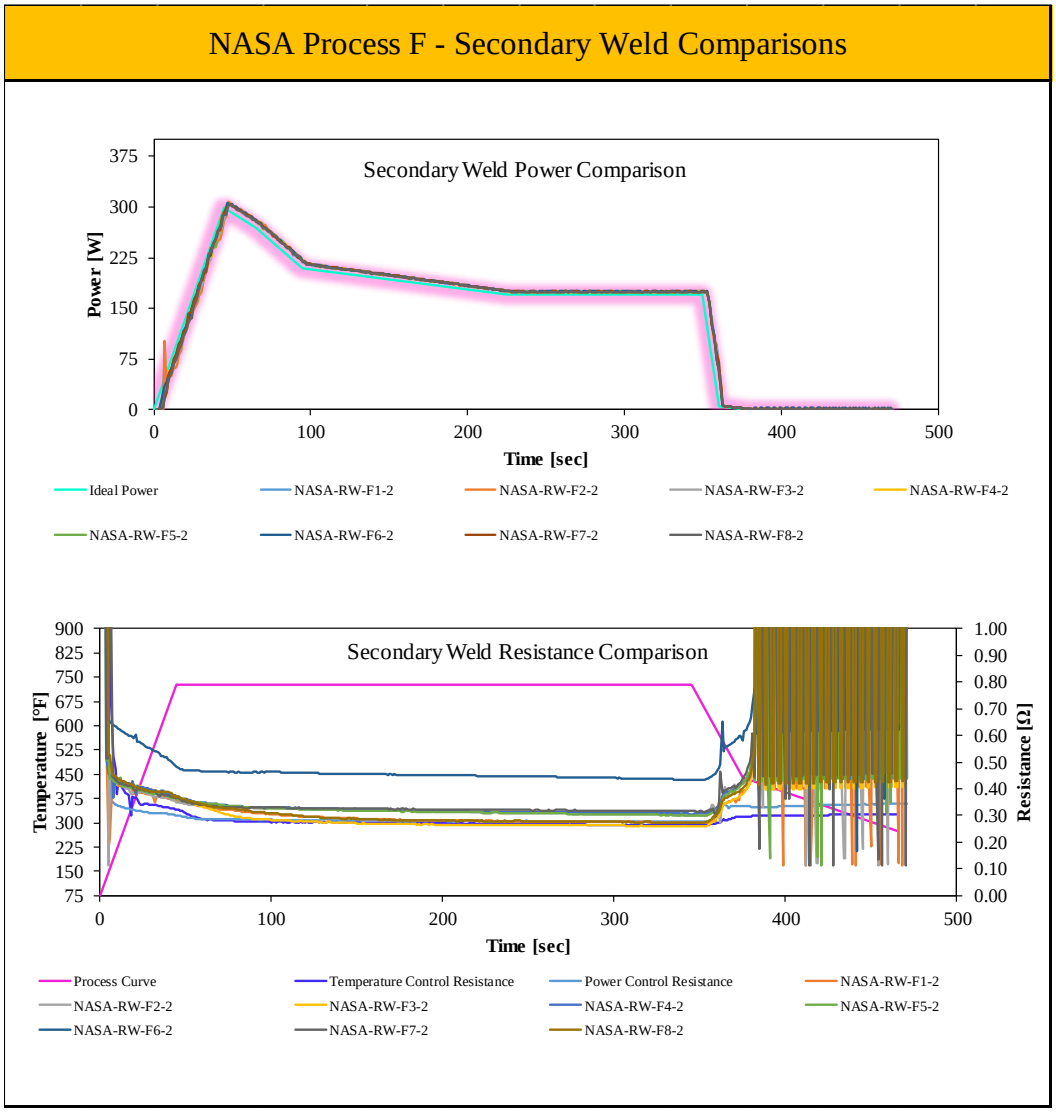

Figure 32 – Process F2 Weld Summary

4.2.7 Process G Welding Metric Summary

It can be seen in the resistance comparison below that the resistance values are more wide-spread than the previous weld processes. This can result in a larger spread of welding temperatures and a higher COV when it comes to weld strengths.

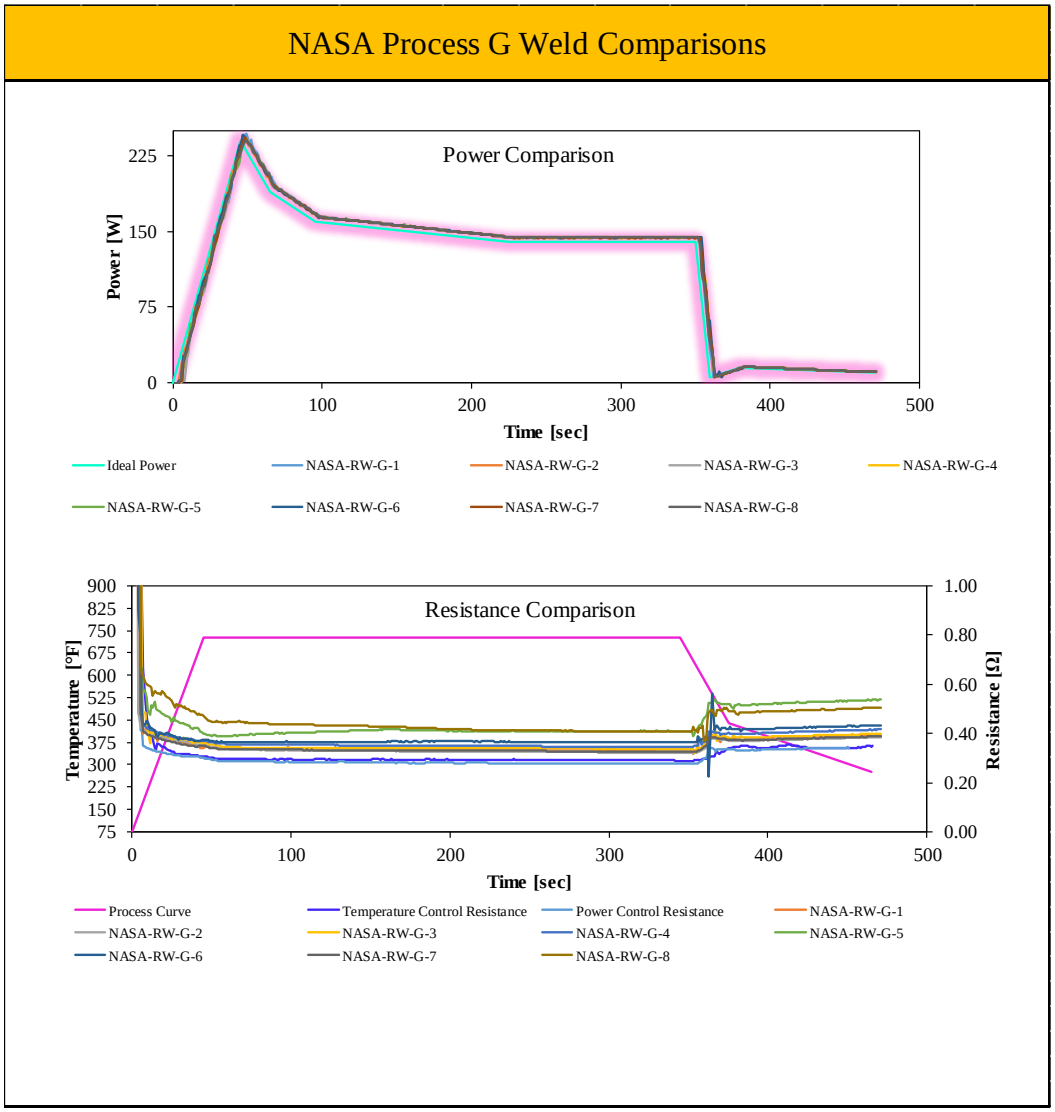

Figure 33 – Process G Weld Summary

4.2.8 Process H Welding Metric Summary

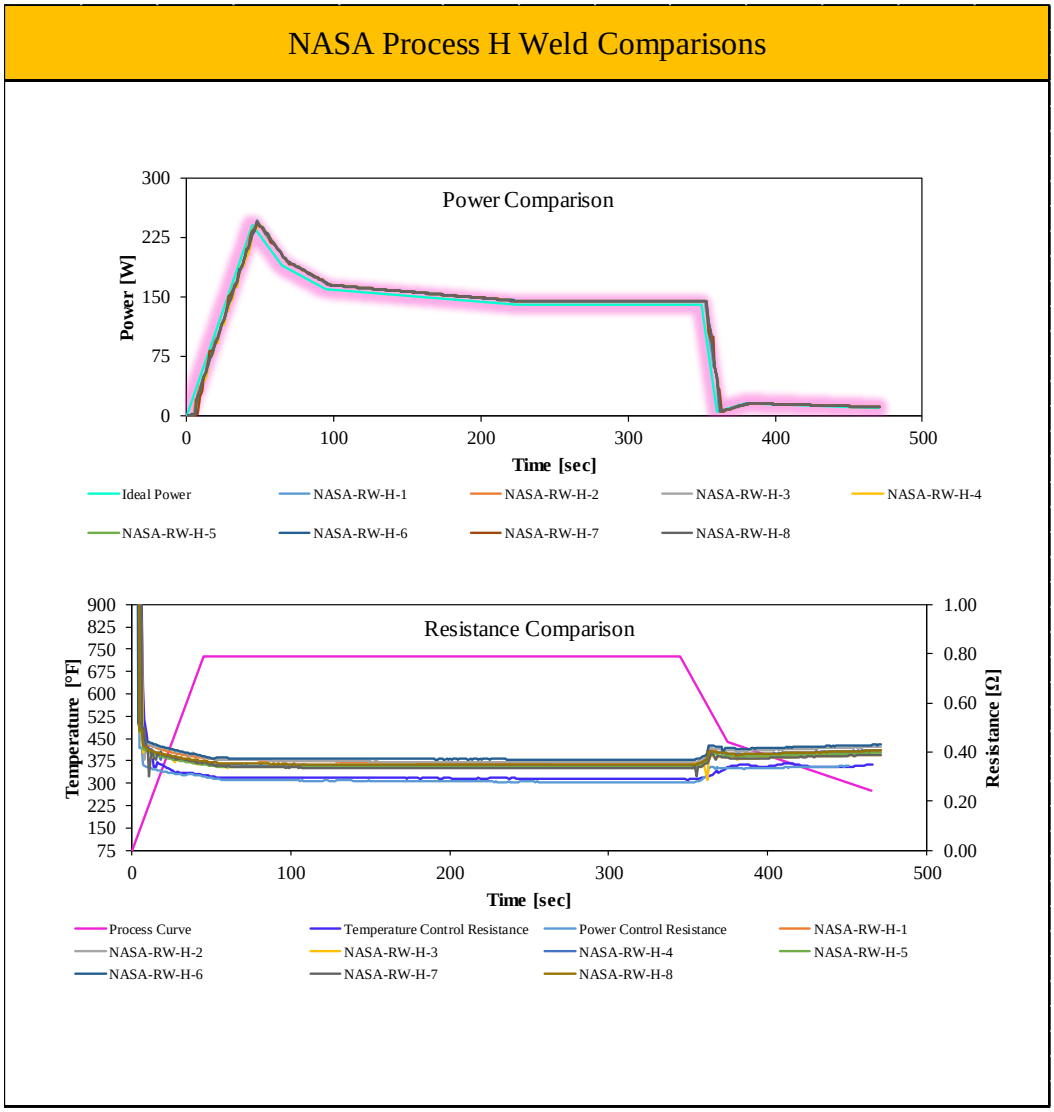

Figure 34 – Process H Weld Summary

4.2.9 Process I Welding Metric Summary

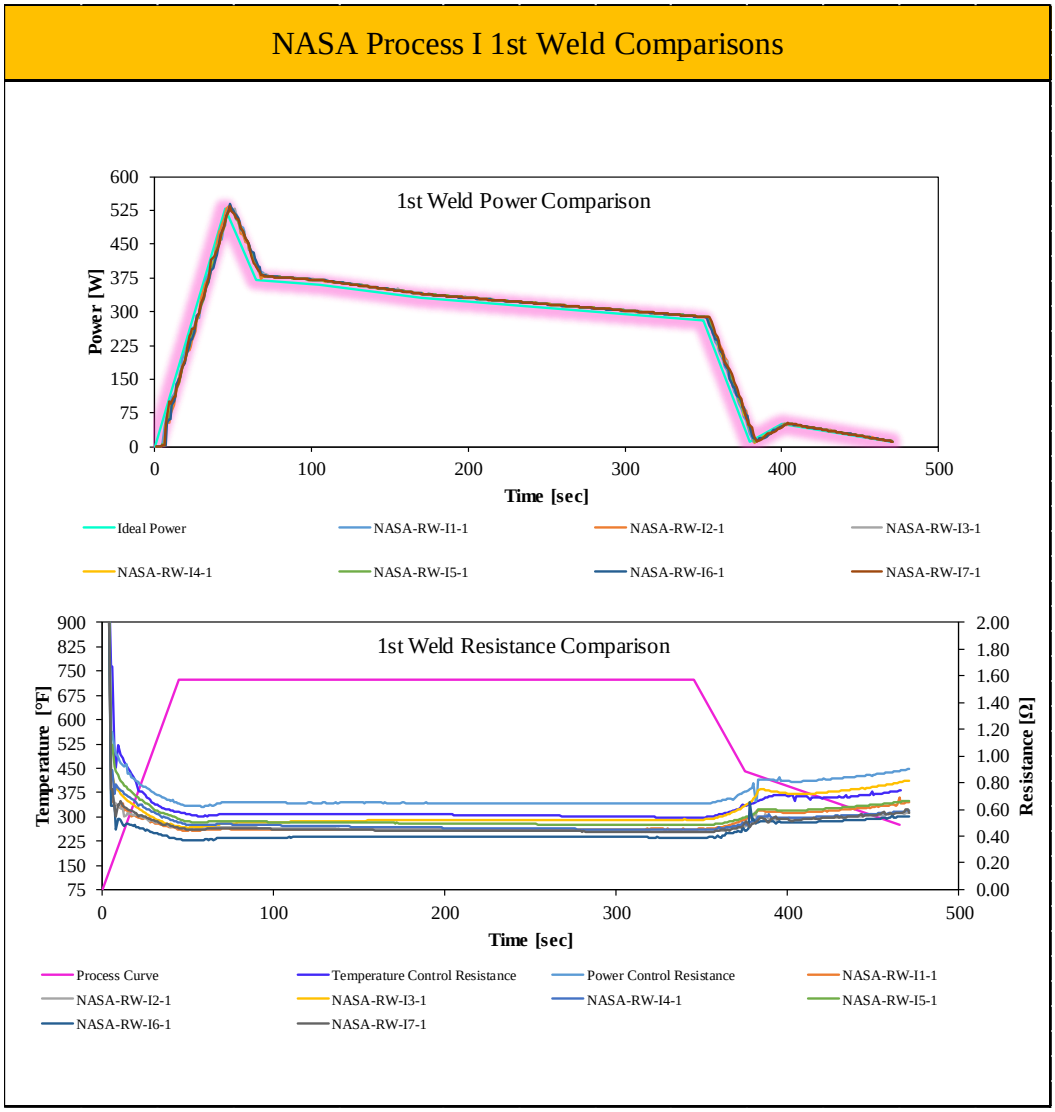

Figure 35 – Process I 1st Weld Summary

The process I 2nd weld summary shows the main issue when welding the PEEK mode I and mode II coupons. Depending on the resistance of the weld the power supply limit was reached and the peak power was not reached in some of the welds. This could contribute to unstable crack growth in the mode I / and mode II testing. To fix this issue, a power supply with a higher amperage must be used. The previous anomaly can also be seen below in Figure 36 where the resistance spikes as soon as the cooling stage is started.

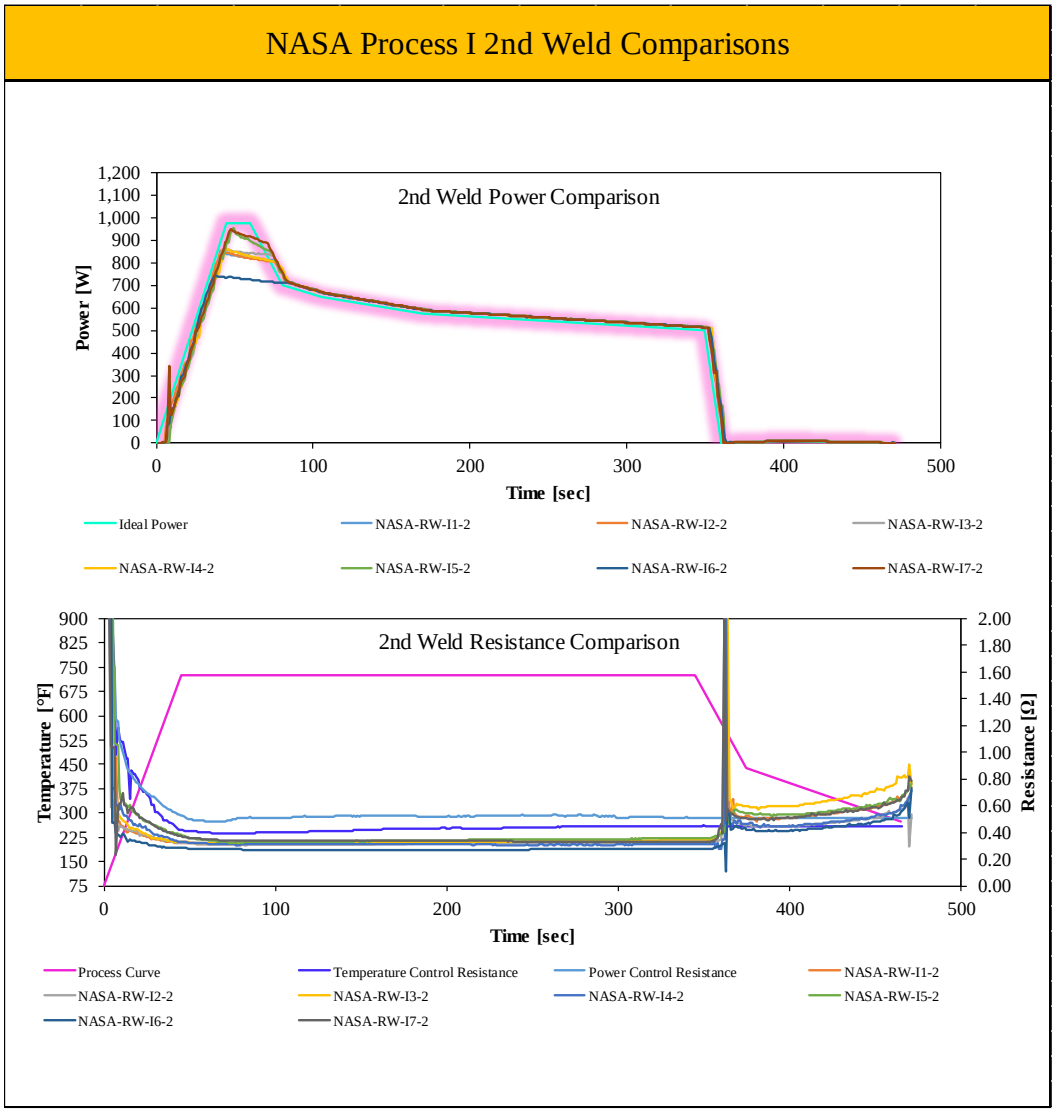

Figure 36 – Process I 2nd Weld Summary

4.2.10 Process J Welding Metric Summary

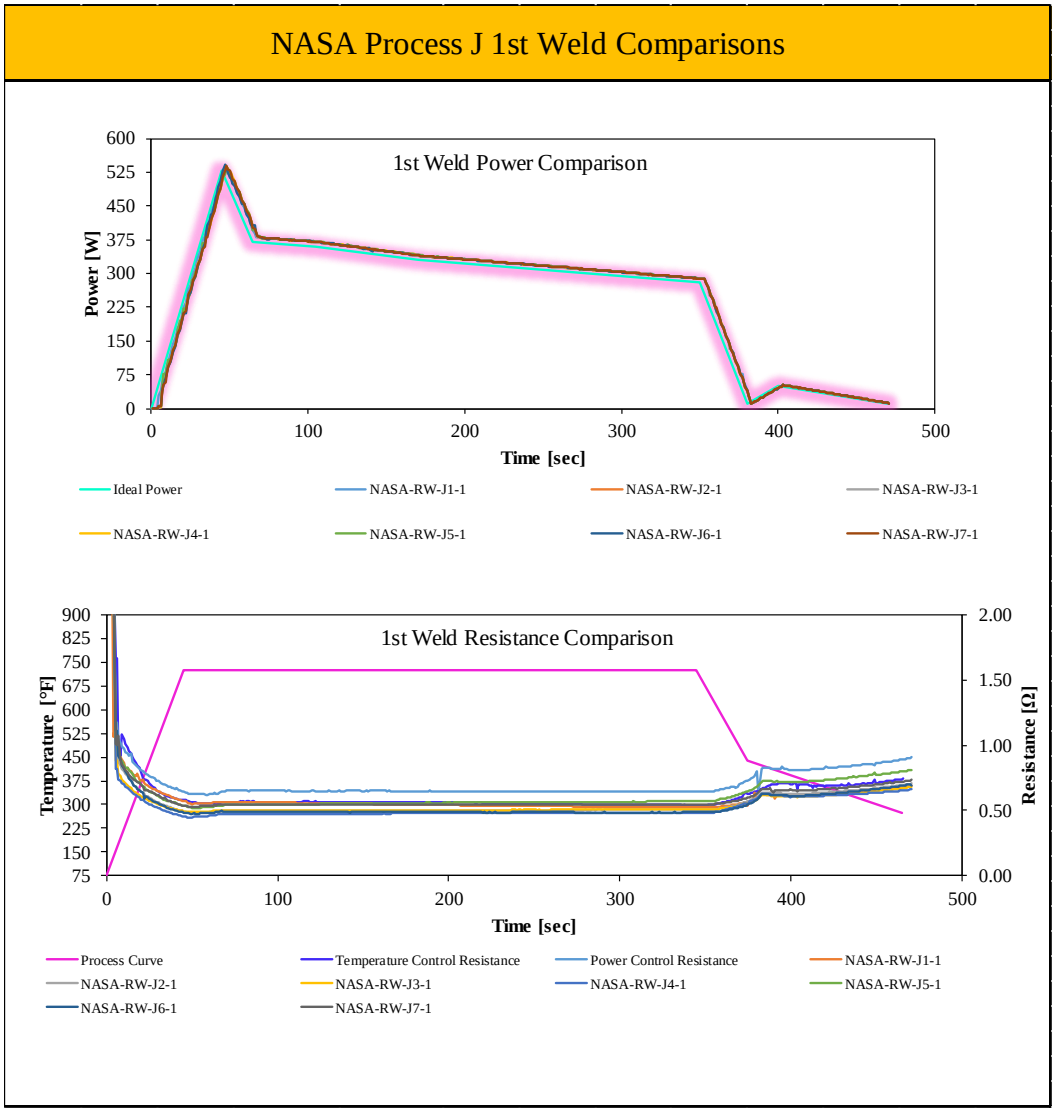

Figure 37 – Process J 1st Weld Summary

In the process J 2nd weld summary it can be seen that all welds reached the maximum power except for NASA-RW-J4-2. This could have been due to a defect in the heating element or oxidation during welding. The major difference in resistance seen in the cooling stage is due to a lower power being commanded from the welding module.

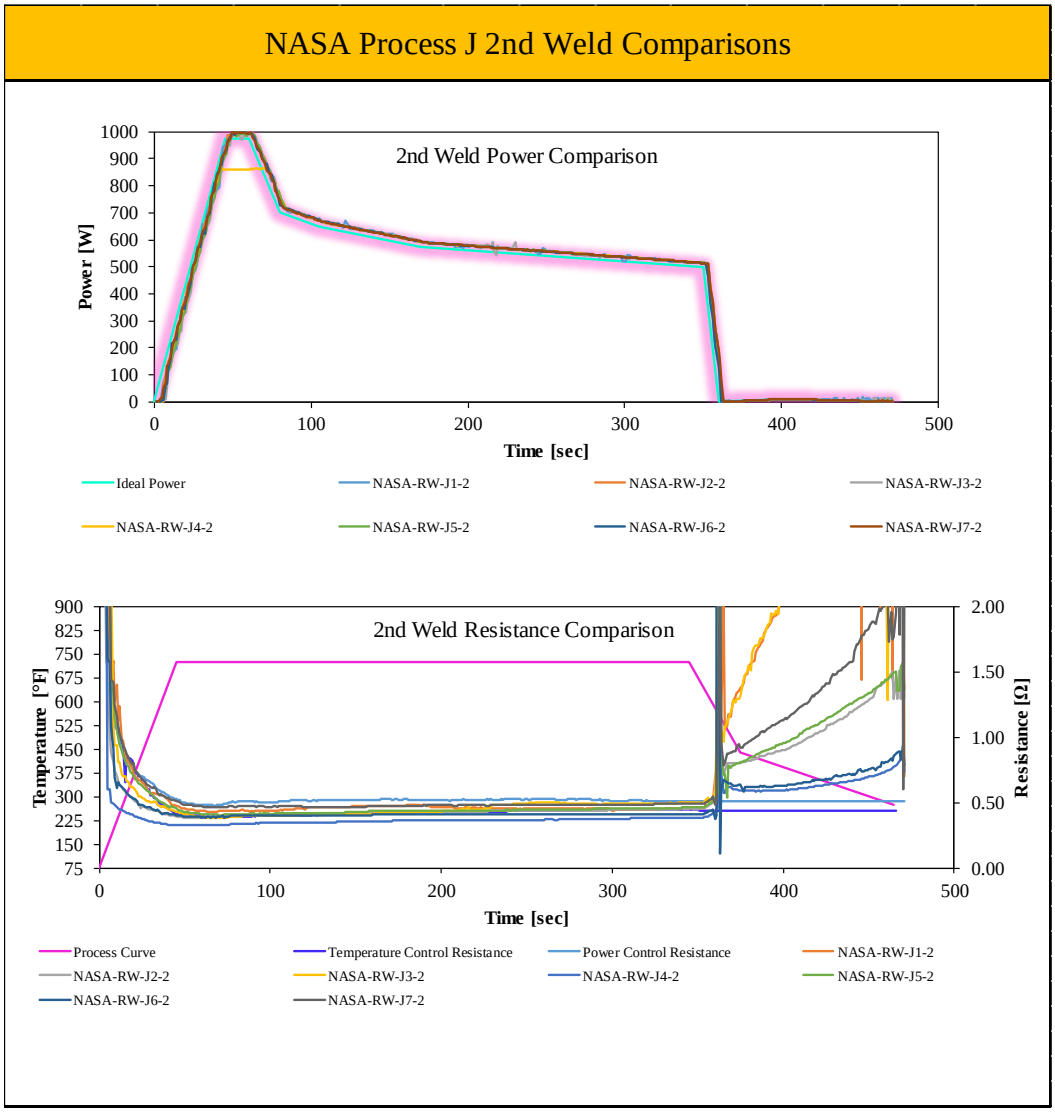

Figure 38 – Process J 2nd Weld Summary

4.2.11 Process K Welding Metric Summary

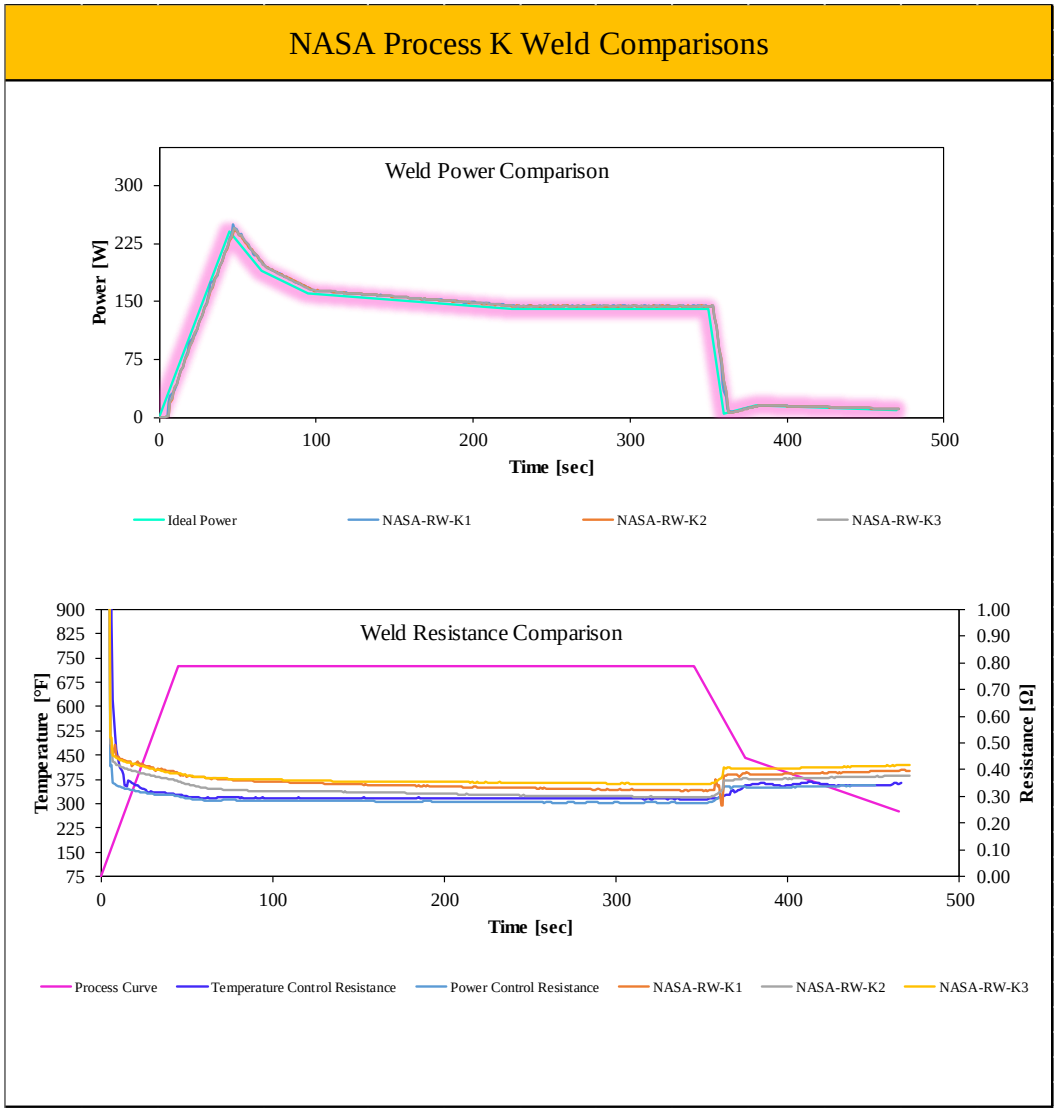

Figure 39 – Process K Weld Summary

5.0 Non-Destructive Inspection: C-Scan Imaging

NDI was performed on every welded specimen in the test matrix. C-Scan is important in thermoplastic welding as it enables the detection of defects, ensures the quality of the welded joint, aids in process optimization, and provides a non-destructive testing method. By utilizing C-Scan, manufacturers can enhance the reliability and performance of thermoplastic welds, leading to safer and more durable products. The C-Scan data for the requested test matrix can be seen below.

5.1 Process A NDI Results

Being a double lap shear configuration, process A required precise shimming for an acceptable pressure application. This C-Scan shows that there were definitely areas that were degraded or showed some porosity. This will later be validated with a cross-sectional photomicrograph. One possible solution to this would be a different shimming strategy or weld tooling.

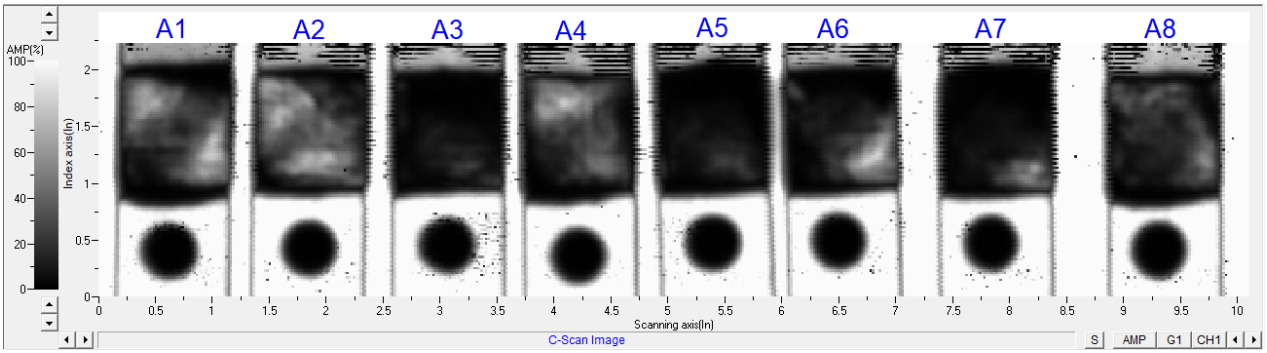

Figure 40 – Process A NDI Results

5.2 Process B NDI Results

The single lap shear configuration shows a much better weld quality. There are still some areas with possible degradation or porosity but overall is better than the process A scans.

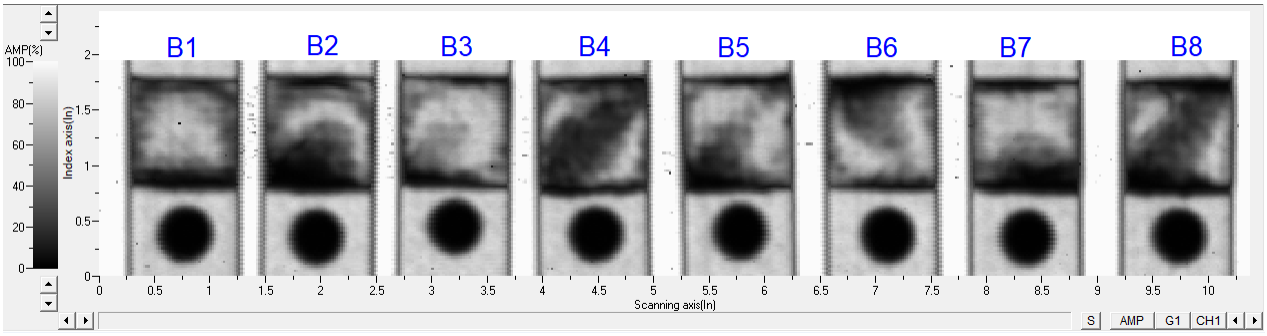

Figure 41 – Process B NDI Results

5.3 Process C NDI Results

The NDI scans for process C show an anomaly happening in the center of the weld line. This could possibly be degradation or porosity at the weld line. Photomicrographs will need to be examined later in this report to prove out which defect is present.

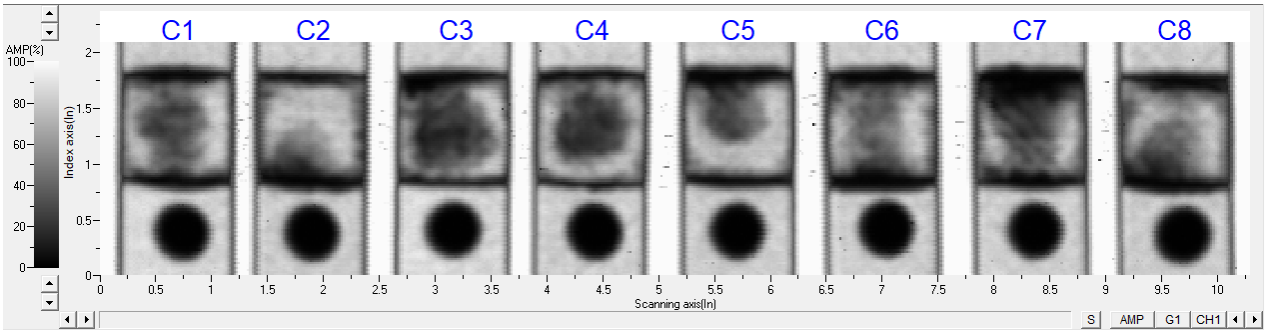

Figure 42 – Process C NDI Results

5.4 Process D NDI Results

The defect that is most likely seen here is porosity. The main problem with sequential welding is applying acceptable pressure during each weld as the pressure block is applying pressure across the entire specimen. The Kapton tape can be clearly seen at the interface as well.

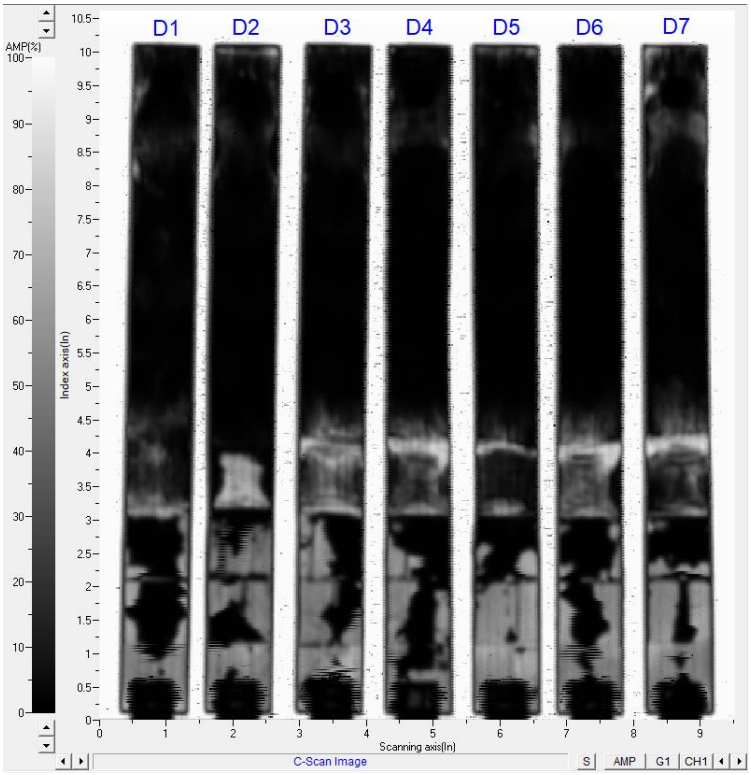

Figure 43 – Process D NDI Results

5.5 Process E NDI Results

As can be expected, process E NDI results show the same defect since it is the same process used as process D.

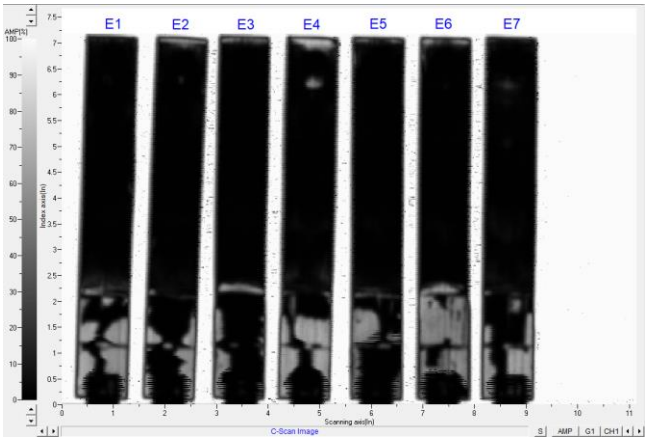

Figure 44 – Process E NDI Results

5.6 Process F NDI Results

As in process A, there are defects seen through the weld line, most likely porosity as the shimming technique must be very precise in order to obtain adequate pressure uniformity.

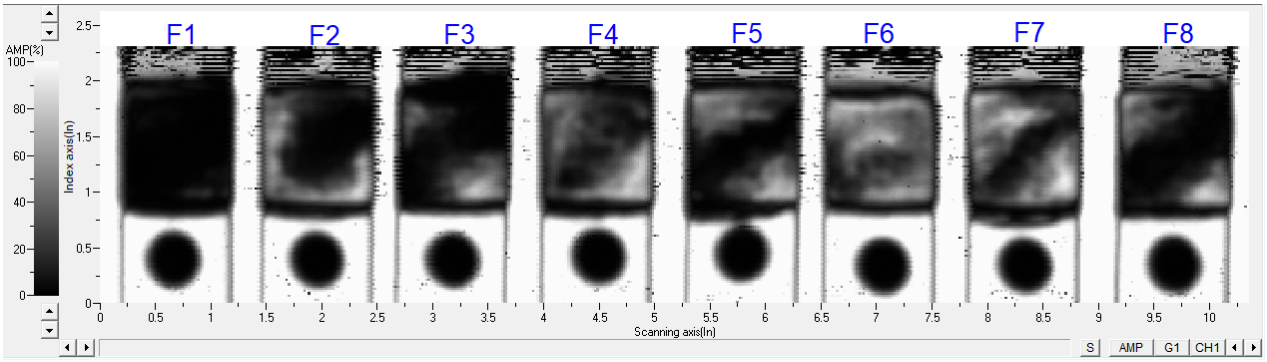

Figure 45 – Process F NDI Results

5.7 Process G NDI Results

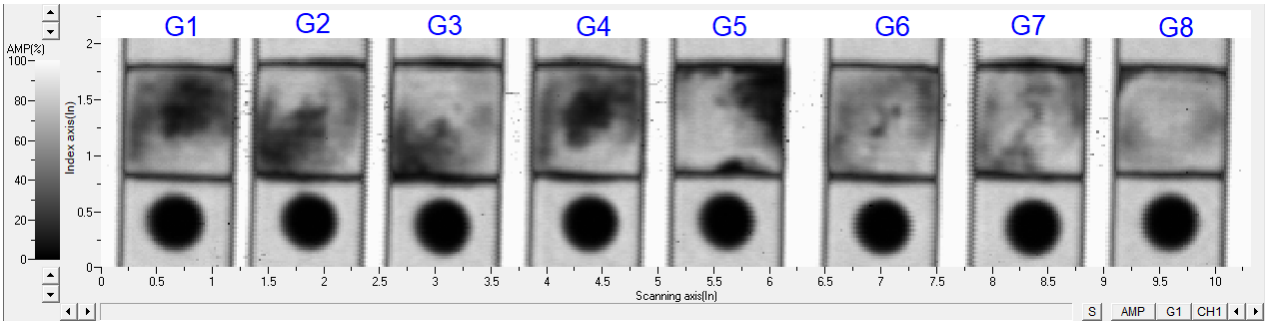

Figure 46 – Process G NDI Results

5.8 Process H NDI Results

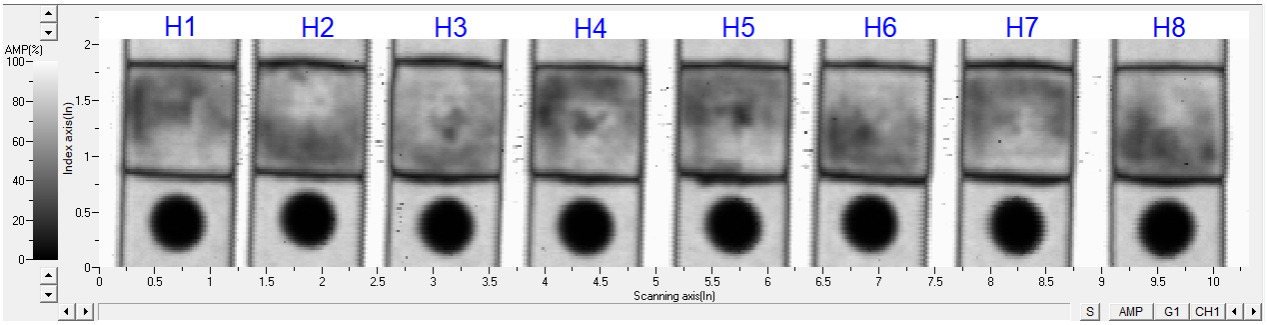

Figure 47 – Process H NDI Results

5.9 Process I NDI Results

Process I NDI Results show that the center of the weld is mainly free of defects but the edges are either being degraded or contain porosity (must be validated by photomicrograph). The Kapton tape can also be clearly seen in the scan.

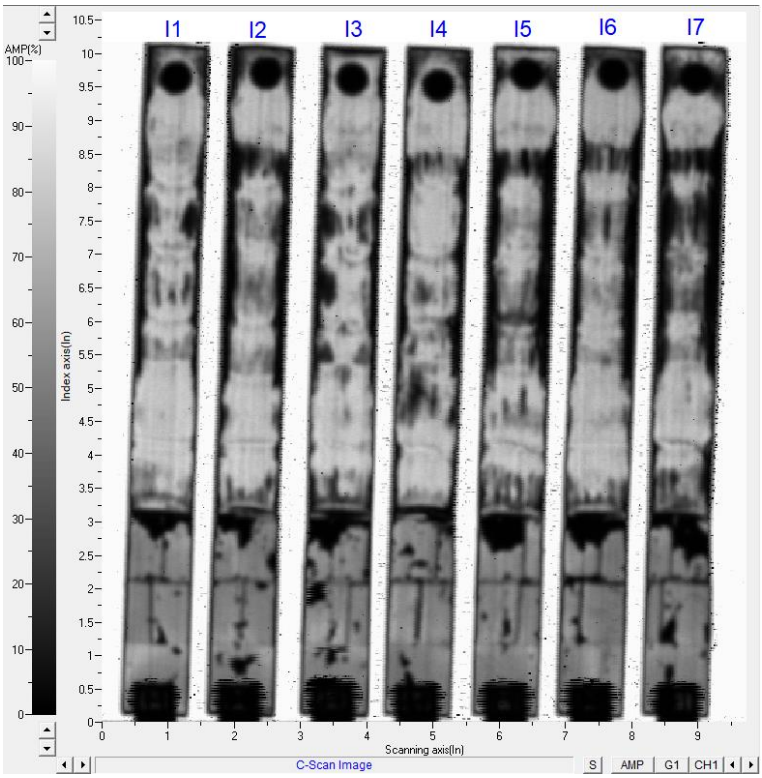

Figure 48 – Process I NDI Results

5.10 Process J NDI Results

Process J NDI results show the middle three welds as being the best quality with porosity or degradation occurring in the end weld sections.

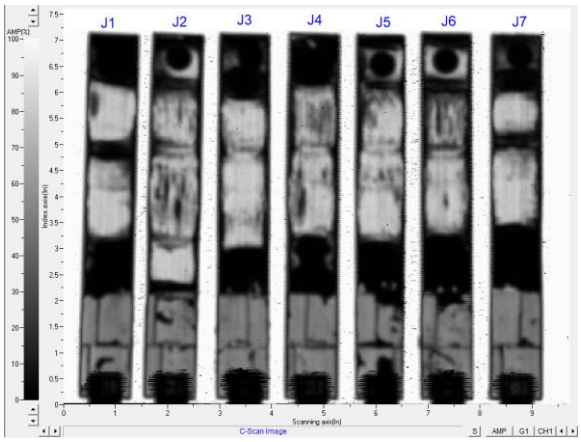

Figure 49 – Process J NDI Results

5.11 Process K NDI Results

With process K being the hybrid weld it is possible that the defect in this weld is degradation of the PEI composite as the weld process used reached 725°F. It's also possible to be porosity, but with the same single lap shear configuration other processes showed minimal defects.

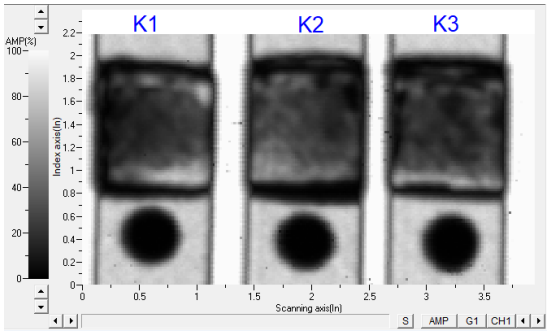

Figure 50 – Process K NDI Results

6.0 Photomicrographs

Photomicrographs are essential in thermoplastic welding as they enable visual inspection, defect analysis and process optimization. One photomicrograph specimen was manufactured from each process except for process K. These results can be seen below.

6.1 Process A Photomicrograph Results

This photomicrograph shows the probable cause of the defect seen in Process A NDI Results. As the secondary weld is being welded there seems to be a loss of pressure in the center area causing a small amount of porosity. This seems to be an issue springing from the fibers flowing out at the edge.

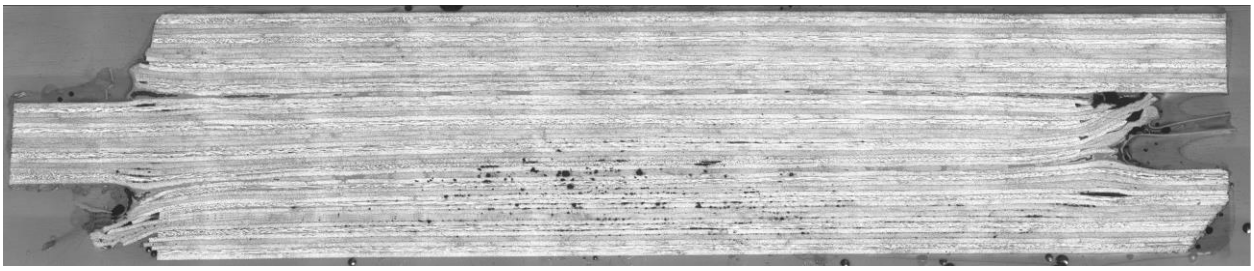

Figure 51 – Process A Photomicrograph

6.2 Process B Photomicrograph Results

This photomicrograph confirms the defect shown in Process B NDI Results as porosity. It's possible that as the fibers squeeze out at the edges there is a separation between the remaining layers creating an air gap or porosity.

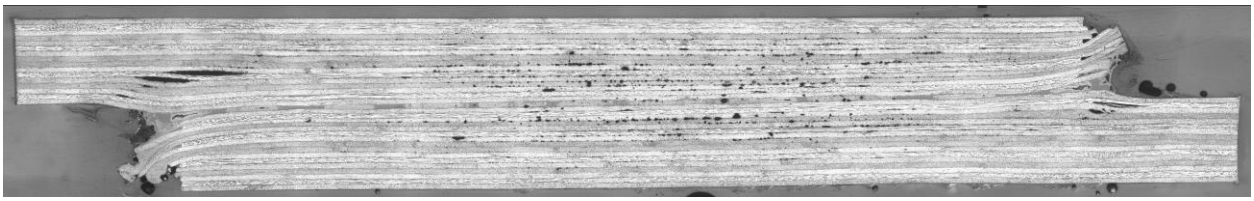

Figure 52 – Process B Photomicrograph

6.3 Process C Photomicrograph Results

This photomicrograph confirms the findings were porosity in the Process C NDI Results. Depending on the amount of fiber flow at the edge, the porosity will be more or less prevalent. In order to solve this problem precise thickness shims must be used to mitigate fiber distortion.

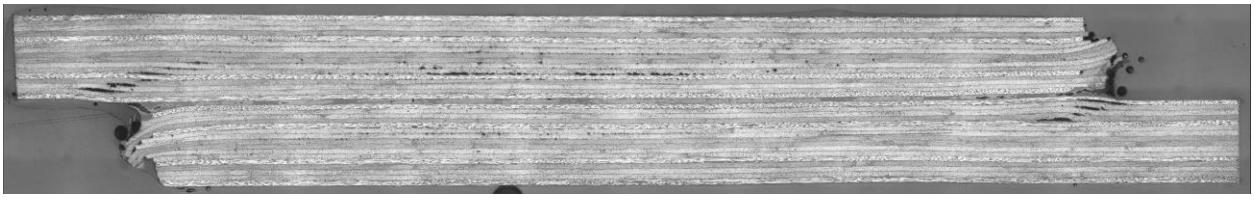

Figure 53 – Process C Photomicrograph

6.4 Process D Photomicrograph Results

This photomicrograph confirms the findings seen in Process D NDI Results. As this specimen was welded the fibers flowed outwards towards the sides and as the fibers moved out it created gaps where fibers used to be. It can be seen that only the layers closest to the heating element (where the heat is being generated from) are showing these pockets of air. In mode 1 testing this could contribute to unsteady crack propagation as the crack would want to jump into the porous region.

Figure 54 – Process D Photomicrograph

6.5 Process E Photomicrograph Results

This photomicrograph shows that the process E specimens exhibited the same behavior as the process D specimens. When the fibers would move out of the edge, air gaps were created causing porosity in the laminate. Again, the layers furthest away from the heating element do not show porosity.

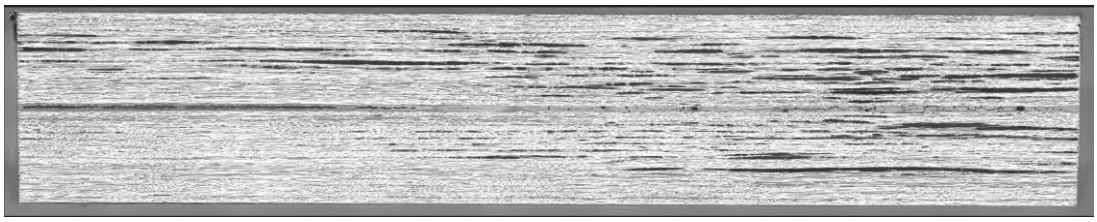

Figure 55 – Process E Photomicrograph

6.6 Process F Photomicrograph Results

This photomicrograph confirms that the defect in Process F NDI Results was porosity. This is most likely a combination of fiber flow and incorrect shimming that causes the porosity as it is only prevalent on the secondary weld.

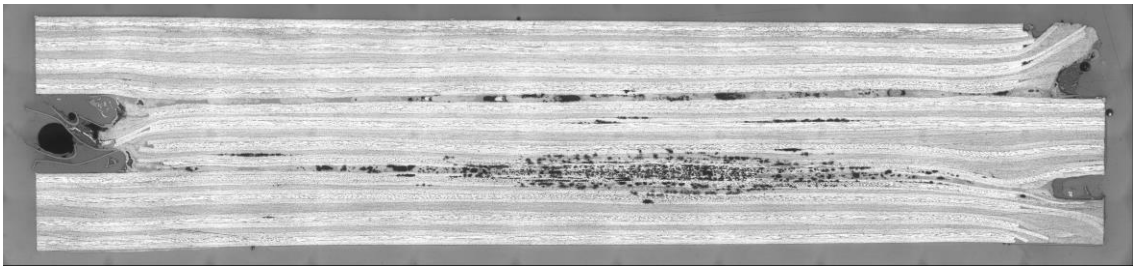

Figure 56 – Process F Photomicrograph Results

6.7 Process G Photomicrograph Results

This photomicrograph agrees with the NDI findings in Process G NDI Results. When fiber distortion is limited, the presence of porosity is mitigated. The same pressure application was used in this process as the other processes but a combination of weld temperature and shimming strategy mitigated the fiber distortion.

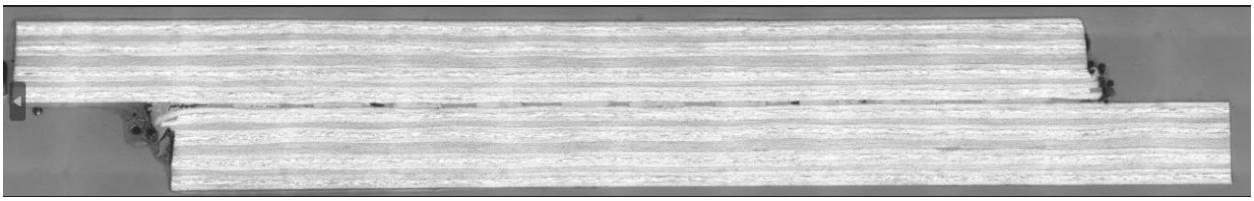

Figure 57 – Process G Photomicrograph

6.8 Process H Photomicrograph Results

This photomicrograph, like process G agrees with the fact that when fiber distortion is limited, porosity at the weld line is mitigated.

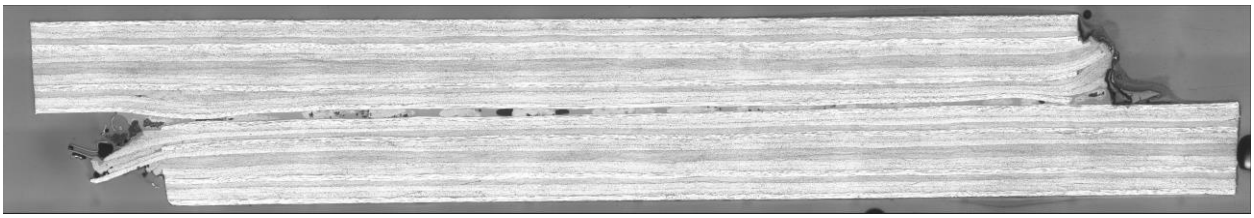

Figure 58 – Process H Photomicrograph

6.9 Process I Photomicrograph Results

This photomicrograph proves what was happening in the scans in the Process I NDI Results. The fiber distortion was only happening at the edges therefore the only porosity was at the edge instead of through the center of the specimen.

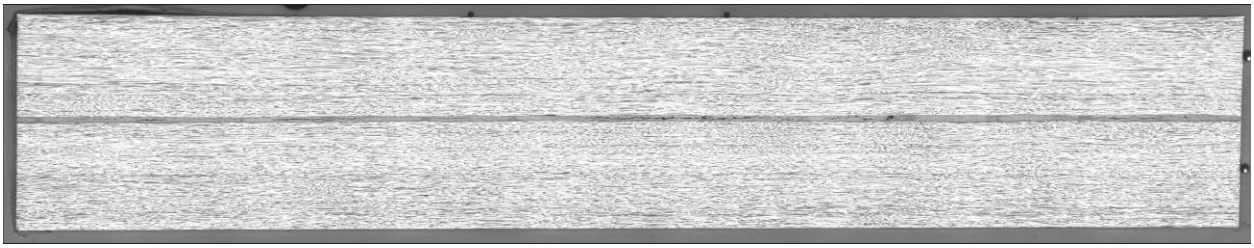

Figure 59 – Process I Photomicrograph

6.10 Process J Photomicrograph Results

This photomicrograph also agrees with the process I photomicrograph. Less fiber distortion at the edge means less porosity in the middle of the specimen.

7.0 Differential Scanning Calorimetry

DSC data is important in thermoplastic welding as it provides valuable insights into the thermal behavior and properties of the materials involved. This information aids in optimizing welding parameters, selecting compatible materials, and assessing the quality of weld joints, ultimately leading to improved welding processes and reliable final products.

7.1 Test Specimen Extraction Plan

DSC Specimens extracted from resistance welds were taken from the center of the 1” weld overlap. These DSC specimens were then ground down on either side to 0.04” (≈8 Plies) according to Figure 60.

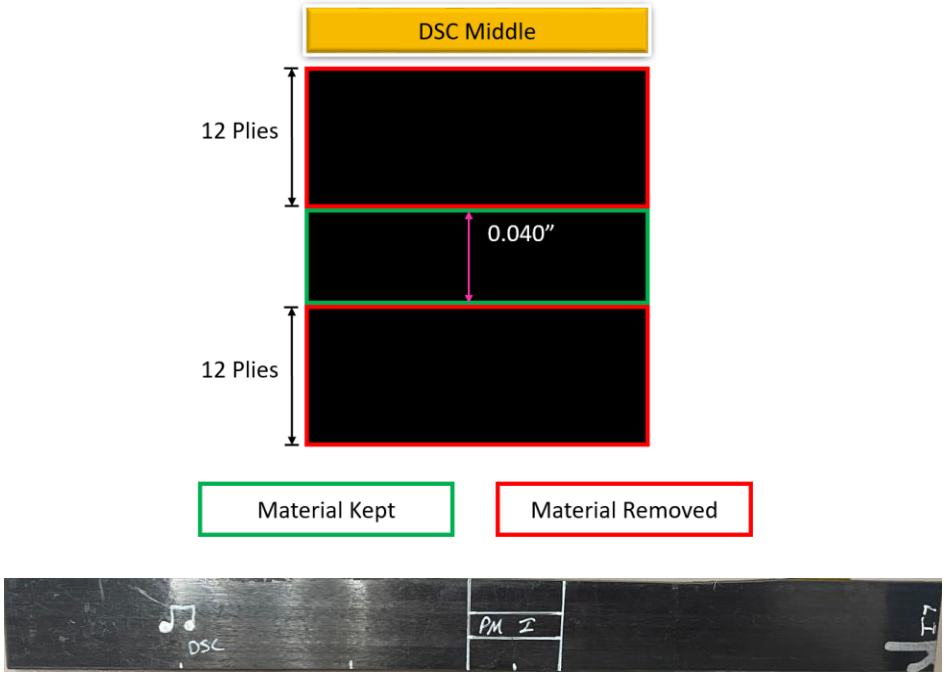

Figure 60 - DSC Specimen Extraction Plan

~~7.1~~7.2 PEI DSC Data Summary (Processes A-E)

PEI is primarily amorphous, meaning it lacks a regular and ordered arrangement of polymer chains. The amorphous structure of PEI limits the formation of crystalline regions within the material. Amorphous polymers have a random molecular arrangement, which hinders the formation of long-range ordered structures necessary for crystallinity. Which is why in the PEI results in Figure 61, there is only the glass transition temperature as there is no enthalpy of crystallization. Individual results can be seen in Appendix II – DSC Results.

NIAR Wichita State University National Institute for Aviation Research

DSC Results

NASA RW 80NSSC22PB269 DSC

Sample ID	Glass Transition Temperature T_g [°C]	T_g [°F]
NASA-RW-A	210.13	410.23
NASA-RW-B	211.22	412.20
NASA-RW-C	210.12	410.22
NASA-RW-D	204.62	400.32
NASA-RW-E	213.21	415.78

Test Parameters:

Instrument:	TA Instruments Discovery DSC 2500
Pan Type:	Tzero Aluminum
Test Method:	ASTM D3418
Ramp Rate:	10°C/min
Temperature Range:	50°C to 390°C
Atmosphere:	Nitrogen

Figure 61 – PEI DSC Results

~~7.2~~7.3 PEEK DSC Data Summary (Processes F-J)

Unlike PEI, PEEK has a higher tendency to form crystalline regions, especially in composite form. There are a couple factors that contribute to the higher crystallinity achievable in PEEK composites. The molecular structure of PEEK promotes the formation of crystalline regions. PEEK consists of repeating units of aromatic rings connected by ether and ketone linkages. The rigid and planar structure of the aromatic rings allows for close packing of polymer chains, facilitating the formation of ordered crystalline regions. PEEK is also more compatible with reinforcing materials (carbon fibers), and the presence of these materials can aid in the growth of crystalline regions. The results for the PEEK processes can be seen in Figure 62. The average degree of crystallinity achieved was 38.78%. Individual results can be seen in Appendix II – DSC Results.

NIAR Wichita State University National Institute for Aviation Research

DSC Results

NASA RW 80NSSC22PB269 DSC

Sample ID	Melting Peak Temperature T_m [°C]	T_m [°F]	Enthalpy of Melting ΔH_m [J/g]	Crystallization Peak Temperature T_c [°C]	T_c [°F]	Enthalpy of Crystallization ΔH_c [J/g]	Degree of Crystallinity %
NASA-RW-F	341.90	647.42	16.694	298.27	568.89	17.143	37.77
NASA-RW-G	340.59	645.06	17.064	296.00	564.80	17.963	38.61
NASA-RW-H	340.43	644.77	17.232	298.02	568.44	18.222	38.99
NASA-RW-I	340.50	644.90	17.601	292.35	558.23	16.874	39.82
NASA-RW-J	344.77	652.59	17.111	298.86	569.95	15.682	38.71

ΔH_f° (theoretical maximum heat of fusion for a fully crystalline sample) 130 J/g

Theoretical R_c (resin content) 34 %

Test Parameters:

Instrument: TA Instruments Discovery DSC 2500

Pan Type: Tzero Aluminum

Test Method: ASTM D3418

Ramp Rate: 10°C/min (Heat & Cool)

Temperature Range: 50°C to 380°C (Heating)

Atmosphere: Nitrogen

Figure 62 – PEEK DSC Results

8.0 Single Lap Shear Summary (ASTM D5868-01)

8.1 Shear Strength Summary

ASTM D5868-01 plays a crucial role in the assessment, characterization, and selection of continuous fiber-reinforced matrix composites. By providing a standardized method for measuring tensile properties, it helps ensure consistent and reliable evaluation of these materials, supporting quality control, design optimization, and performance prediction. The test setup for these specimens is shown in Figure 63.

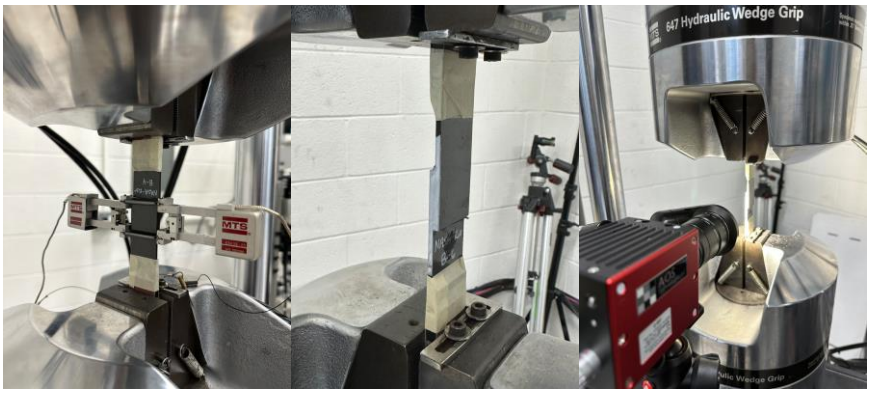

Figure 63 – Single Lap Shear Test Setup

It can be seen in Figure 64 that the highest apparent shear strength for the single lap shear testing was process H, which was the PEEK material with a 0 degree fiber orientation at the interface. The lowest strength was process K, which was the PEEK/PEI hybrid weld. It's also important to note that in each material, the specimen with a zero degree fiber orientation at the interface was stronger than the specimen with a 45 degree fiber orientation at the interface. Each process had a relatively low COV, all under 15%. This shows a robust weld process even with the presence of porosity in some of the welded specimens.

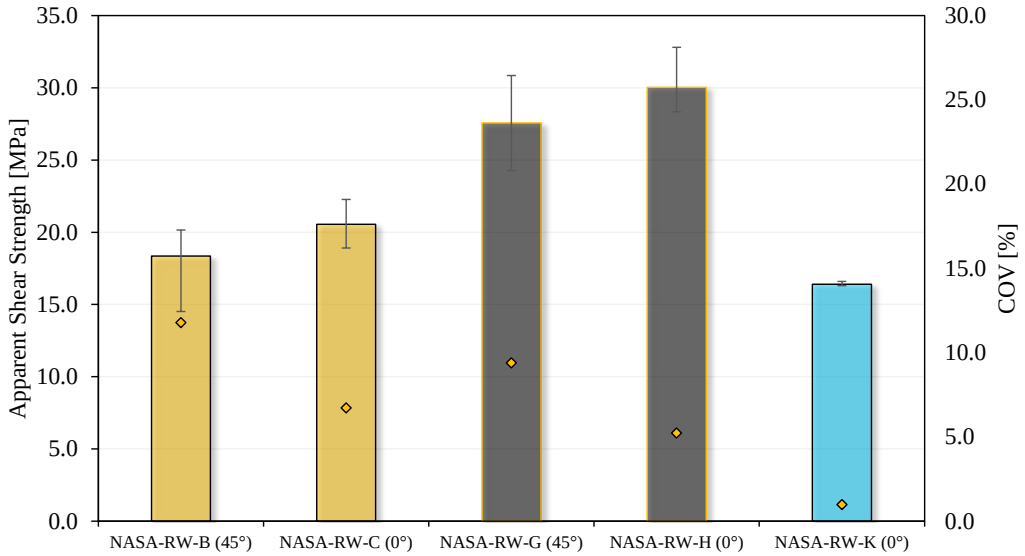

Figure 64 – Single Lap Shear Strength Summary

8.2 Failure Mode Images

Seen below in Figure 65 are the selected representative failure modes for the single lap shear testing. The specimens with a 45 degree fiber orientation at the interface show a substrate failure along the interface fiber angle. The specimens with a 0 degree fiber orientation at the interface also show a failure along the fiber angle. These specimens show a mixture of failure modes between substrate failure and failure at the carbon fiber heating element. All failure modes and failure loads can be found in Appendix III – Single Lap Shear Data.

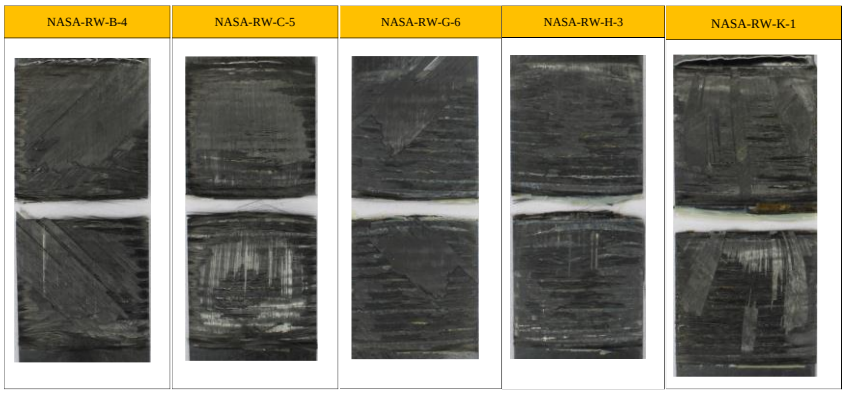

Figure 65 – Single Lap Shear Representative Failure Images

8.3 Crack Propagation Images

All single lap shear crack propagation images show a crack initiating at the edge of the weld and propagating through the center of the weld line. These images were captured at the exact time of failure.

8.3.1 Process B High Speed Images

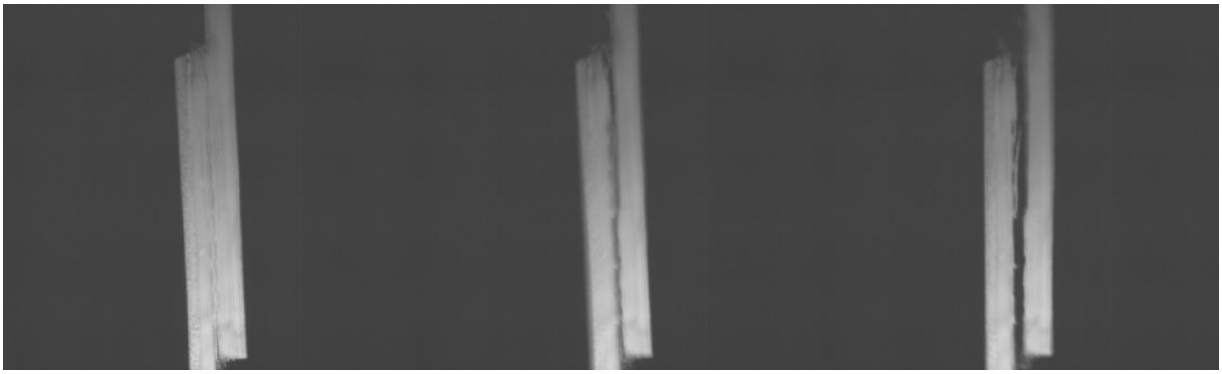

Figure 66 – Process B High Speed Images

8.3.2 Process C High Speed Images

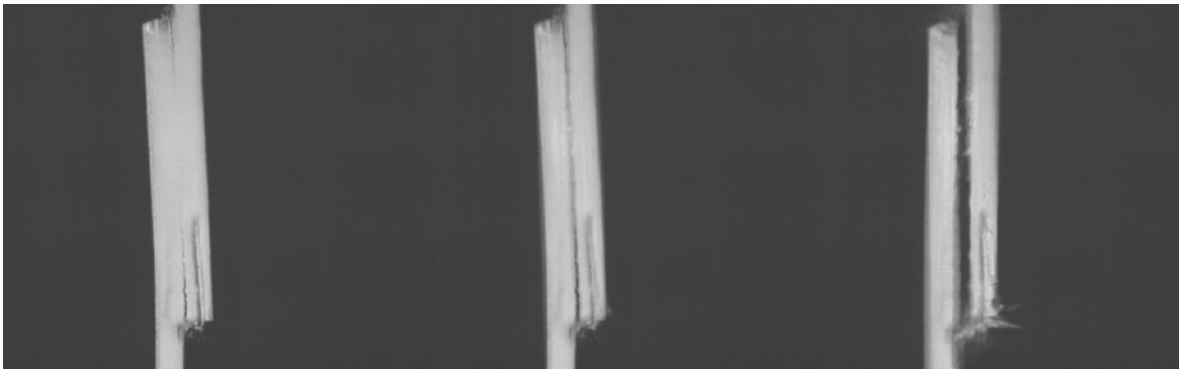

Figure 67 – Process C High Speed Images

8.3.3 Process G High Speed Images

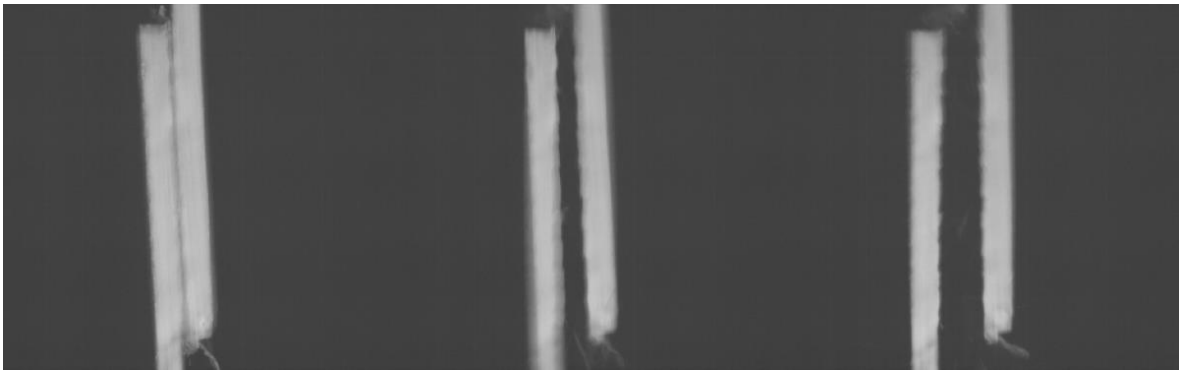

Figure 68 – Process G High Speed Images

8.3.4 Process H High Speed Images

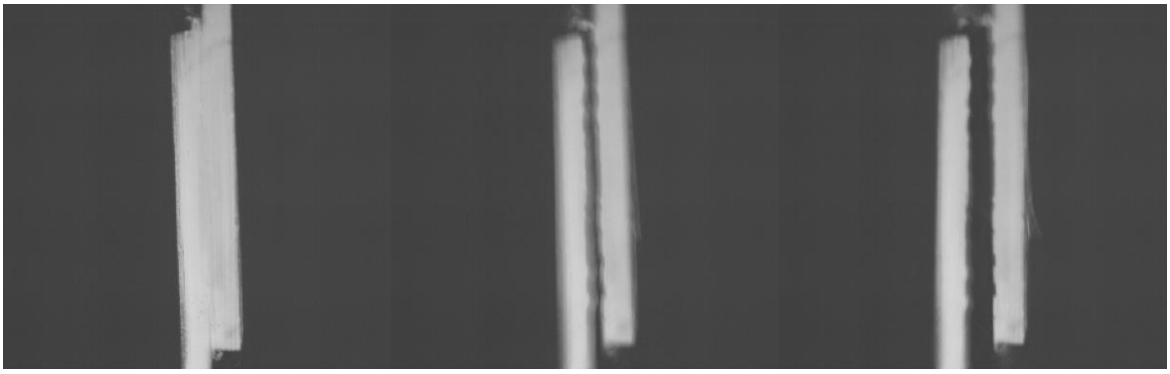

Figure 69 – Process H High Speed Images

8.3.5 Process K High Speed Images

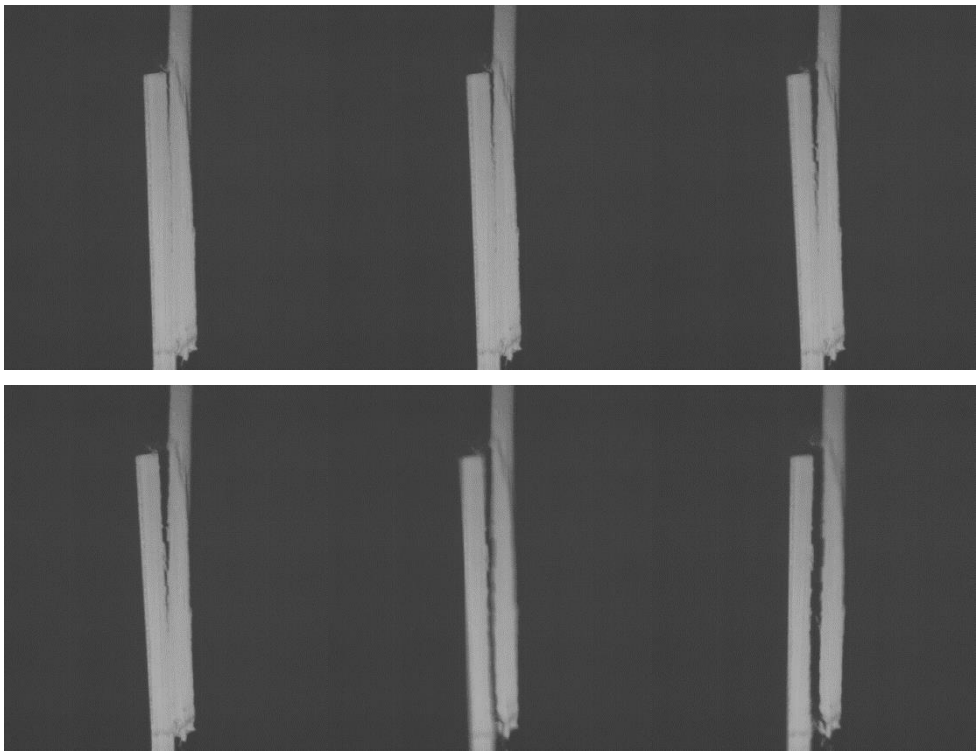

Figure 70. Process K High Speed Images

8.4 Load vs. Displacement

The load vs. displacement summary charts for PEI, PEEK, and PEEK/PEI single lap shear testing can be found in Figure 71, Figure 72, and Figure 73 respectively. These charts show a similar loading pattern for most of the specimens tested. Individual load vs. displacement charts and extensometer data can be found in Appendix III – Single Lap Shear Data.

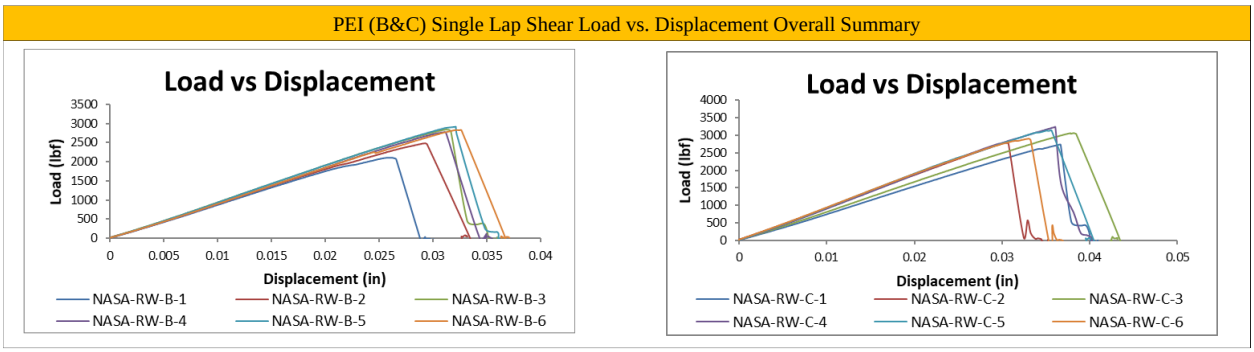

Figure 71 – PEI SLS Load vs. Displacement Summary

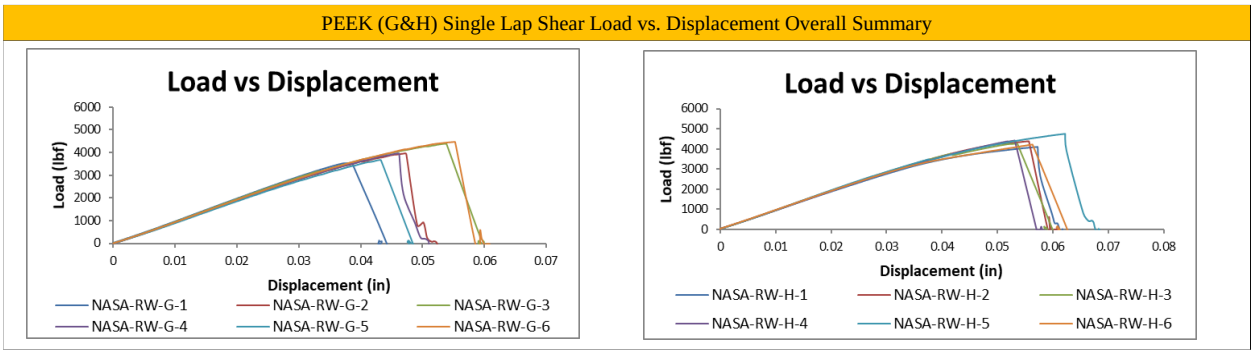

Figure 72 – PEEK SLS Load vs. Displacement Summary

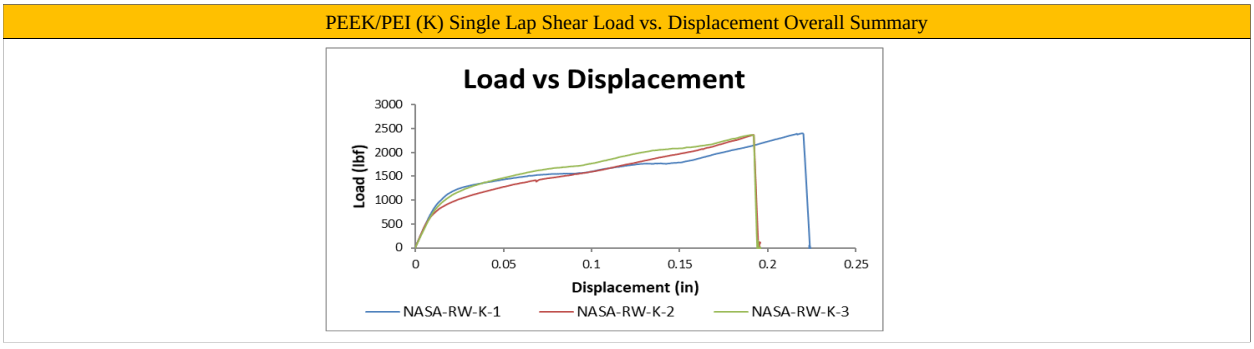

Figure 73 – PEEK/PEI SLS Load vs. Displacement Summary

9.0 Double Lap Shear Summary (ASTM D3528-96)

9.1 Shear Strength Summary

ASTM D3528-96 measures the strength of the bond between two thermoplastic components. It subjects the welded joint to an applied load in a shear mode, simulating the type of stress the joint may experience in real-world applications. By measuring the maximum force required to cause failure in the joint, it provides an indication of the joint strength and the effectiveness of the welding process. The test setup for double lap shear is shown in Figure 74.

Figure 74 – Double Lap Shear Test Setup

As shown in Figure 75 below, the PEEK material performed slightly higher than the PEI material although the PEEK material also exhibited a slightly higher COV percentage than the PEI material. Each COV percentage is below 20% which shows the robustness of the welding process even with some porosity present at the weld line.

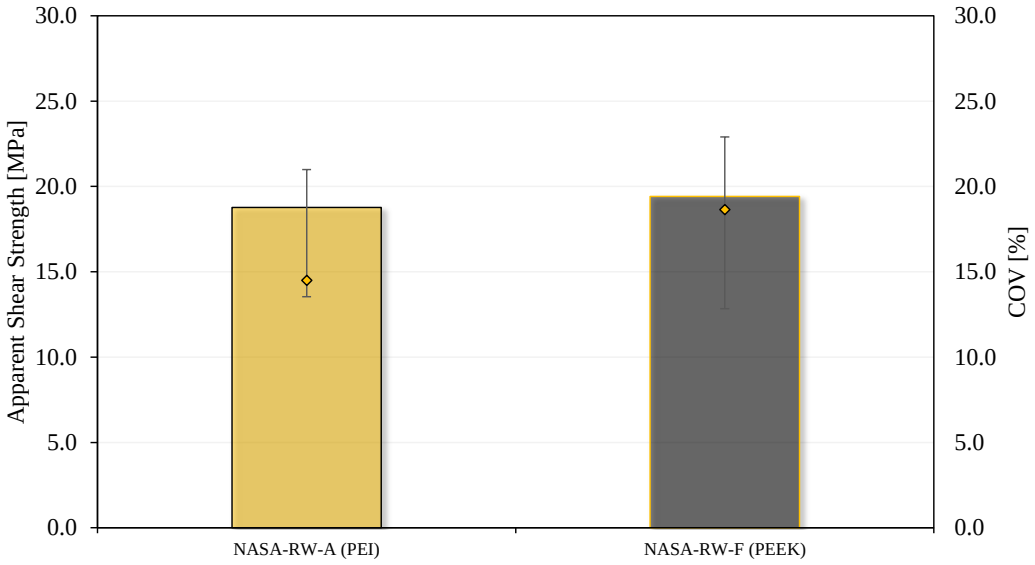

Figure 75 – Double Lap Shear Strength Summary

9.2 Failure Mode Images

Seen below in Figure 76 are the selected representative failure modes for the double lap shear testing. These specimens have a 45 degree fiber orientation at the interface and show a substrate failure along the interface fiber angle. These specimens also show a mixture of failure modes between substrate failure and failure at the carbon fiber heating element. All failure modes and failure loads can be found in Appendix IV – Double Lap Shear Data.

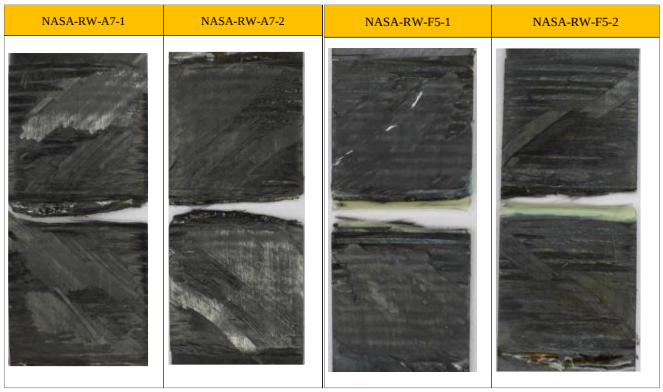

Figure 76 – Double Lap Shear Representative Failure Images

9.3 Crack Propagation Images

The double lap shear coupons also display a crack propagation initiating from the edge of one of the welds. It was unclear if it was the same weld (primary or secondary) every time, but it would always initiate from the edge and propagate through the center of the weld.

9.3.1 Process A High Speed Images

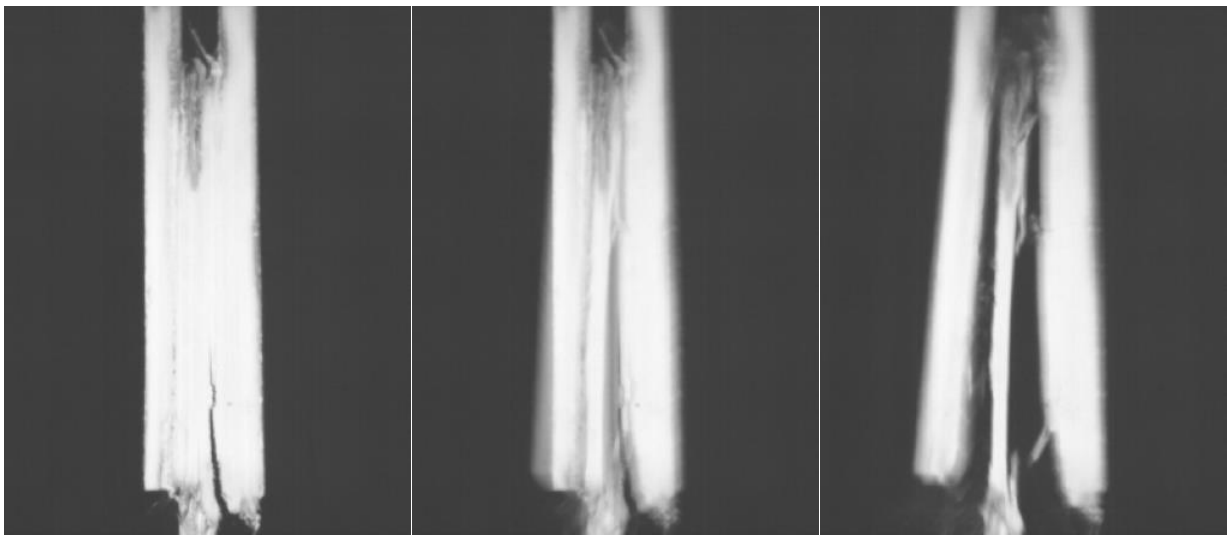

Figure 77 – Process A High Speed Images

9.3.2 Process F High Speed Images

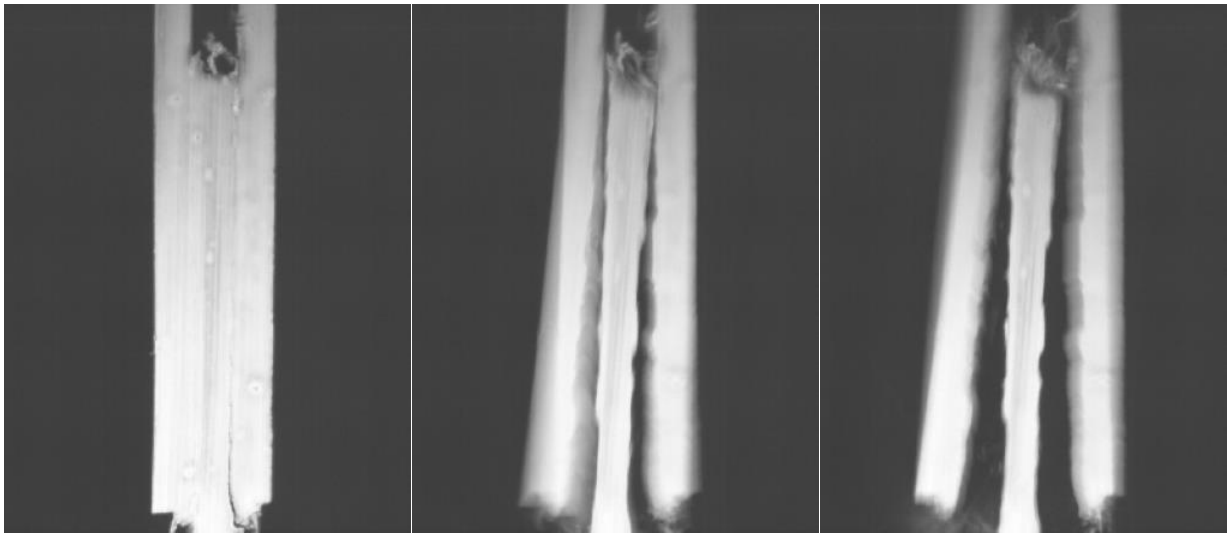

Figure 78 – Process F High Speed Images

9.4 Load vs. Displacement

The load vs. displacement summary charts for PEI and PEEK double lap shear testing can be found in Figure 79. These charts show a similar loading pattern for most of the specimens tested. Individual load vs. displacement charts and extensometer data can be found in Appendix IV – Double Lap Shear Data.

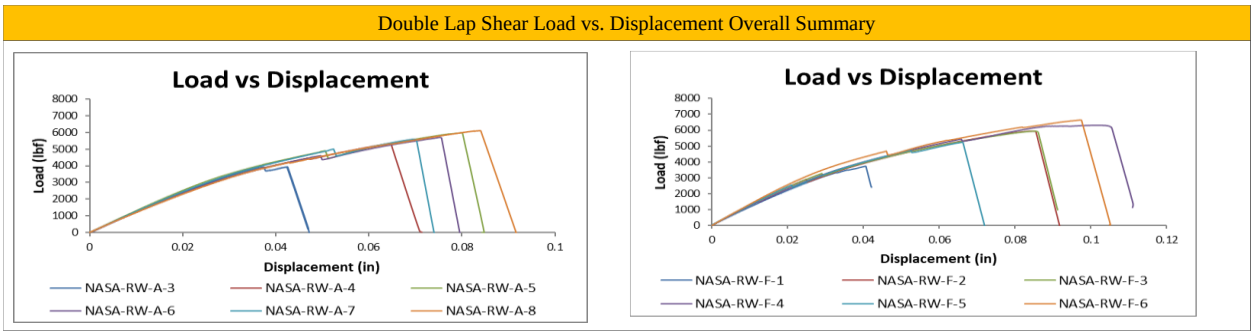

Figure 79 – PEI and PEEK DLS Load vs. Displacement Summary

10.0 Mode I Summary (ASTM D5528-01)

10.1 Mode I Fracture Toughness Summary

ASTM D5528-01 helps assess the resistance of welded joints to crack propagation under tensile or opening loading conditions. Mode I testing plays a crucial role in the evaluation, quality control, performance prediction, and optimization of thermoplastic welds. As can be seen in Figure 80, the pre-crack G_{IC} value was similar between PEI and PEEK but the actual G_{IC} value showed the PEEK material to be higher than the PEI material. The PEI material showed a much higher COV around 70% whereas the PEEK material was less than half of that at a COV of around 30%. This was most likely due to more porosity being present in the PEI material than in the PEEK material, causing unstable crack propagation and a lower mode I fracture toughness.

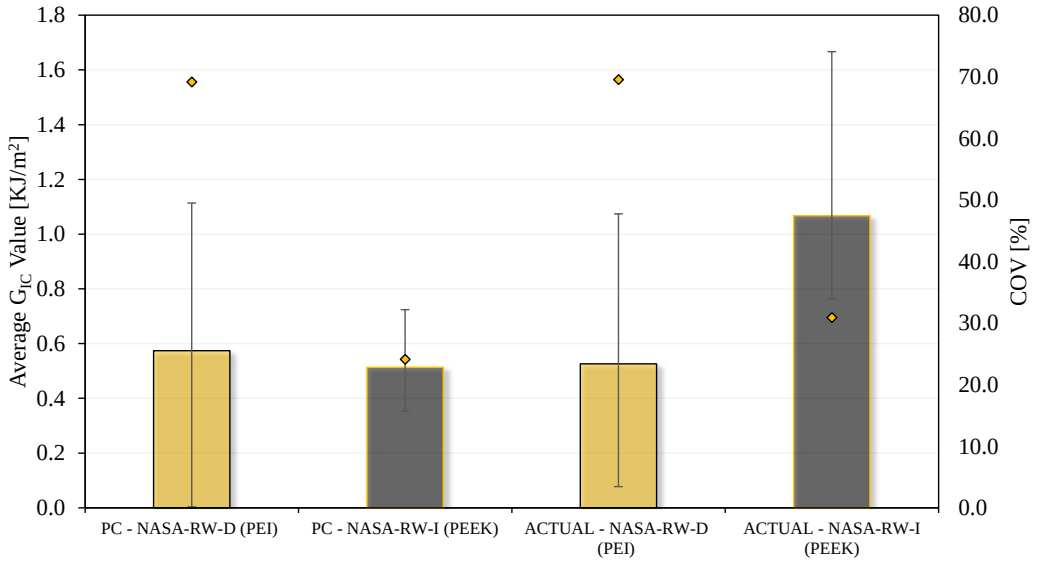

Figure 80 – Average G_{IC} Value Summary

10.2 Failure Mode Images

Seen below in Figure 81 are the selected representative failure modes for the mode I testing. These specimens have a zero degree fiber orientation at the interface and show a substrate failure along the interface fiber angle. These specimens show a mixture of failure modes between substrate failure and failure at the carbon fiber heating element but mainly at the heating element because of the pre-crack present in the weld line. All failure modes and failure loads can be found in Appendix V – Mode I Data.

Figure 81 – Mode I Representative Failure Mode Images

10.3 Load vs. Displacement

The load vs. displacement summary charts for PEI and PEEK mode I testing can be found in Figure 82, and Figure 83 respectively. These charts show a similar loading pattern for most of the specimens tested. Individual load vs. displacement charts and can be found in Appendix V – Mode I Data.

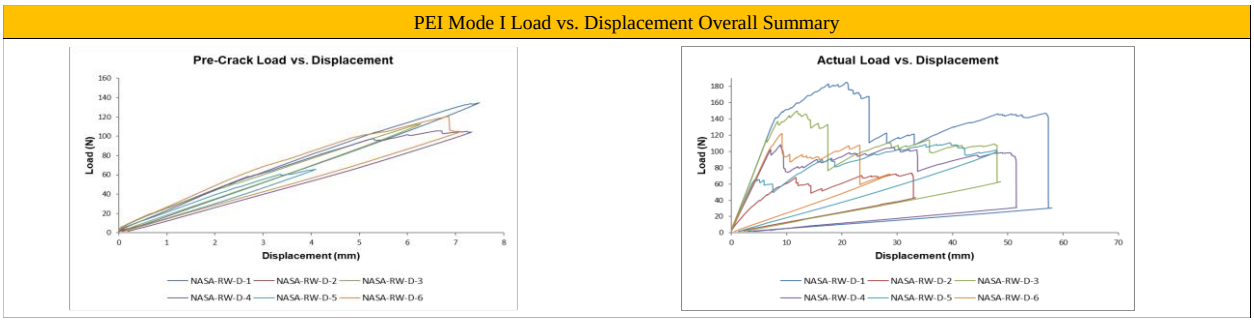

Figure 82 – PEI Mode I Load vs. Displacement Summary

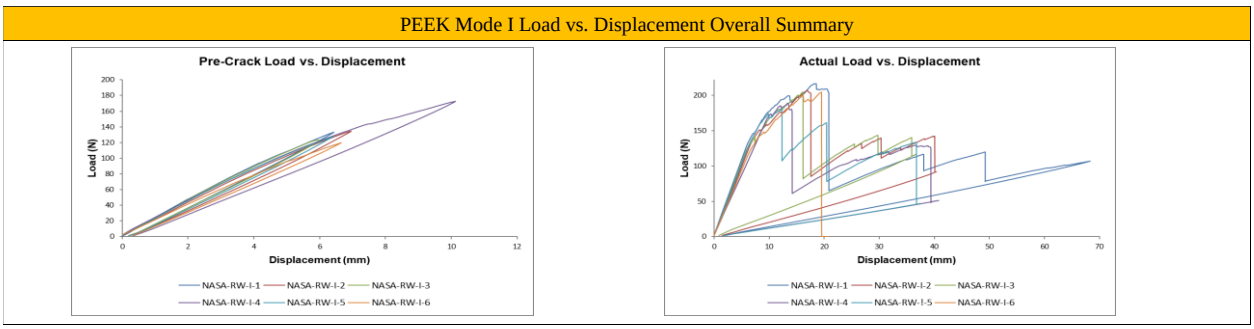

Figure 83 – PEEK Mode I Load vs. Displacement Summary

11.0 Mode II Summary (ASTM D7905)

11.1 Mode II Fracture Toughness Summary

ASTM D7905 specifically focuses on the shear resistance of the welded joint. It measures the ability of the material to withstand sliding forces that can occur parallel to the plane of the weld interface. Shear stresses can arise due to different factors, such as differential cooling rates, residual stresses, or external loads applied to the joint. As can be seen in Figure 84 below, the PEEK material had a higher GIIC value than the PEI material in both the Non Pre-Crack and Pre-Crack scenarios. Most of the testing had a COV at or less than 30% except for the PEI Non Pre-Crack which had a COV of around 50%. This makes sense as the PEI material showed more porosity then the PEEK material in the C-Scan data and photomicrographs which would ultimately lead to an unstable crack growth and a lower mode two fracture toughness.

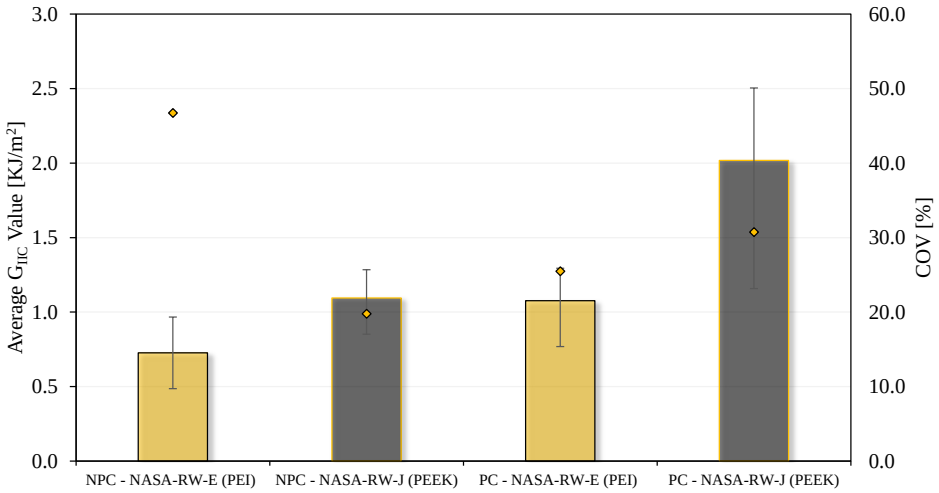

Figure 84 - Average G_{IIC} Value Summary

11.2 Failure Mode Images

Seen below in are the selected representative failure modes for the mode II testing. These specimens have a zero degree fiber orientation at the interface and show a substrate failure along the interface fiber angle. These specimens show a mixture of failure modes between substrate failure and failure at the carbon fiber heating element but mainly at the heating element because of the pre-crack present in the weld line. All failure modes and failure loads can be found in Appendix VI – Mode II Data.

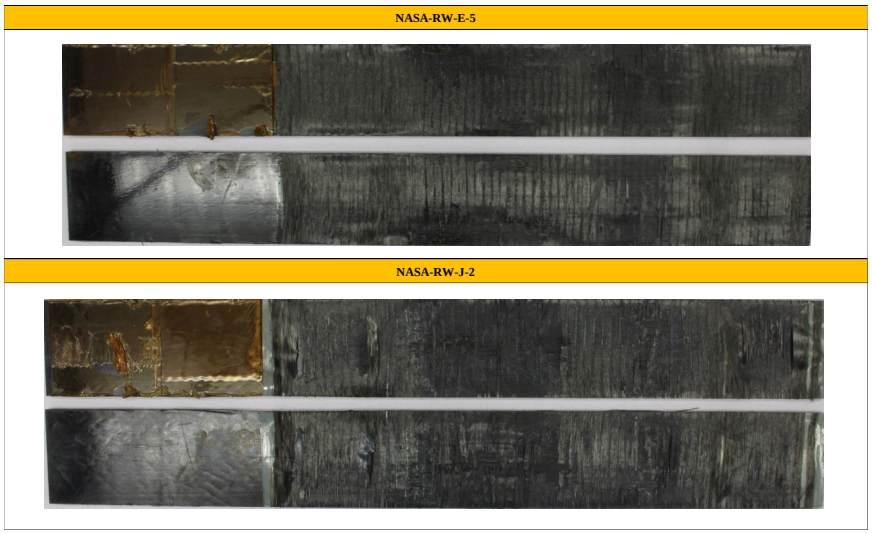

Figure 85 – Mode II Representative Failure Mode Images

11.3 Load vs. Displacement

The load vs. displacement summary charts for PEI and PEEK mode II testing can be found in Figure 86, and Figure 87 respectively. These charts show a similar loading pattern for most of the specimens tested. Individual load vs. displacement charts and can be found in Appendix VI – Mode II Data.

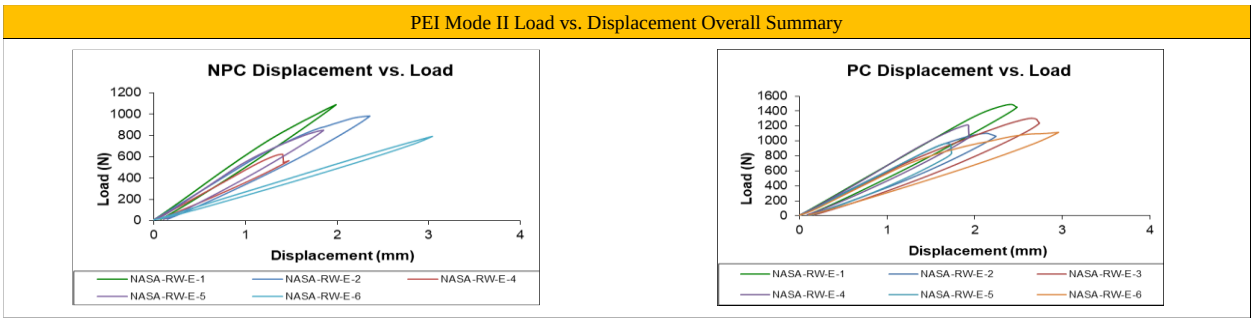

Figure 86 – PEI Mode II Load vs. Displacement Summary

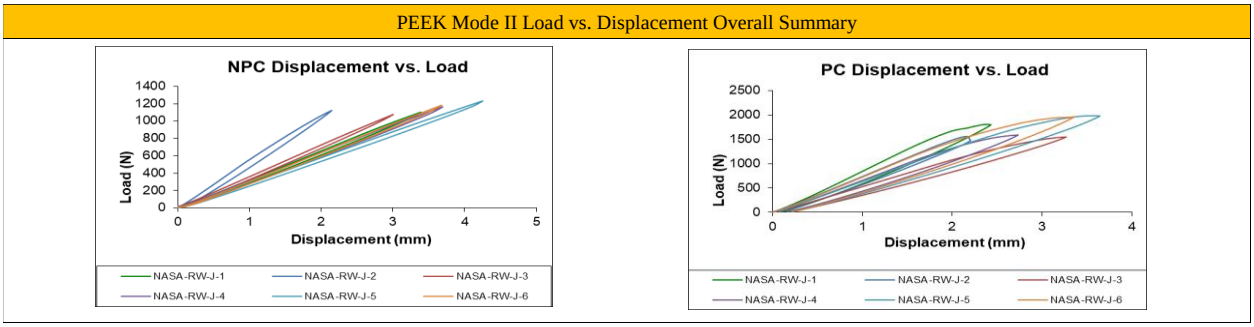

Figure 87 – PEEK Mode II Load vs. Displacement Summary

12.0 Conclusion – Recommendations

Through the manufacturing and testing of resistance welded PEI and PEEK coupons there are a few main takeaways. It is possible to use a Carbon Fiber Heating Element to weld thermoplastic composite together but it would most likely benefit the joint strength if a thinner heating element was used, as the failure almost always happens as the heating element instead of the substrate. It is important to weld all the way to the edge of the substrate as the failure always initiates at the edge as seen in the high speed images, although mitigation of fiber distortion at the edge must occur to prevent porosity at the weld line as we saw in the photomicrograph results. It is possible to weld a PEI composite and PEEK composite together although more research may need to be completed in order to find the optimal processing temperature for joint strength.

Overall, this research has showed that using a carbon fiber heating element in thermoplastic welding is a viable option but more research on mitigating the fiber distortion and porosity must take place in order to lower the COV seen in some of the physical testing. Studies must also be completed in order to improve the consistency of sequential welding and the overall speed as this technique would most likely be used to scale up to weld larger structures. It' possible for future research to look into different types of carbon fiber heating elements to see if higher strengths are achieved and lower COV percentages are present.

13.0 Appendix I – Welding Metrics

13.1 Process D Welding Metrics

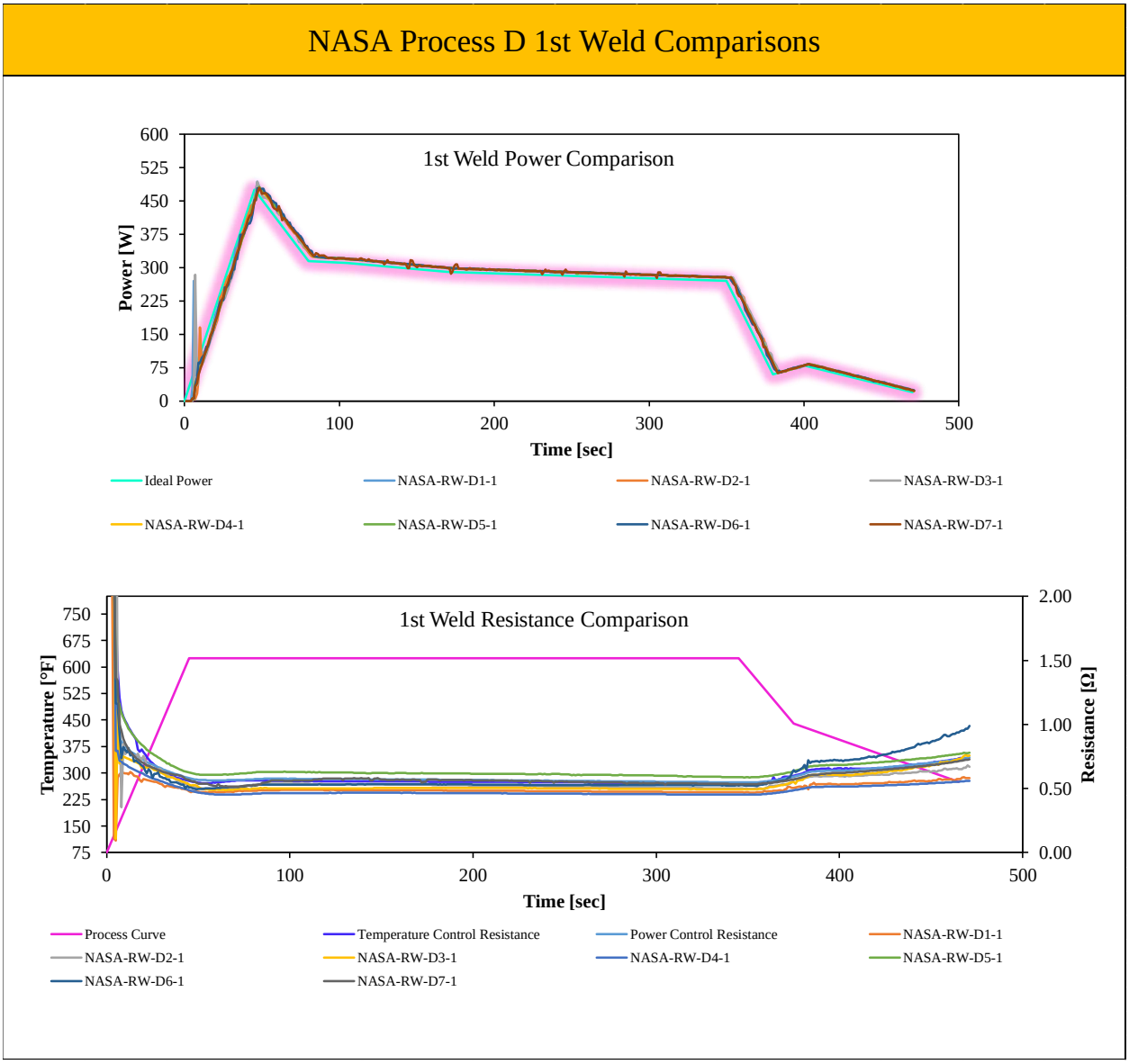

Figure 88 – Process D 1st Weld Comparison

NASA Process D 2nd Weld Comparisons

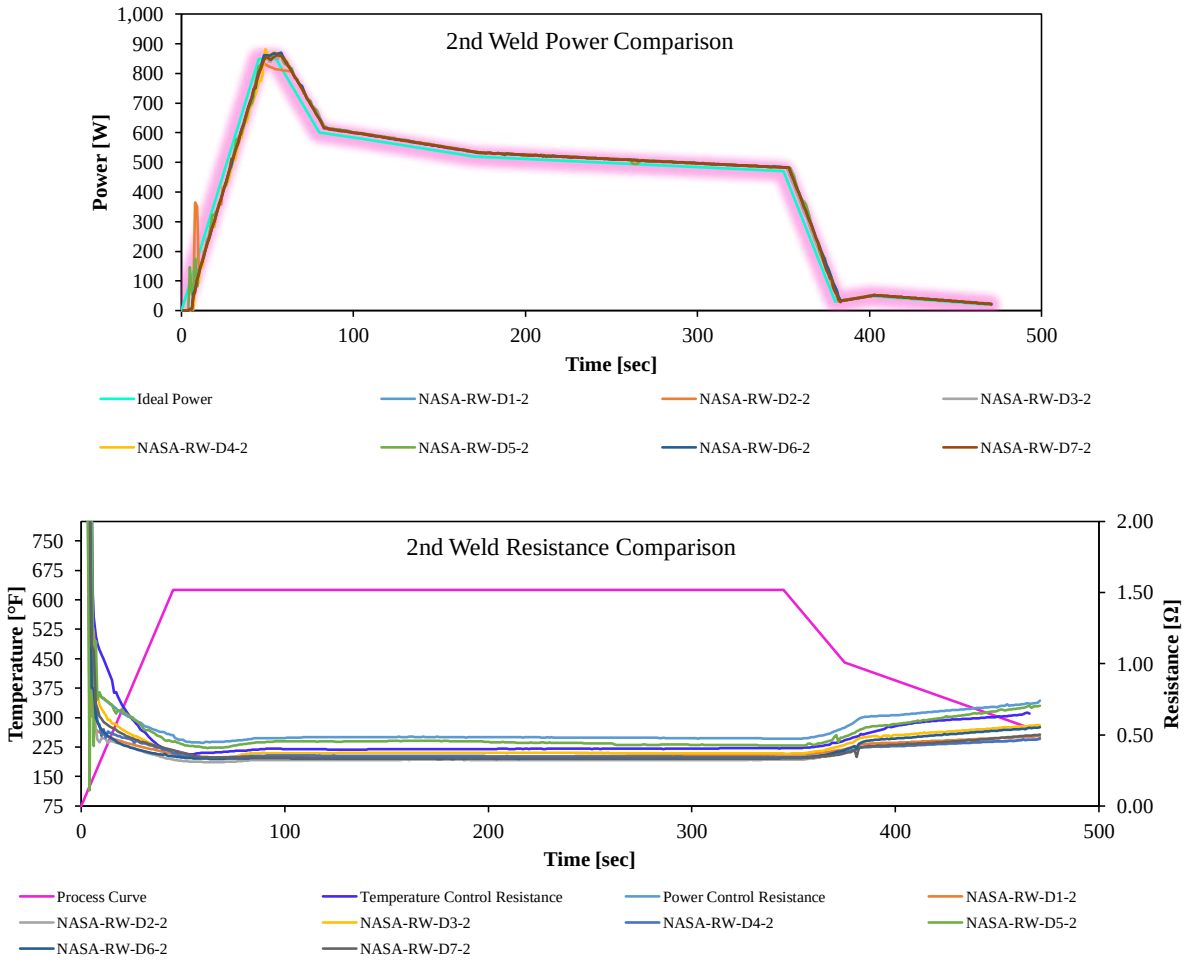

Figure 89 – Process D 2nd Weld Comparison

NASA Process D 3rd Weld Comparisons

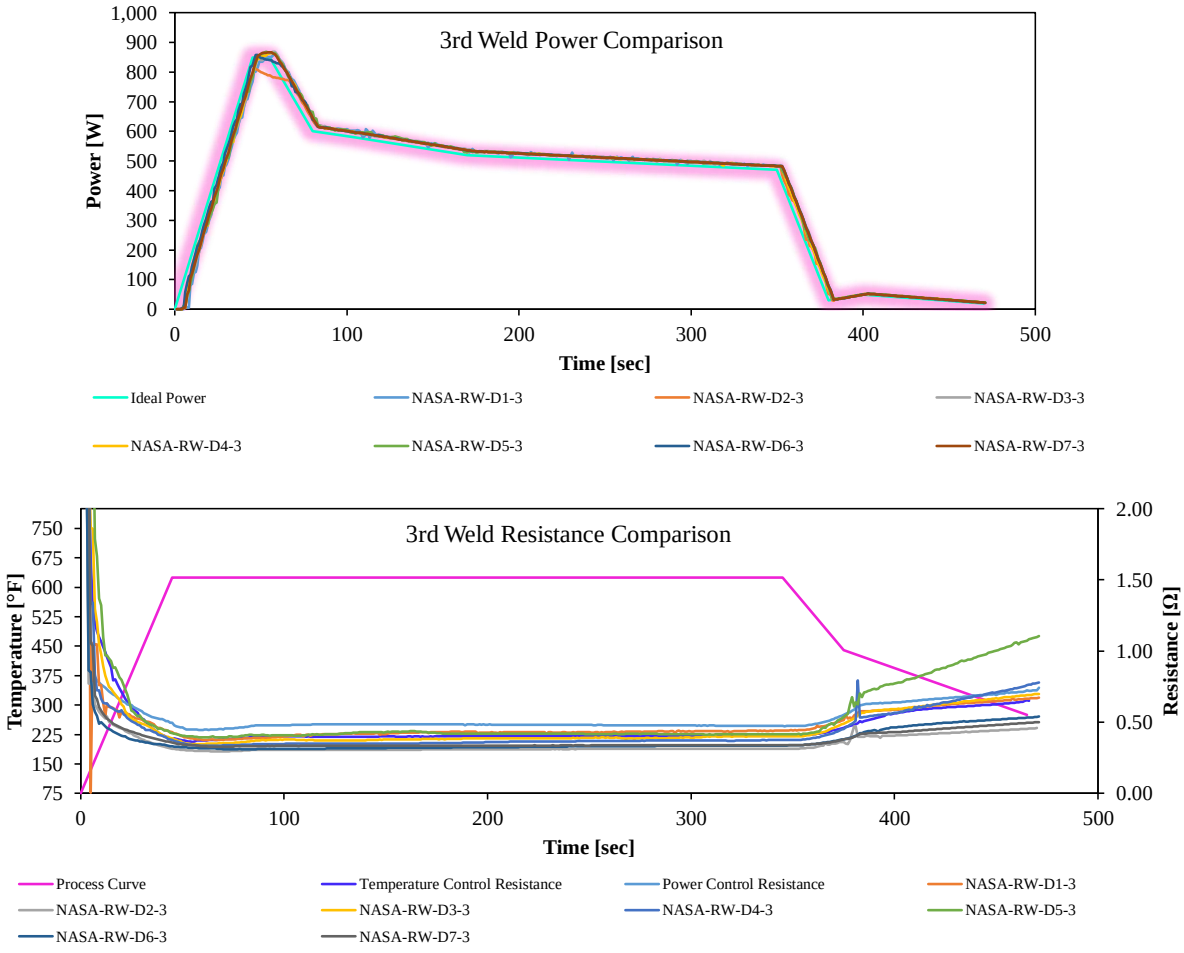

Figure 90 – Process D 3rd Weld Comparison

NASA Process D 4th Weld Comparisons

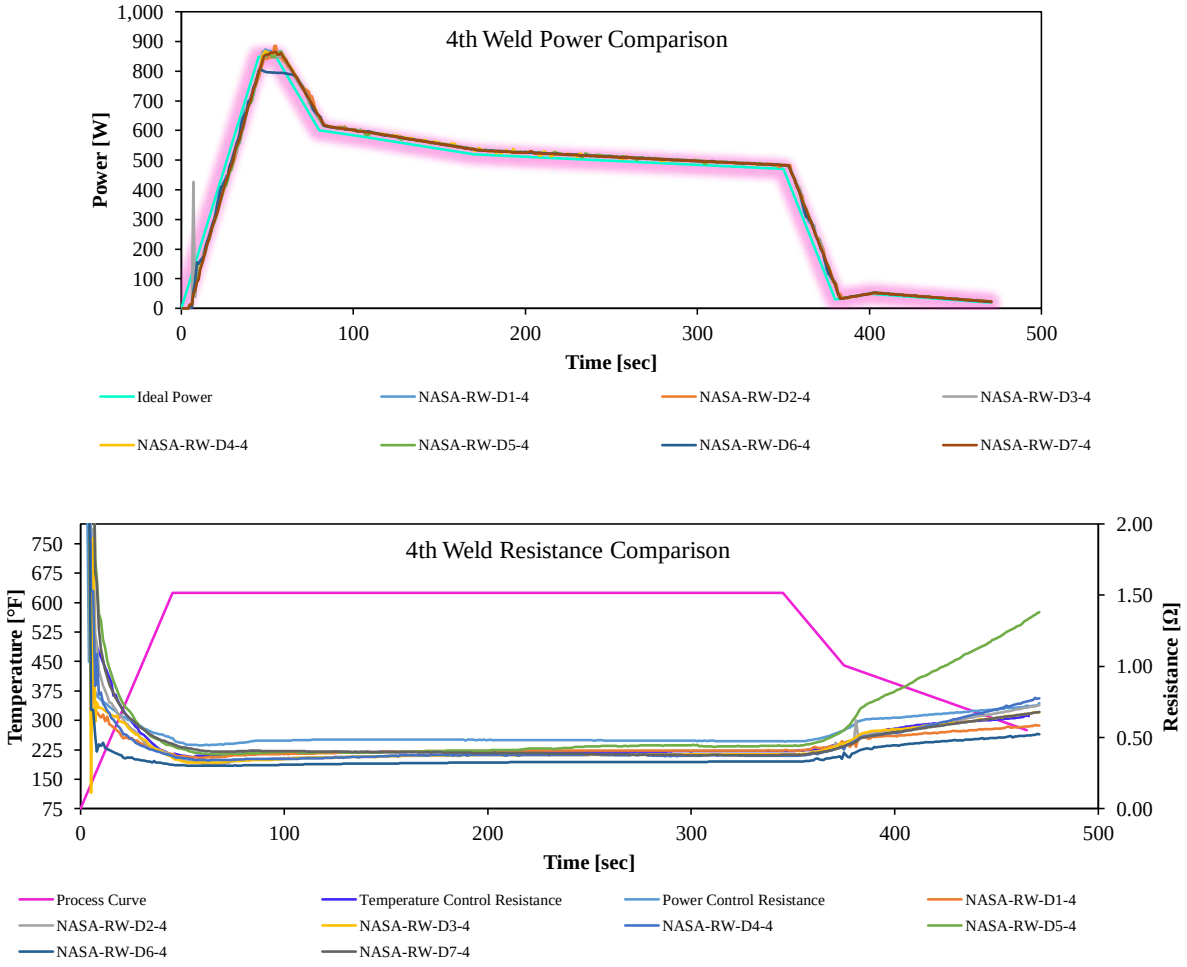

Figure 91 – Process D 4th Weld Comparison

NASA Process D 5th Weld Comparisons

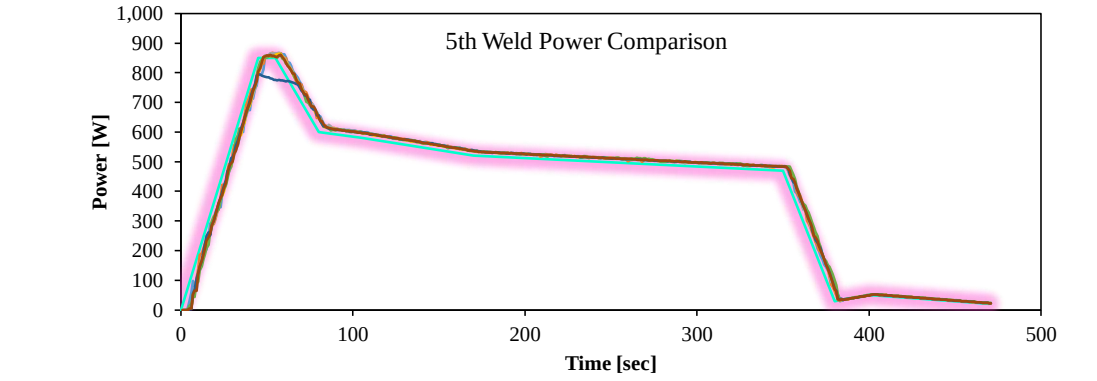

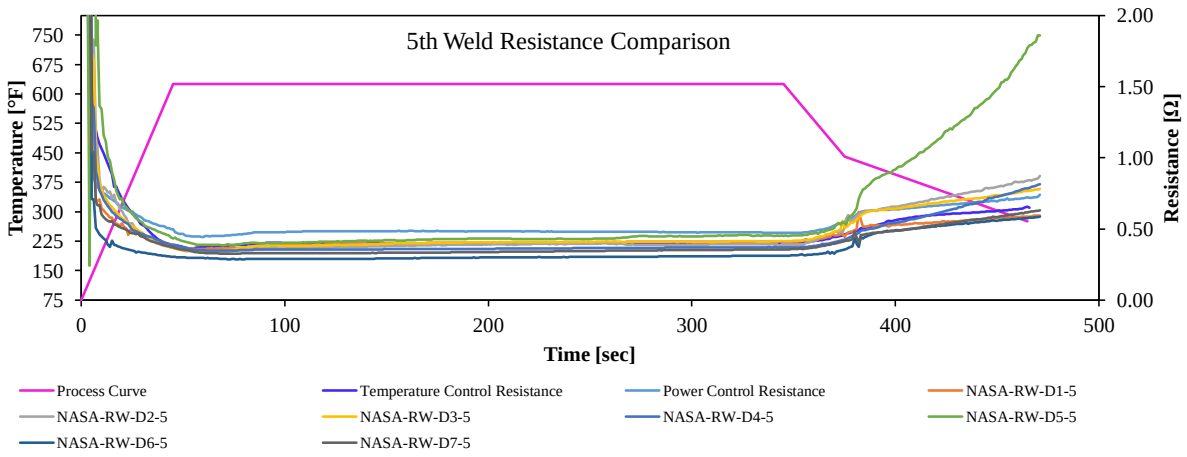

Figure 92 – Process D 5th Weld Comparison

NASA Process D 6th Weld Comparisons

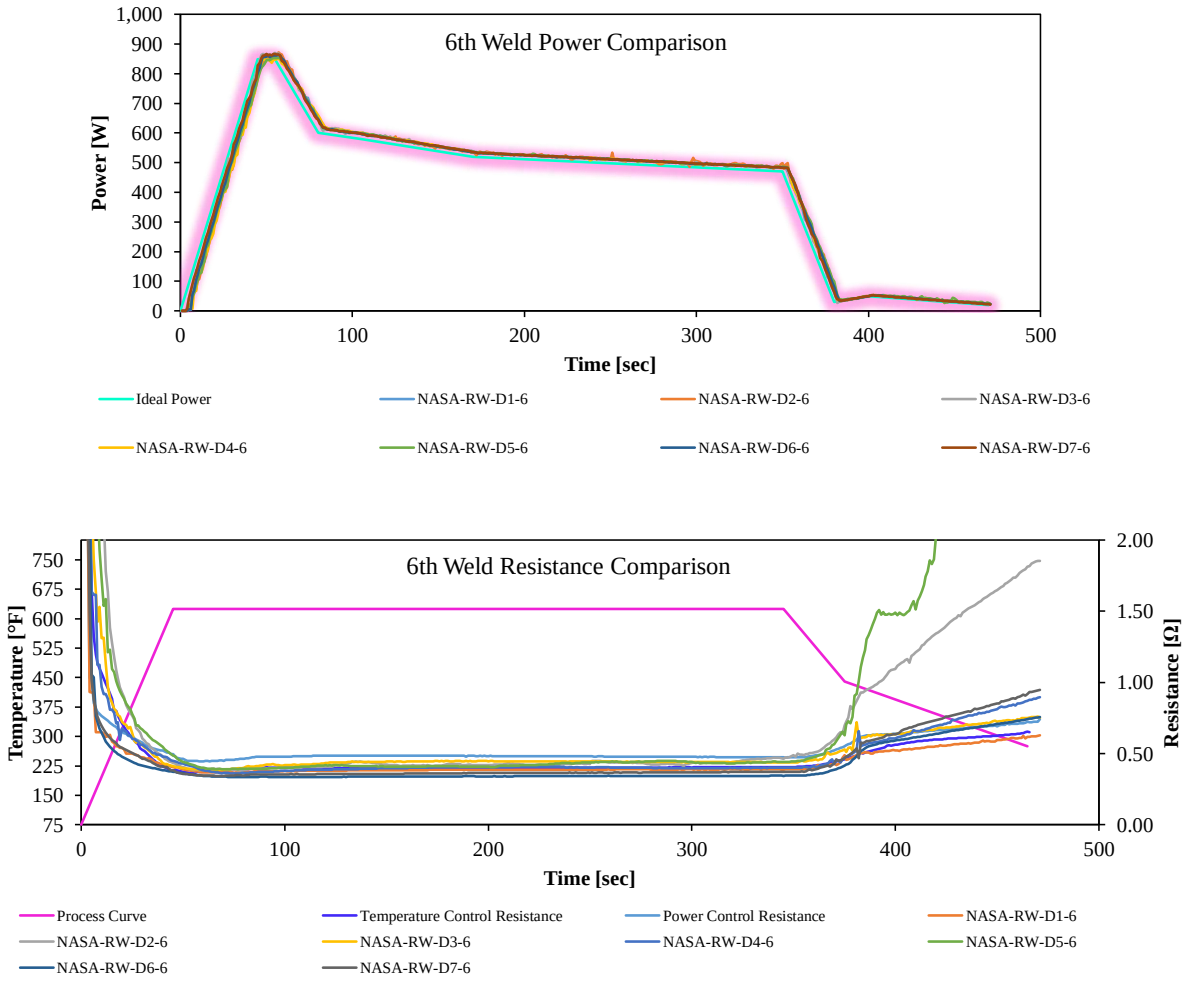

Figure 93 – Process D 5th Weld Comparison

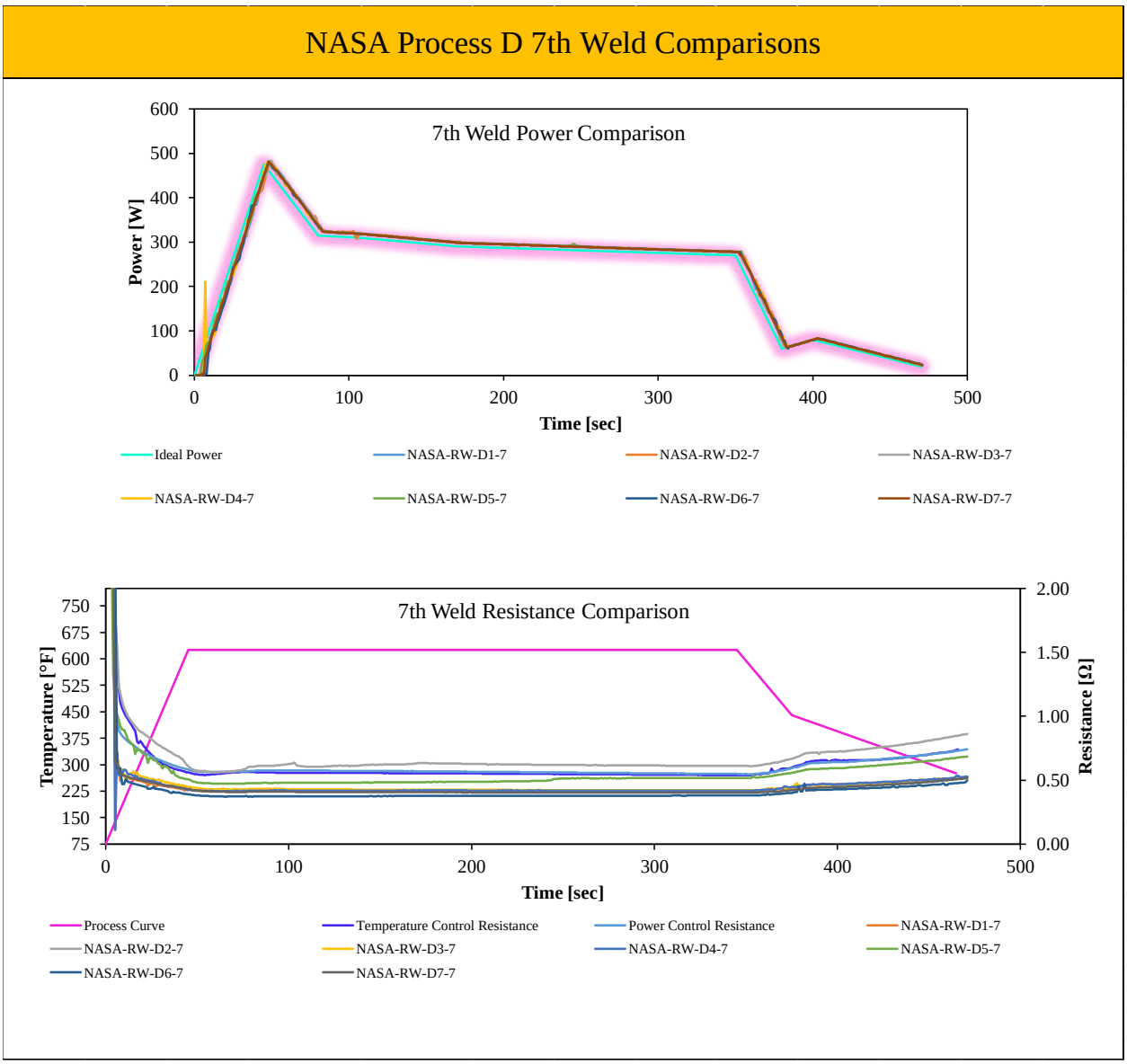

Figure 94 – Process D 7th Weld Comparison

13.2 Process E Welding Metrics

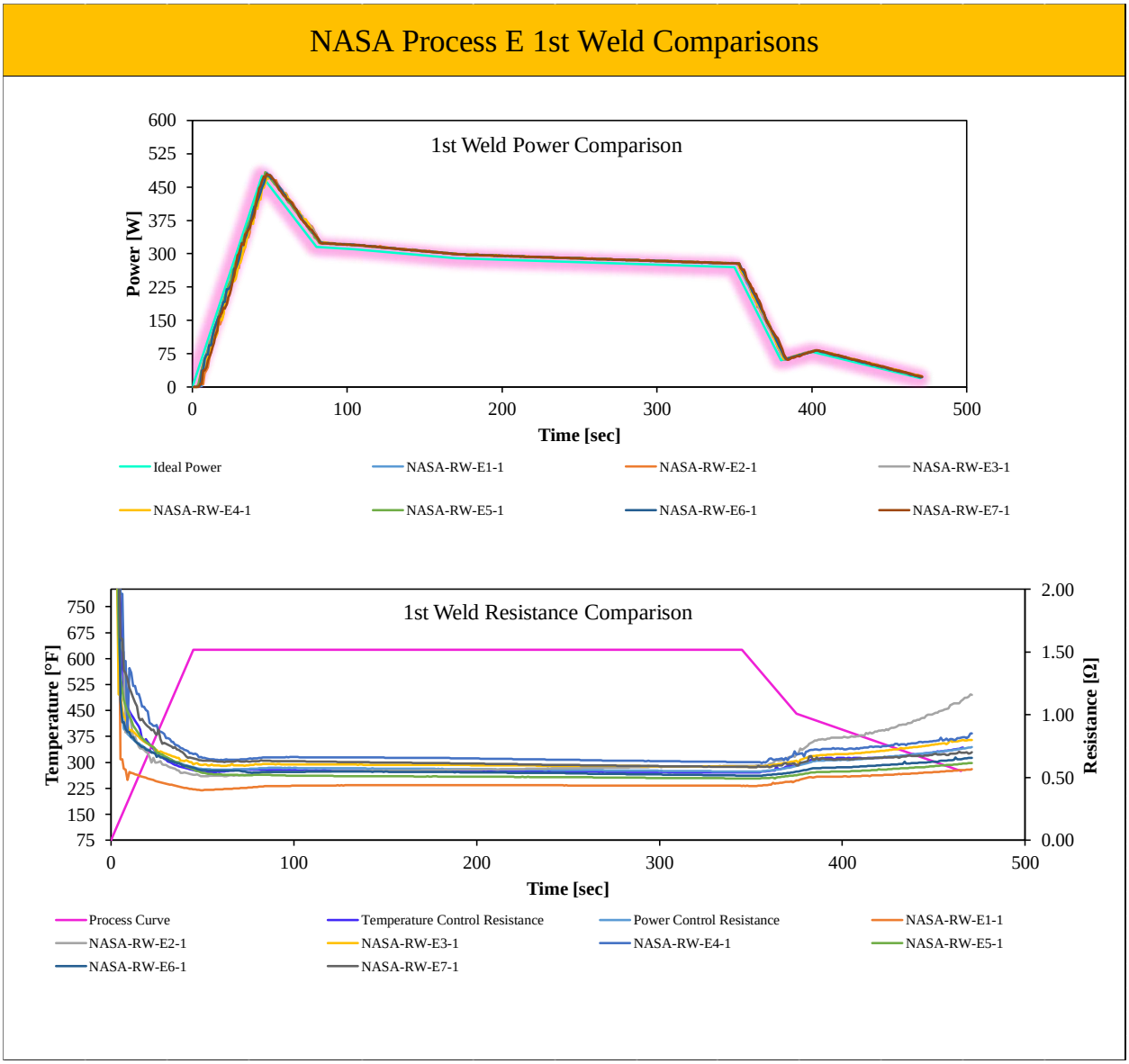

Figure 95 – Process E 1st Weld Comparison

NASA Process E 2nd Weld Comparisons

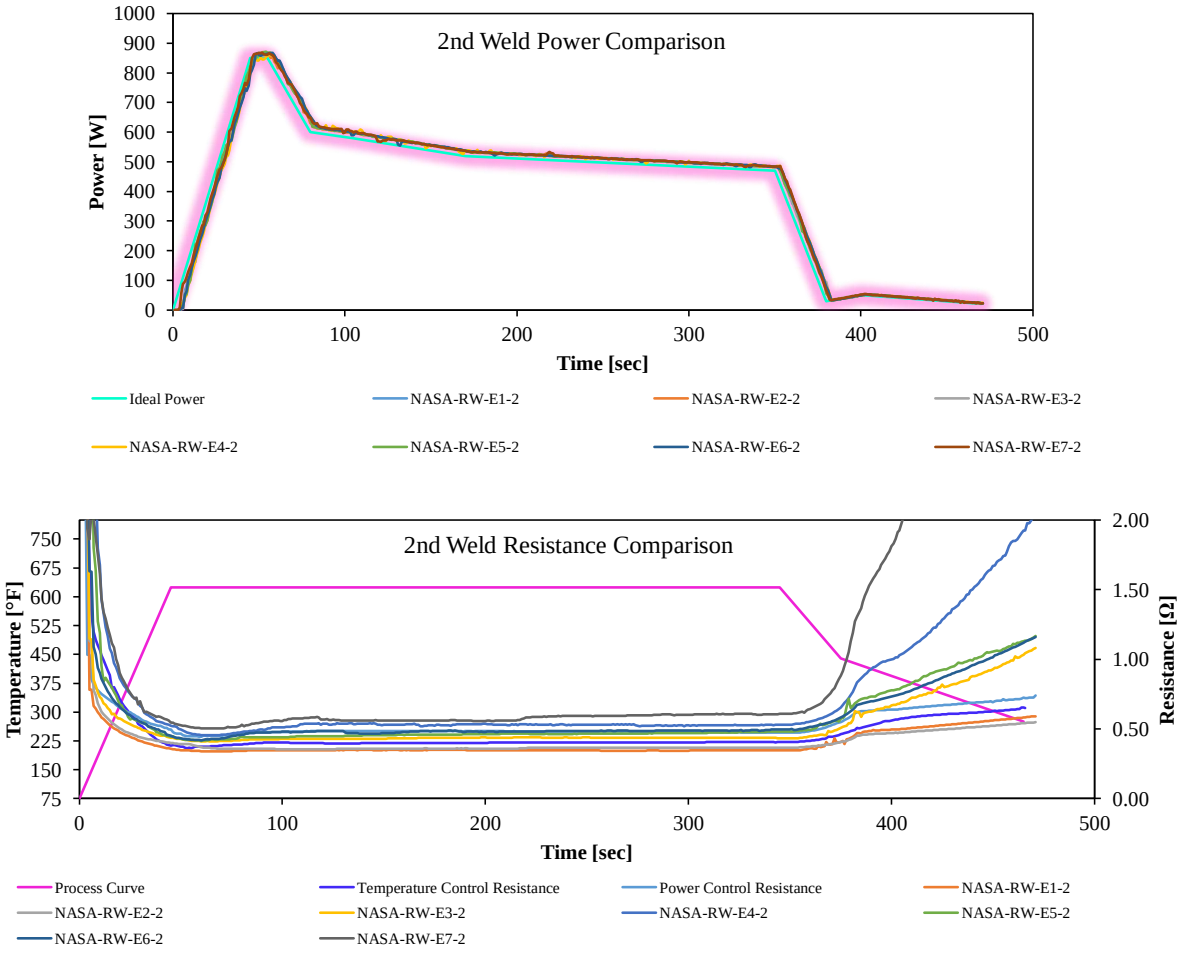

Figure 96 – Process E 2nd Weld Comparison

NASA Process E 3rd Weld Comparisons

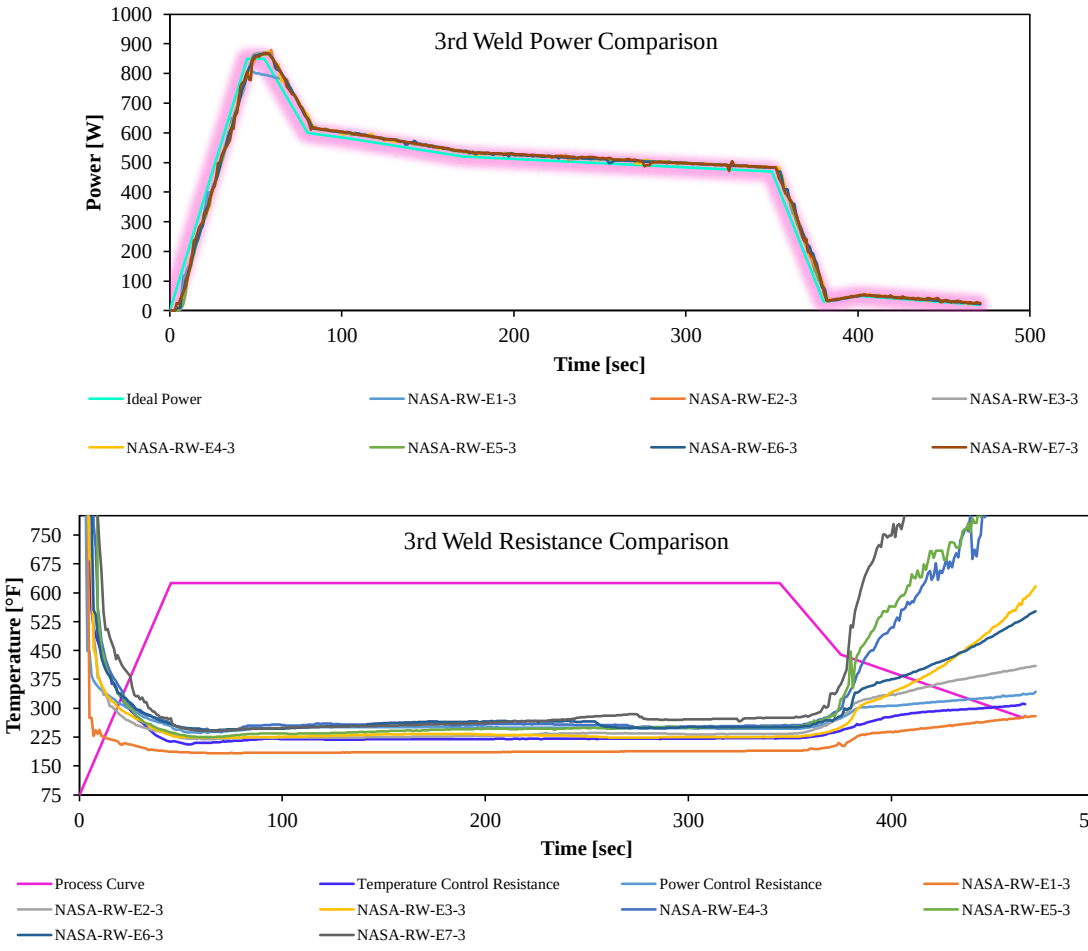

Figure 97 – Process E 3rd Weld Comparison

NASA Process E 4th Weld Comparisons

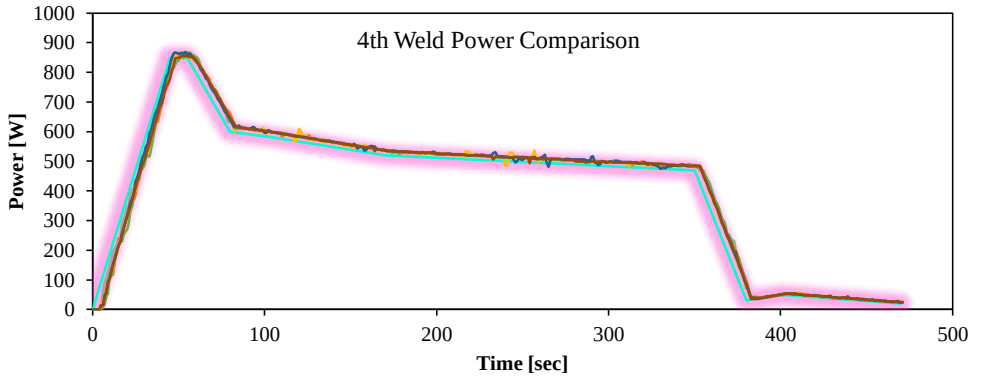

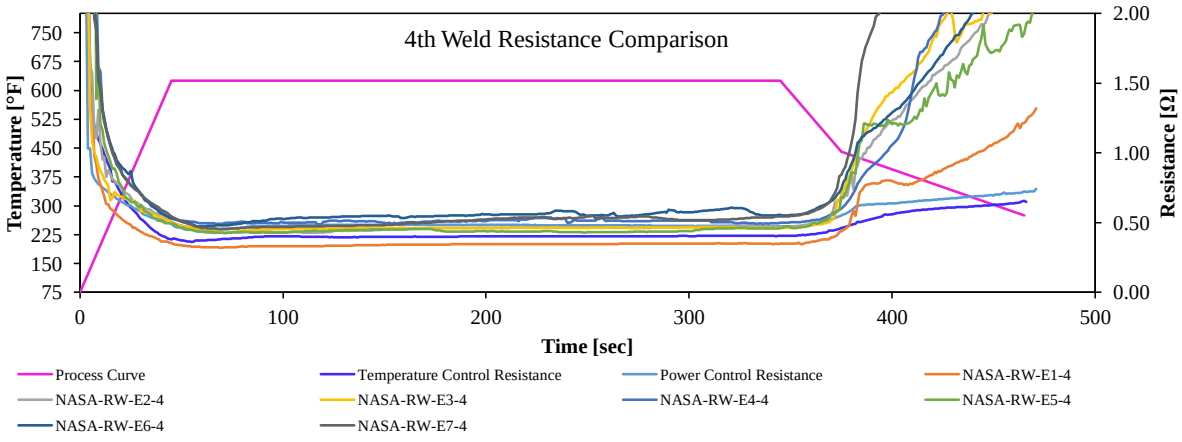

Figure 98 – Process E 4th Weld Comparison

NASA Process E 5th Weld Comparisons

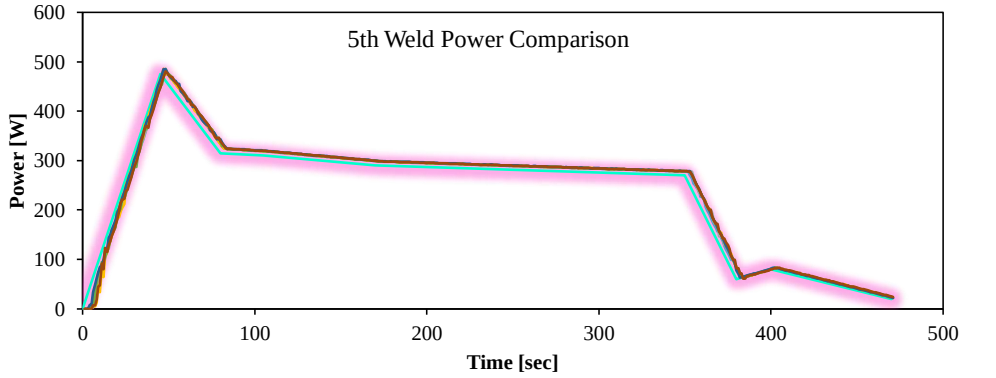

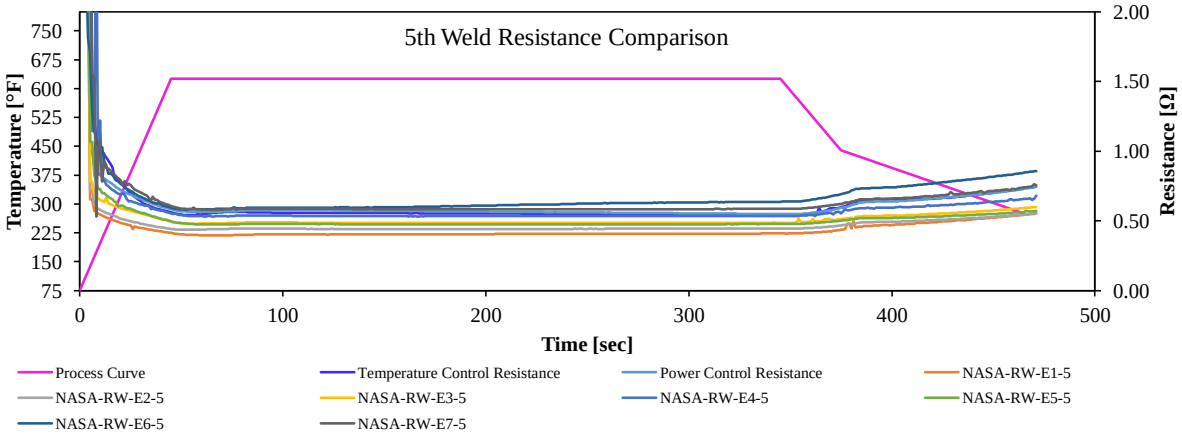

Figure 99 – Process E 5th Weld Comparison

13.3 Process I Welding Metrics

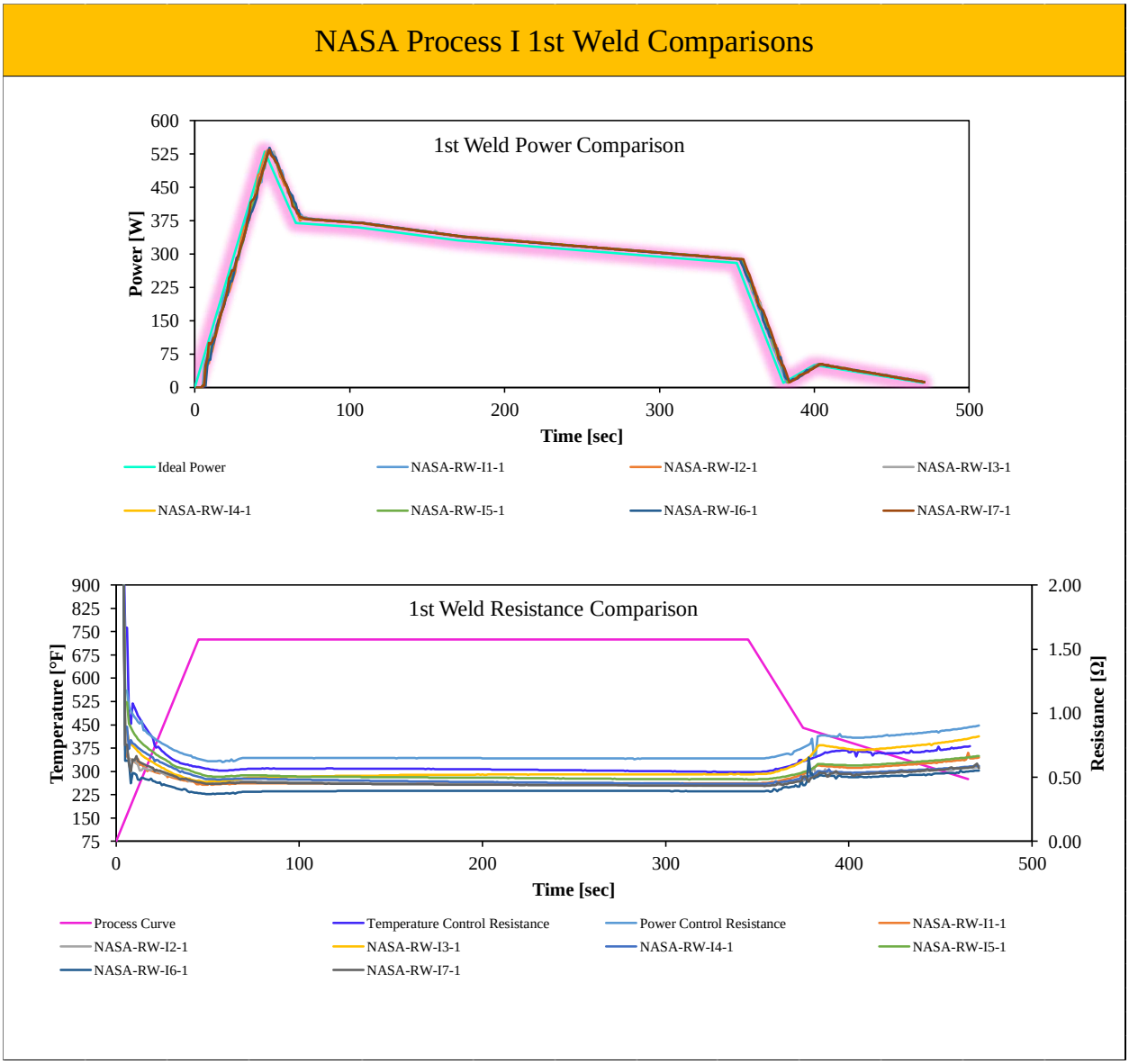

Figure 100 – Process I 1st Weld Comparison

NASA Process I 2nd Weld Comparisons

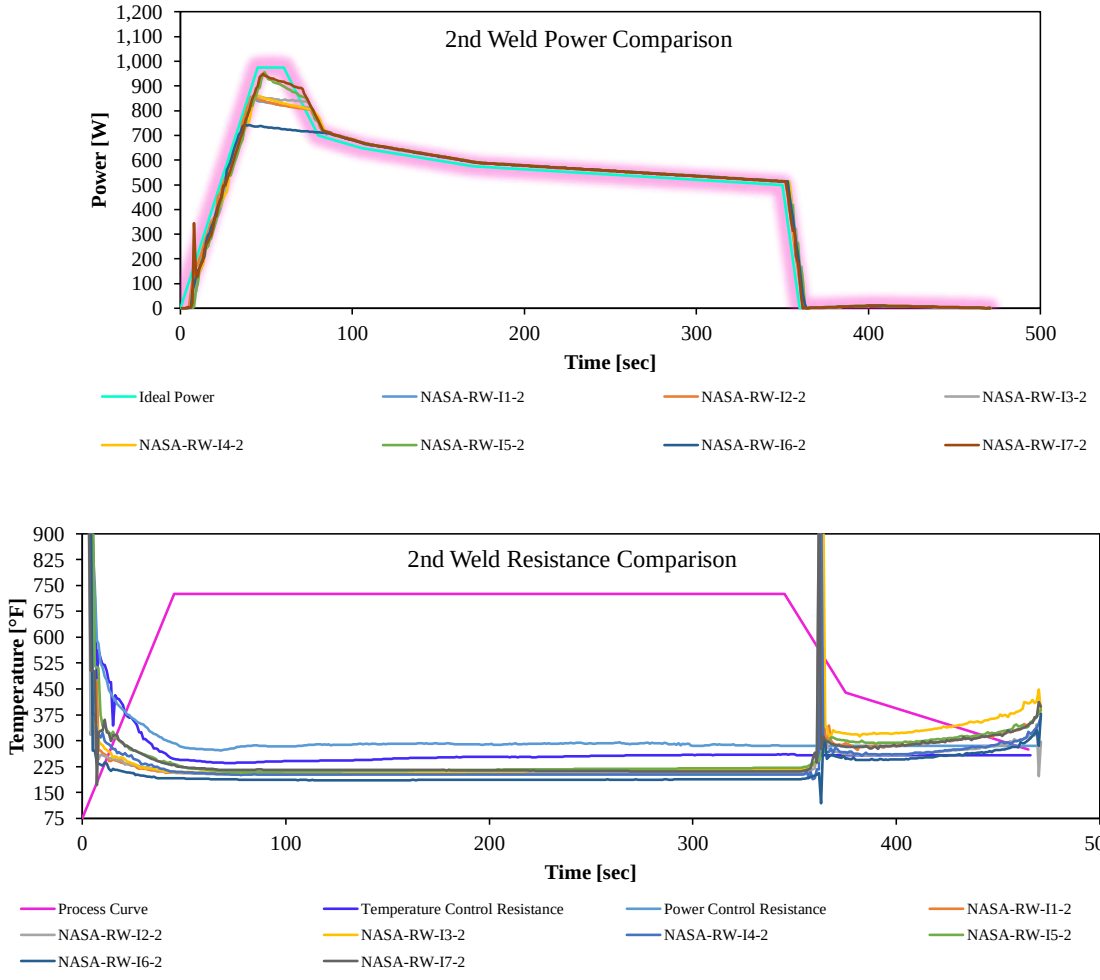

Figure 101 – Process I 2nd Weld Comparison

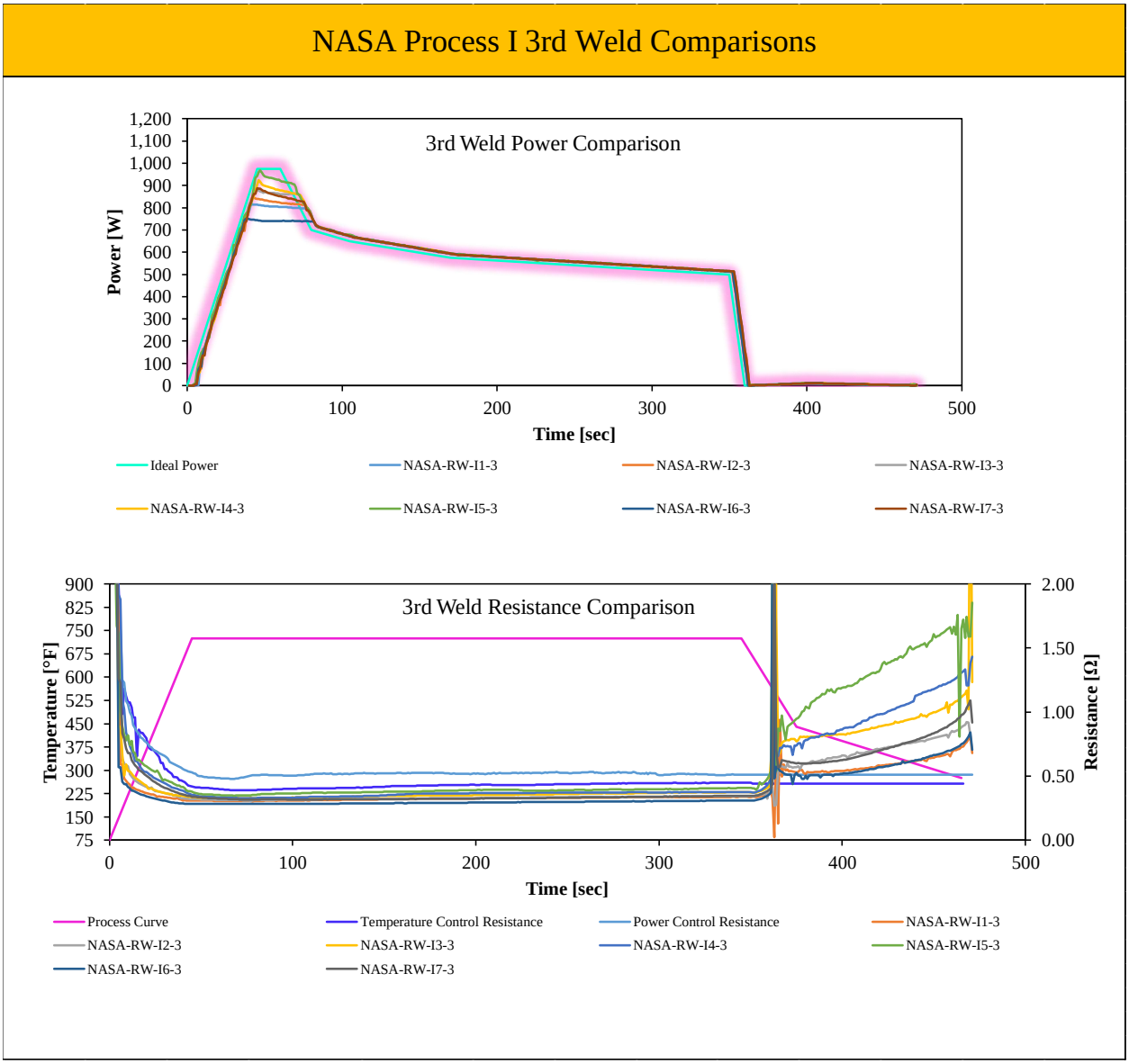

Figure 102 – Process I 3rd Weld Comparison

NASA Process I 4th Weld Comparisons

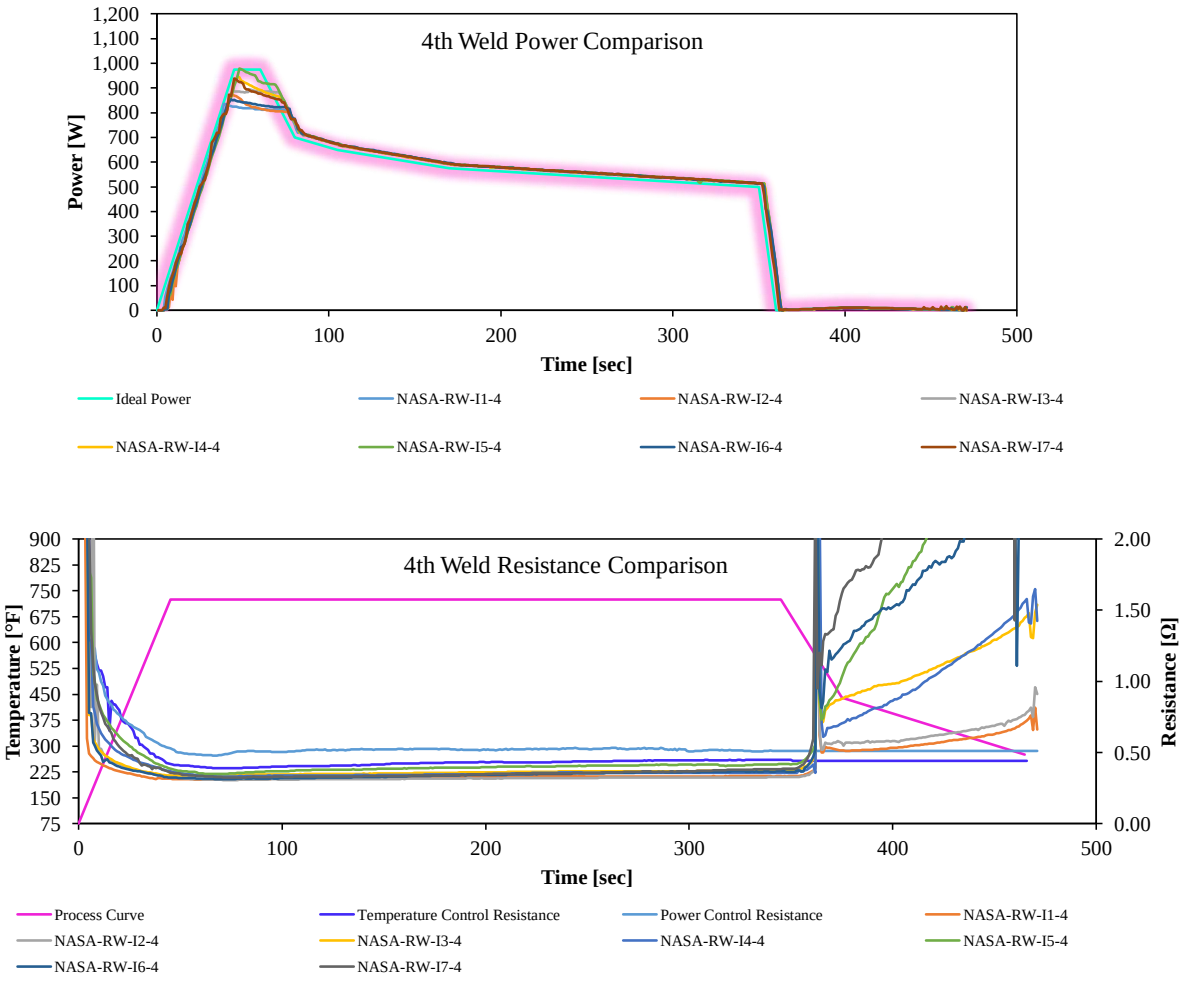

Figure 103 – Process I 4th Weld Comparison

NASA Process I 5th Weld Comparisons

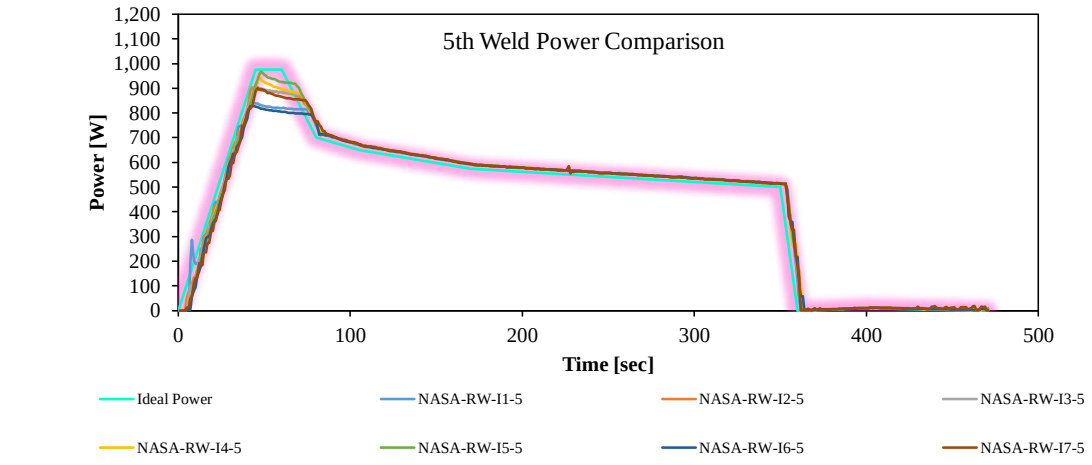

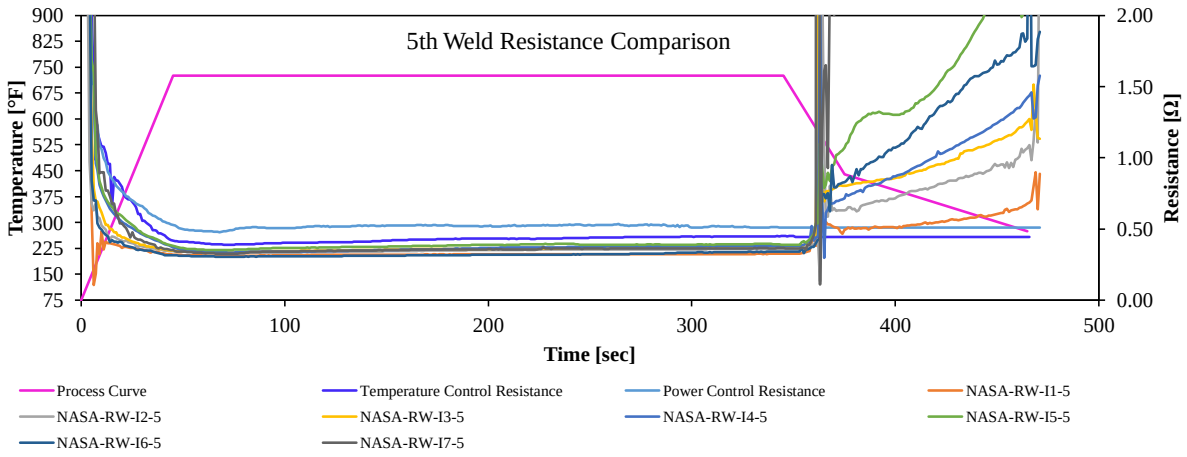

Figure 104 – Process I 5th Weld Comparison

NASA Process I 6th Weld Comparisons

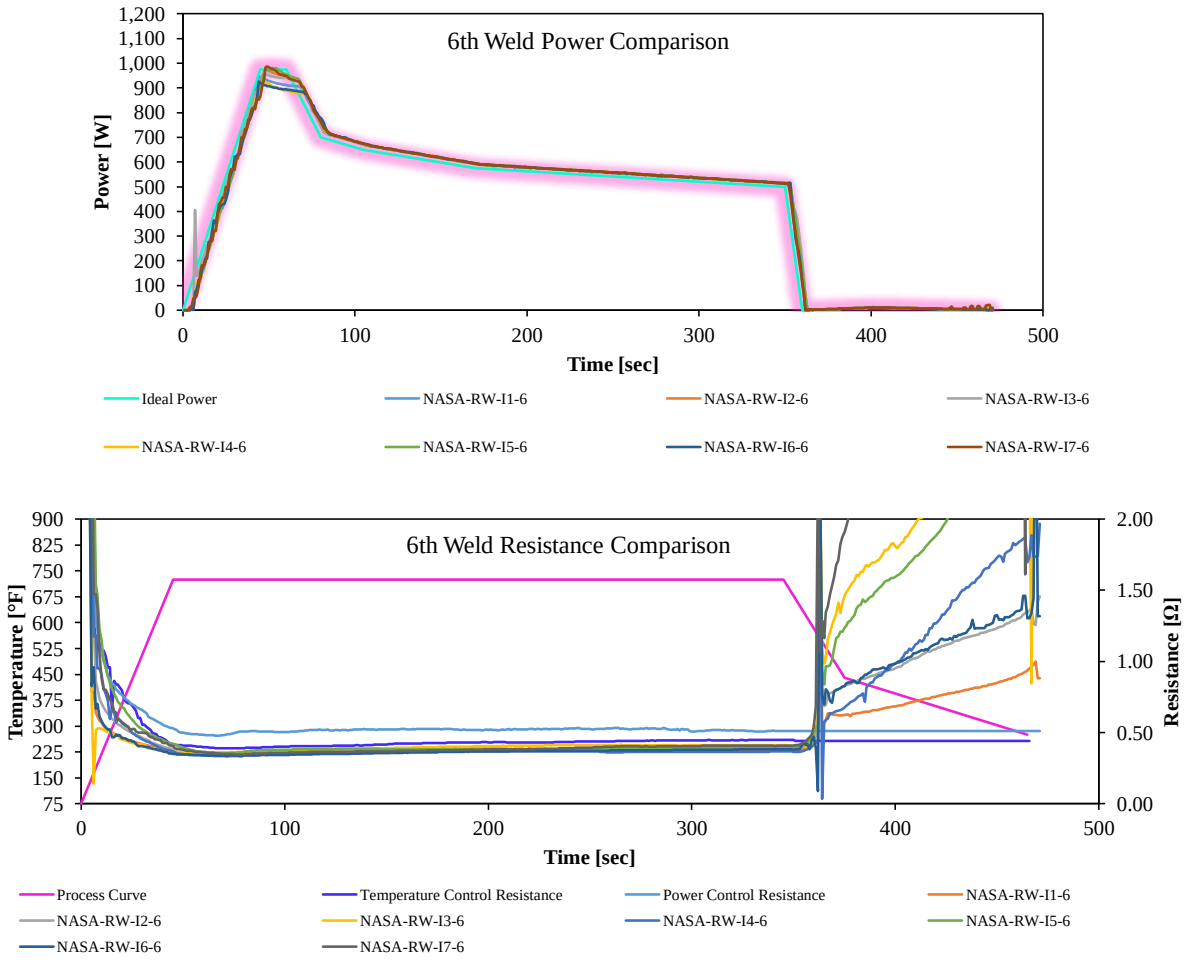

Figure 105 – Process I 6th Weld Comparison

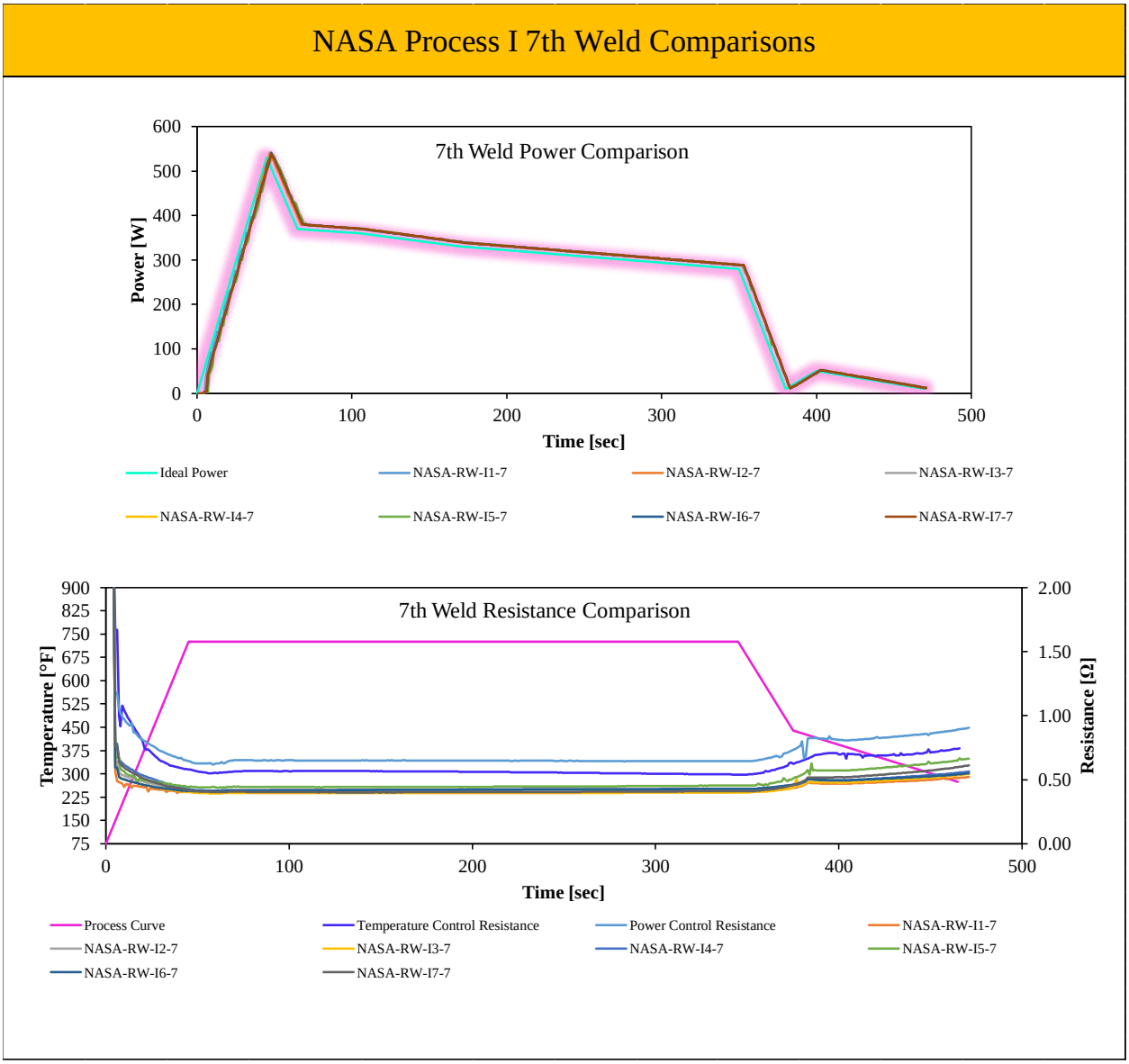

Figure 106 – Process I 7th Weld Comparison

13.4 Process J Welding Metrics

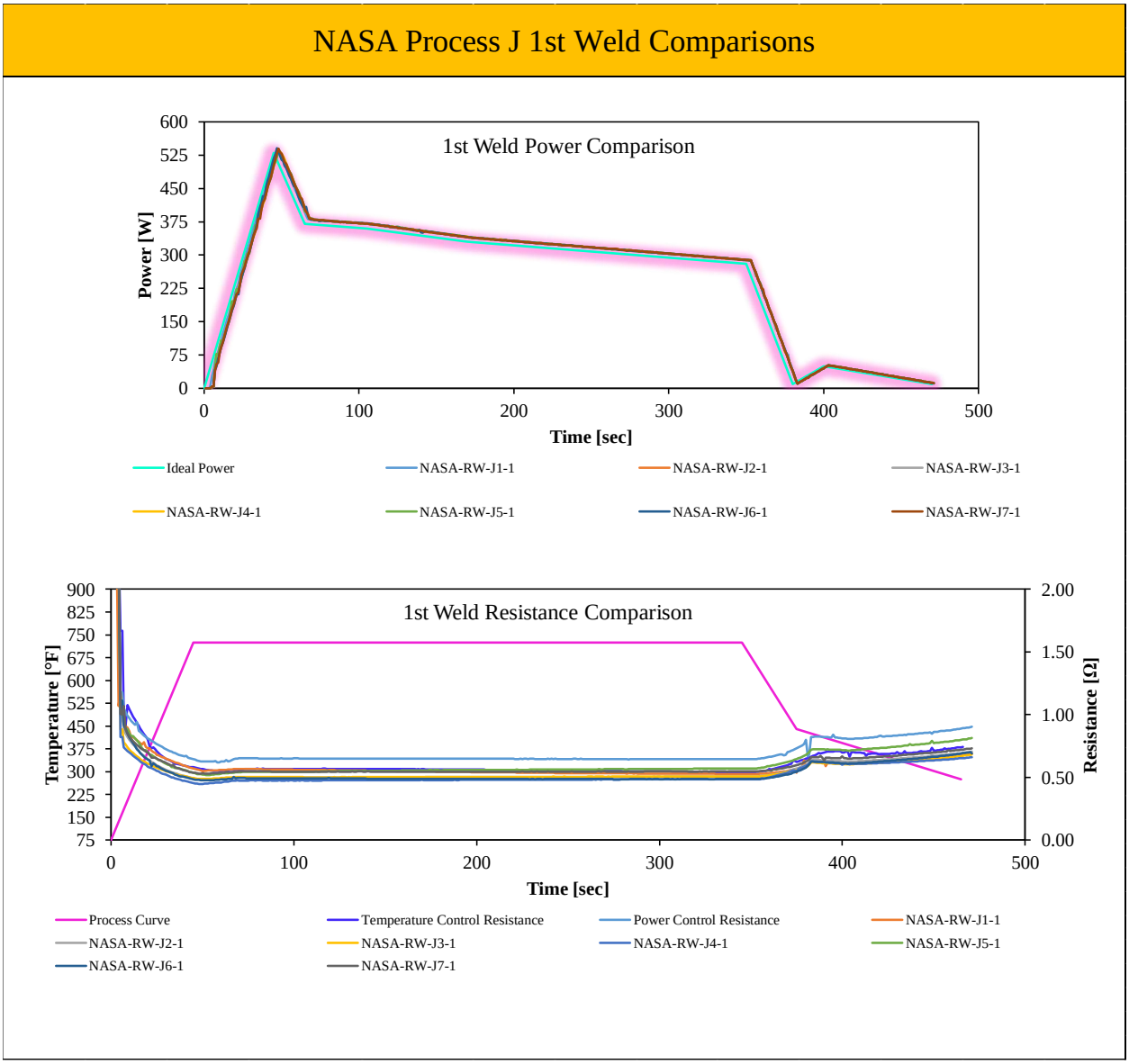

Figure 107 – Process J 1st Weld Comparison

NASA Process J 2nd Weld Comparisons

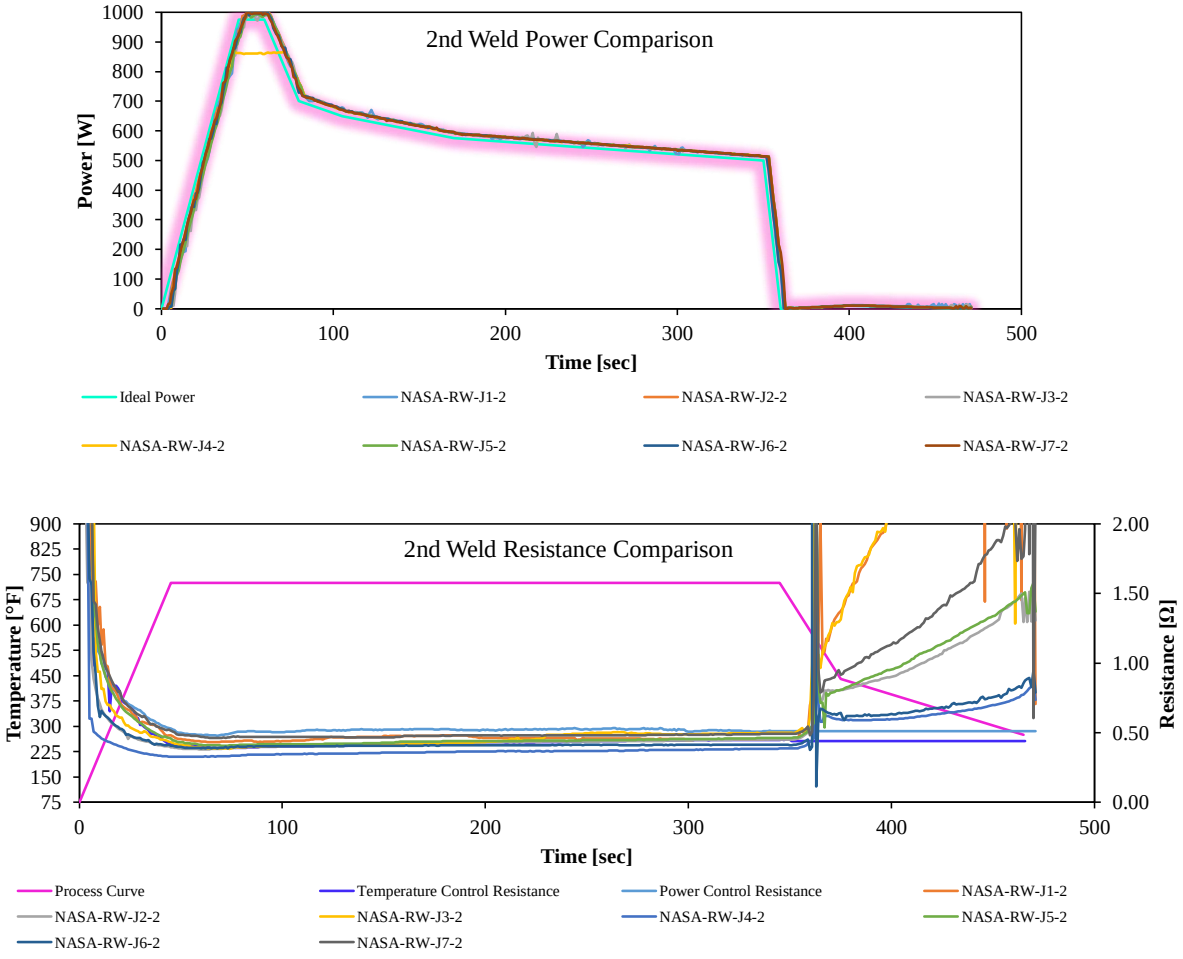

Figure 108 – Process J 2nd Weld Comparison

NASA Process J 3rd Weld Comparisons

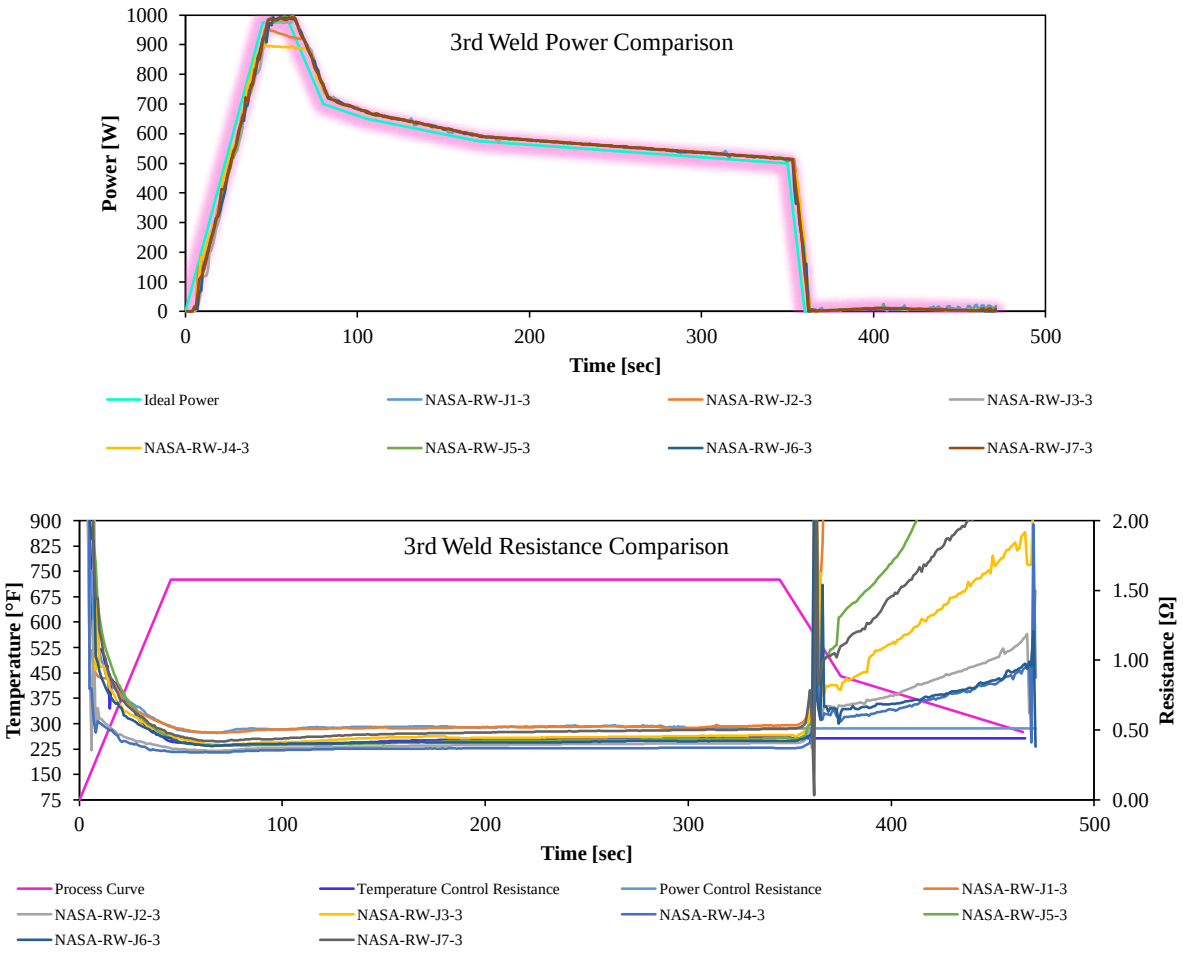

Figure 109 – Process J 3rd Weld Comparison

NASA Process J 4th Weld Comparisons

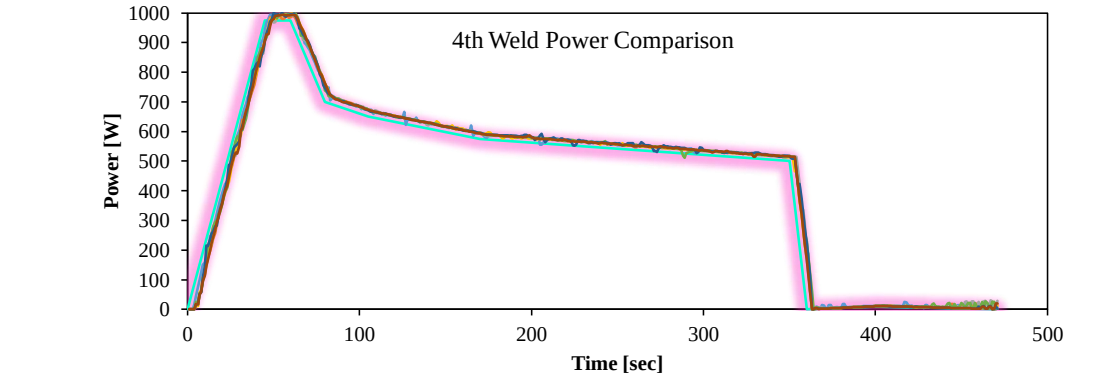

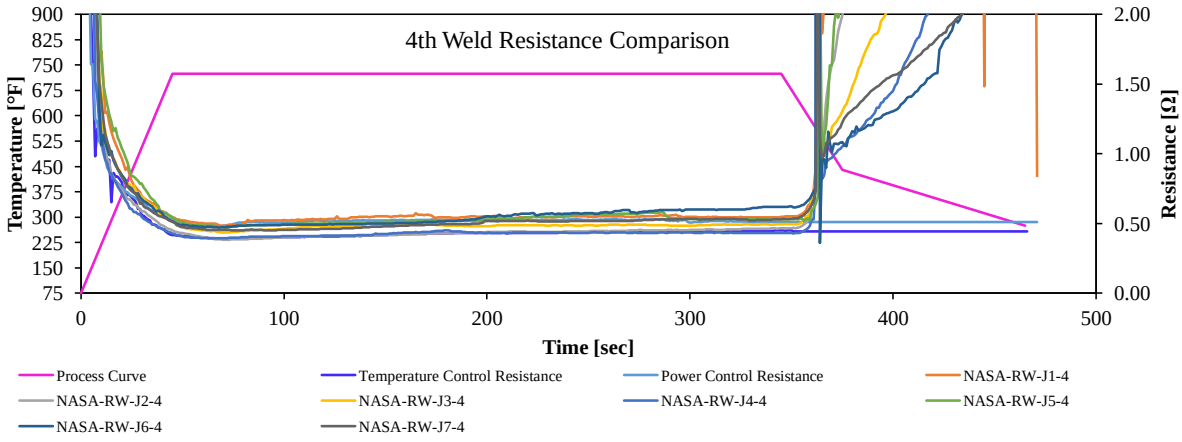

Figure 110 – Process J 4th Weld Comparison

NASA Process J 5th Weld Comparisons

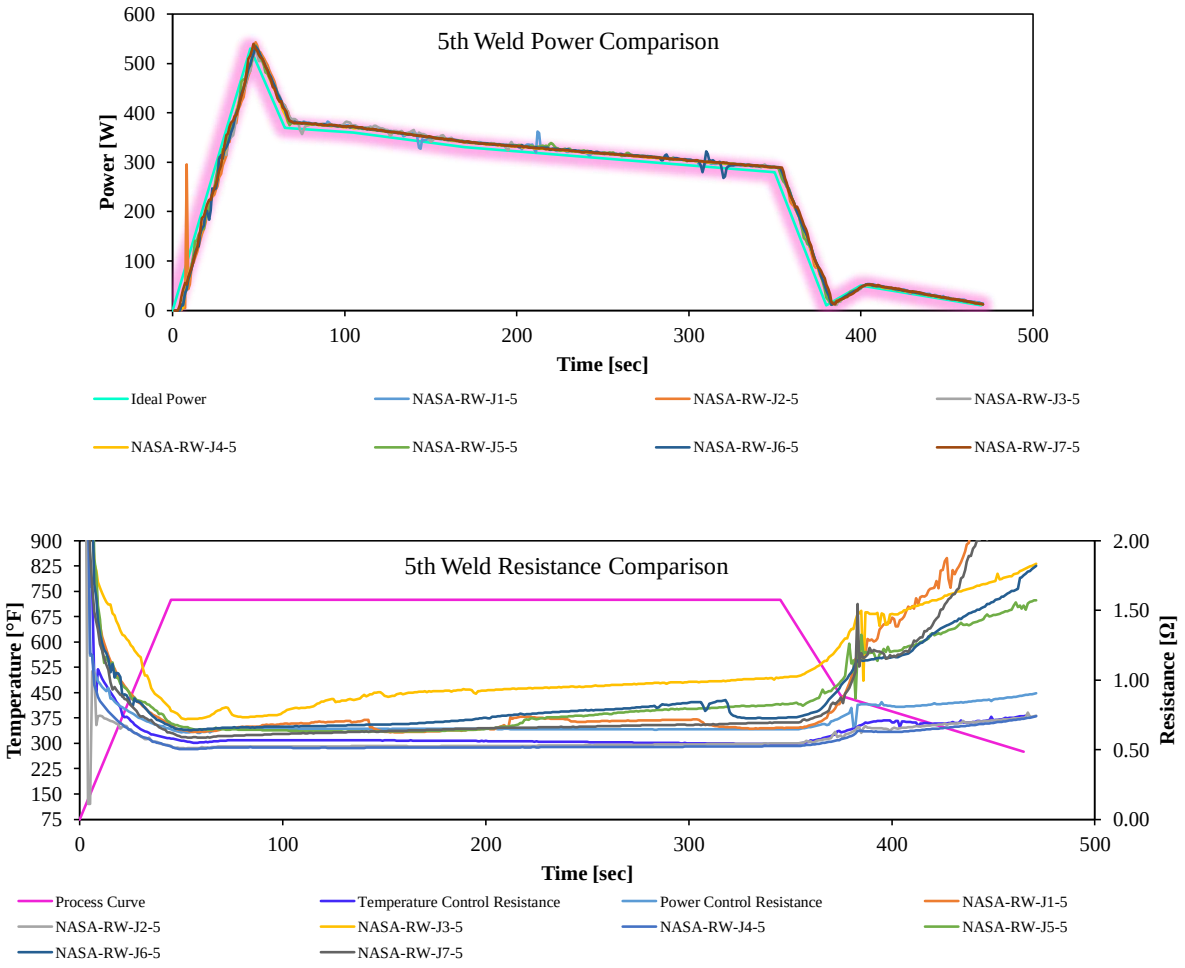

Figure 111 – Process J 5th Weld Comparison

14.0 Appendix II – DSC Results

14.1 Process A DSC Results

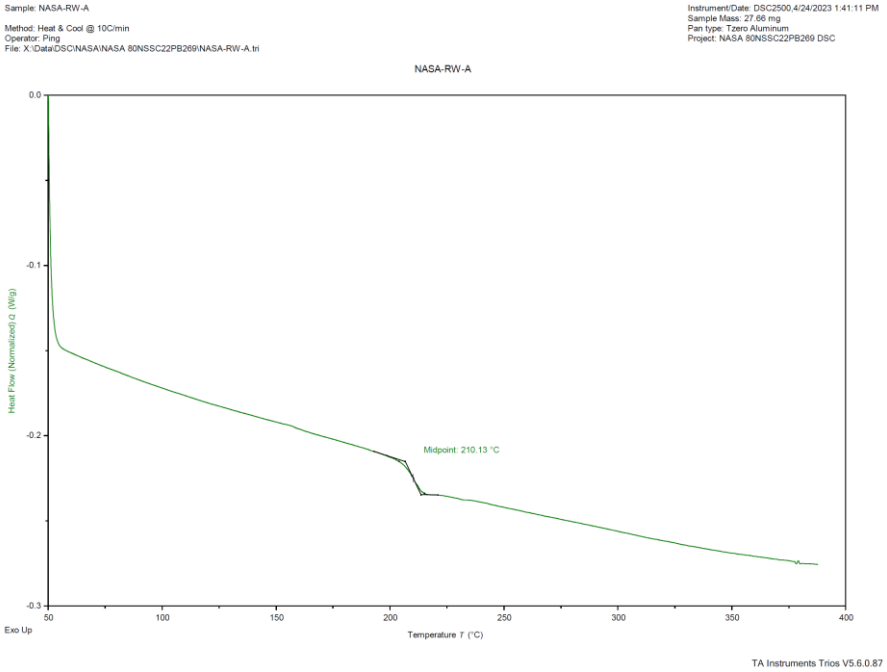

Figure 112 – Process A DSC Results

14.2 Process B DSC Results

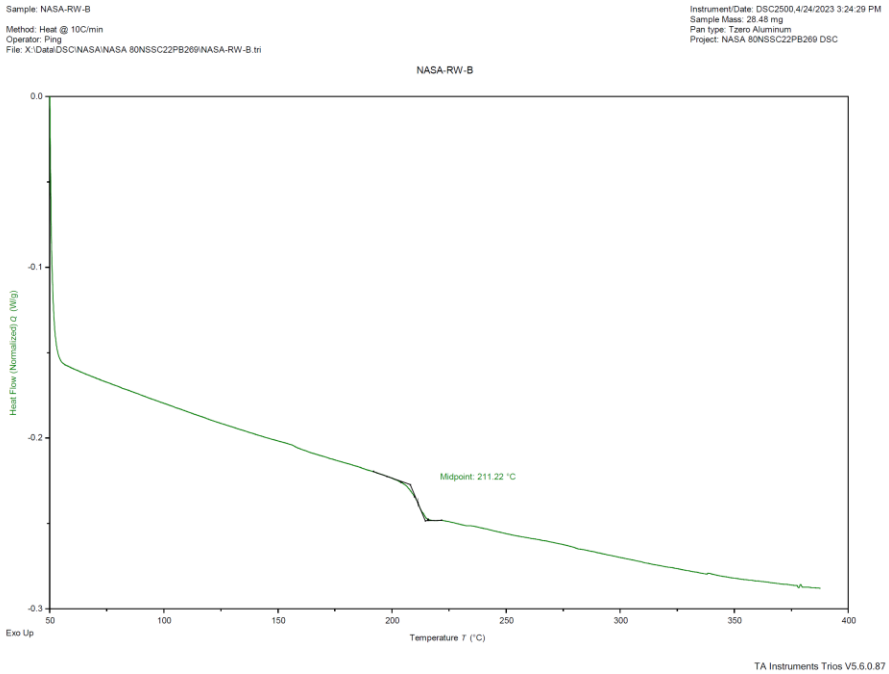

Figure 113 – Process B DSC Results

14.3 Process C DSC Results

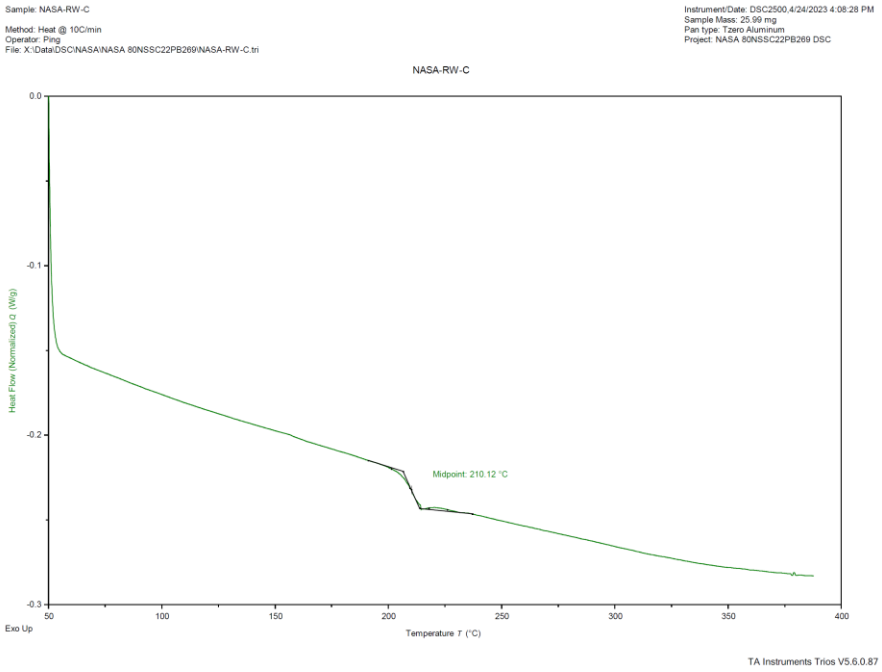

Figure 114 – Process C DSC Results

14.4 Process D DSC Results

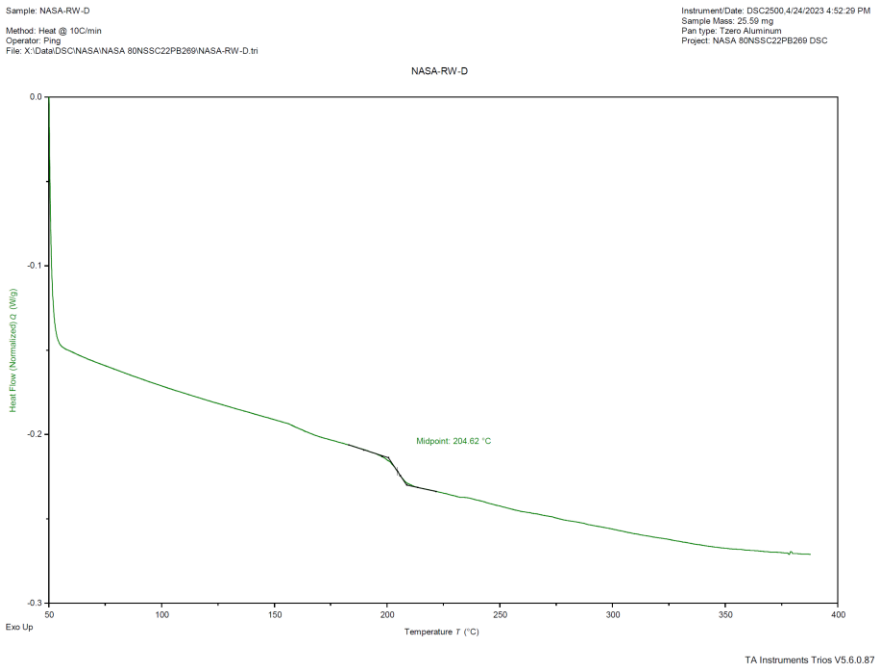

Figure 115 – Process D DSC Results

14.5 Process E DSC Results

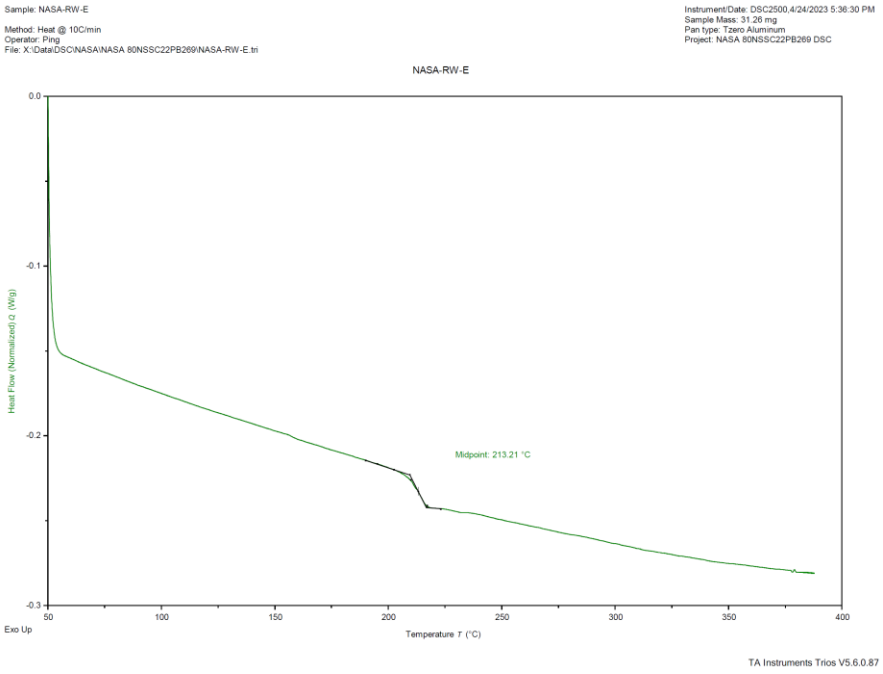

Figure 116 – Process E DSC Results

14.6 Process F DSC Results

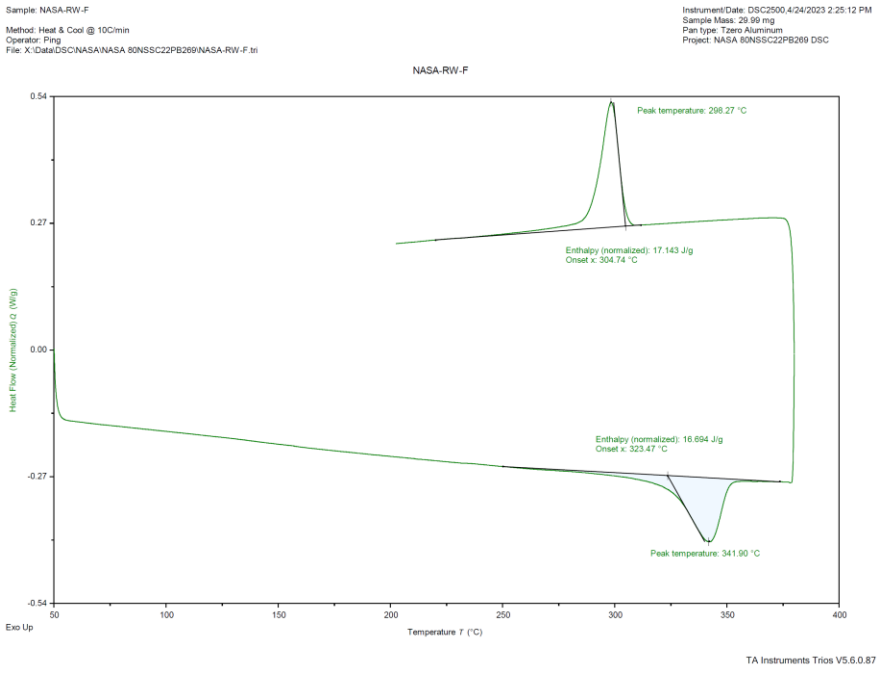

Figure 117 - Process F DSC Results

14.7 Process G DSC Results

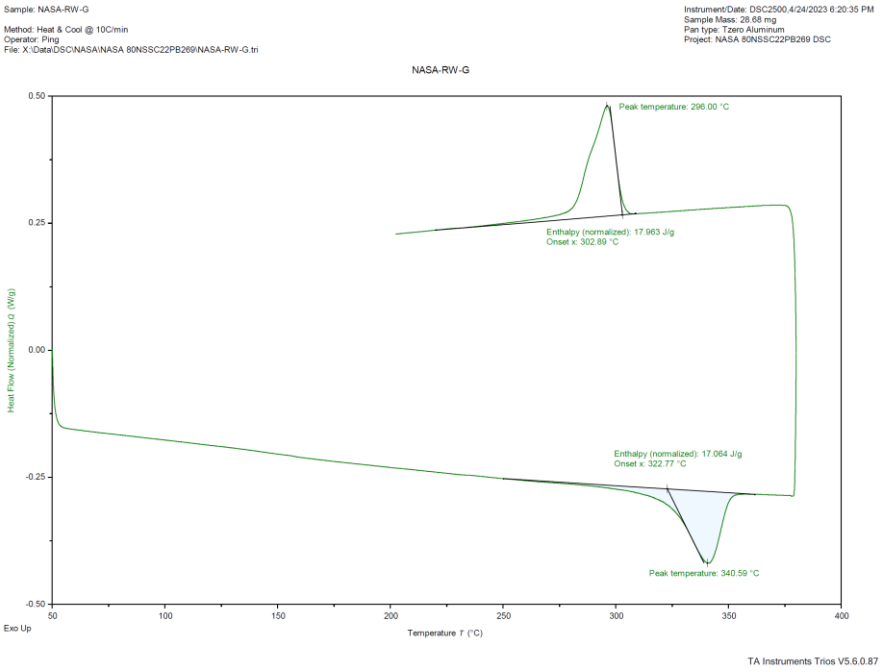

Figure 118 – Process G DSC Results

14.8 Process H DSC Results

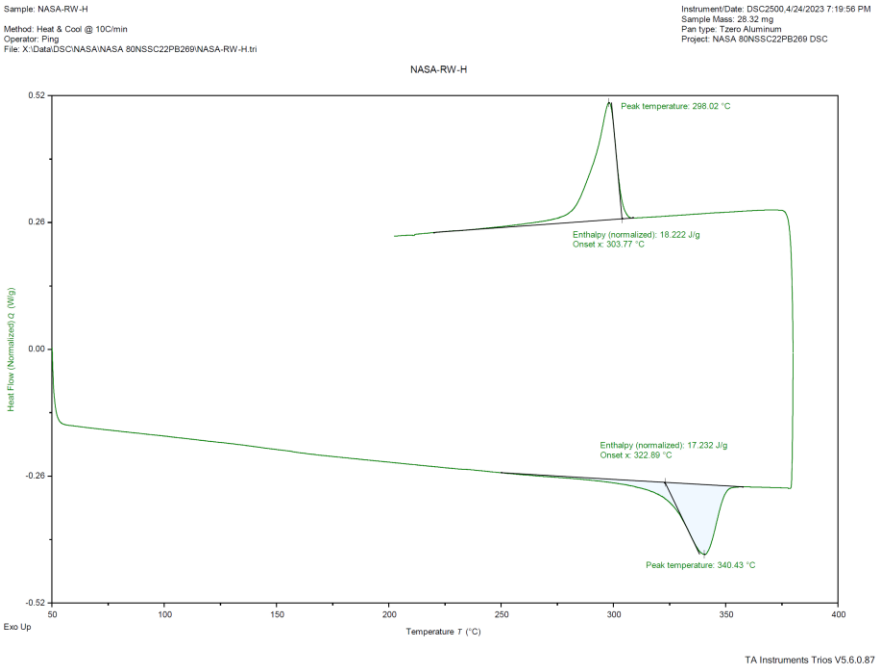

Figure 119 – Process H DSC Results

14.9 Process I DSC Results

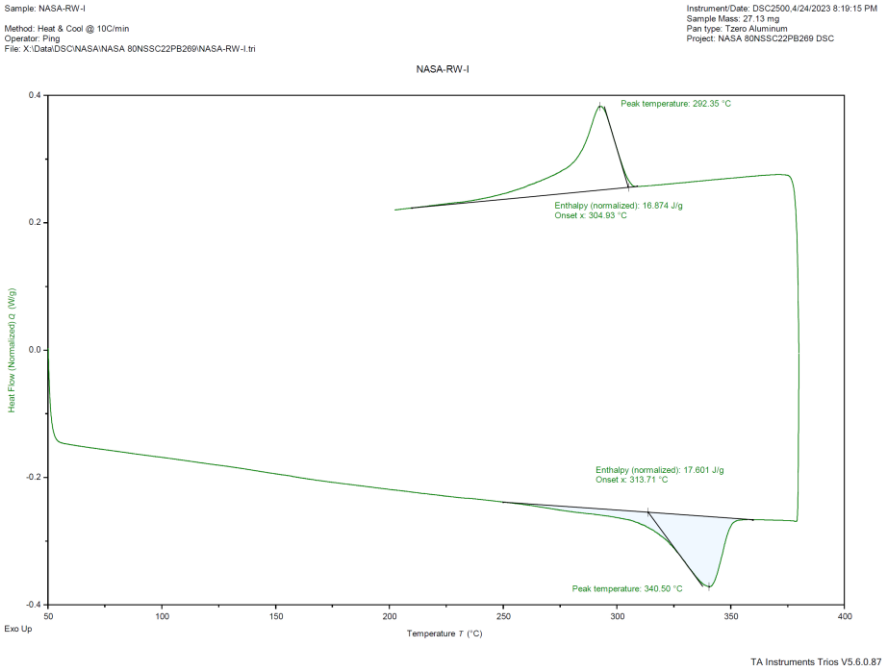

Figure 120 – Process I DSC Results

14.10 Process J DSC Results

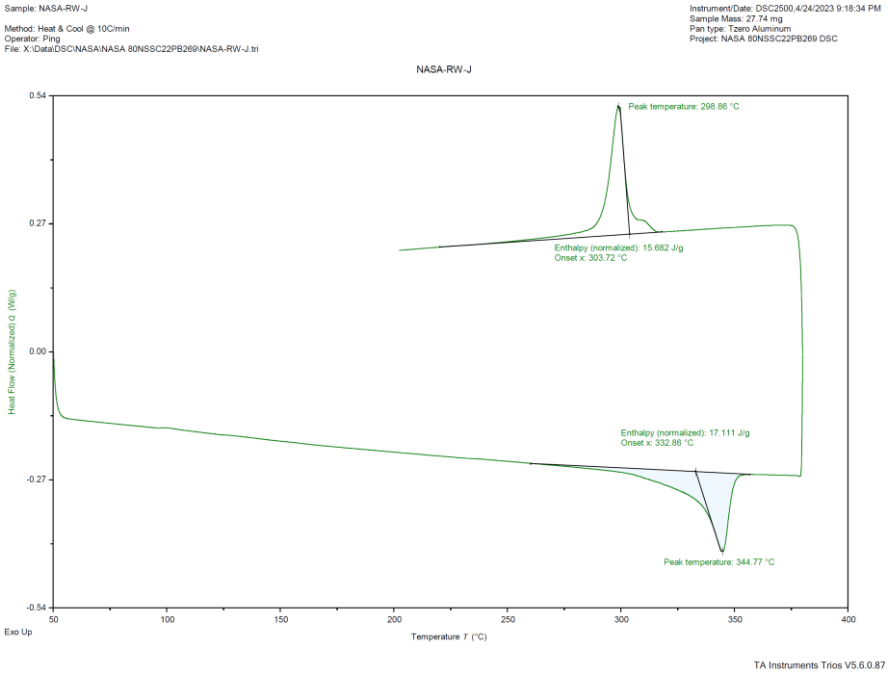

Figure 121 – Process J DSC Results

15.0 Appendix III – Single Lap Shear Data

15.1 Single Lap Shear Data Failure Loads

Category	Specimen Name	Weld Area [in^2]	Failure Load [lbf]	Apparent Shear Strength [psi]	Apparent Shear Strength [MPa]
NASA-RW-B-X	NASA-RW-B-1	1.00	2106.18	2106.18	14.52
	NASA-RW-B-2	1.00	2476.56	2476.56	17.08
	NASA-RW-B-3	1.00	2847.14	2847.14	19.63
	NASA-RW-B-4	1.00	2785.68	2785.68	19.21
	NASA-RW-B-5	1.00	2924.13	2924.13	20.16
	NASA-RW-B-6	1.00	2836.62	2836.62	19.56
NASA-RW-C-X	NASA-RW-C-1	1.00	2742.66	2742.66	18.91
	NASA-RW-C-2	1.00	2778.81	2778.81	19.16
	NASA-RW-C-3	1.00	3075.09	3075.09	21.20
	NASA-RW-C-4	1.00	3230.72	3230.72	22.28
	NASA-RW-C-5	1.00	3142.65	3142.65	21.67
	NASA-RW-C-6	1.00	2907.97	2907.97	20.05
NASA-RW-G-X	NASA-RW-G-1	1.00	3520.52	3520.52	24.27
	NASA-RW-G-2	1.00	3944.81	3944.81	27.20
	NASA-RW-G-3	1.00	4383.83	4383.83	30.23
	NASA-RW-G-4	1.00	3975.64	3975.64	27.41
	NASA-RW-G-5	1.00	3685.61	3685.61	25.41
	NASA-RW-G-6	1.00	4473.71	4473.71	30.85
NASA-RW-H-X	NASA-RW-H-1	1.00	4110.49	4110.49	28.34
	NASA-RW-H-2	1.00	4402.12	4402.12	30.35
	NASA-RW-H-3	1.00	4242.94	4242.94	29.25
	NASA-RW-H-4	1.00	4415.04	4415.04	30.44
	NASA-RW-H-5	1.00	4756.33	4756.33	32.79
	NASA-RW-H-6	1.00	4210.37	4210.37	29.03
NASA-RW-K-X	NASA-RW-K-1	1.00	2406.54	2406.54	16.59
	NASA-RW-K-2	1.00	2363.96	2363.96	16.30
	NASA-RW-K-3	1.00	2368.66	2368.66	16.33

Figure 122 – Single Lap Shear Failure Loads

15.2 Single Lap Shear Data Failure Modes

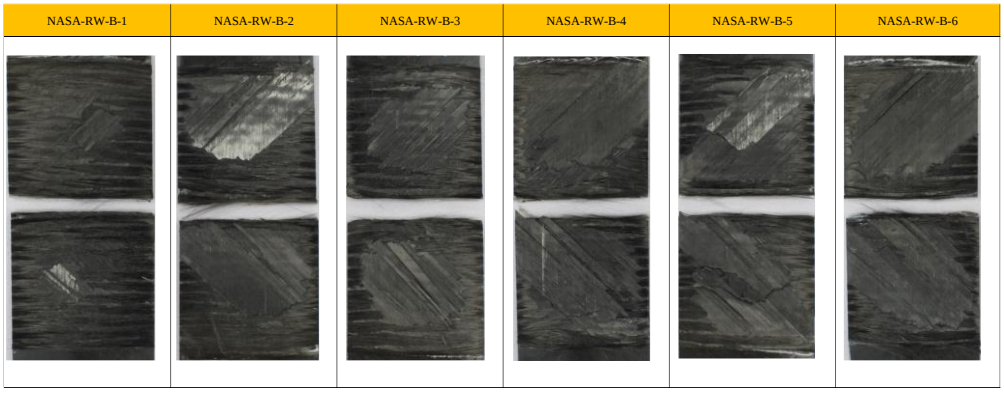

Figure 123 – Process B Failure Modes

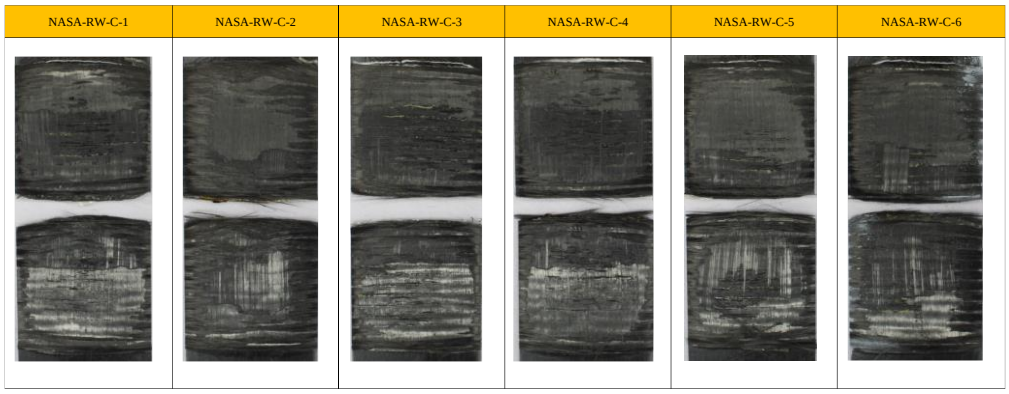

Figure 124 – Process C Failure Modes

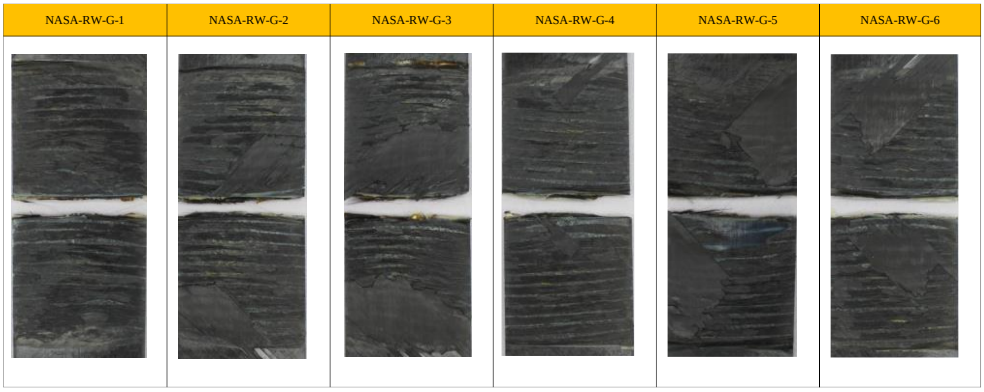

Figure 125 – Process G Failure Modes

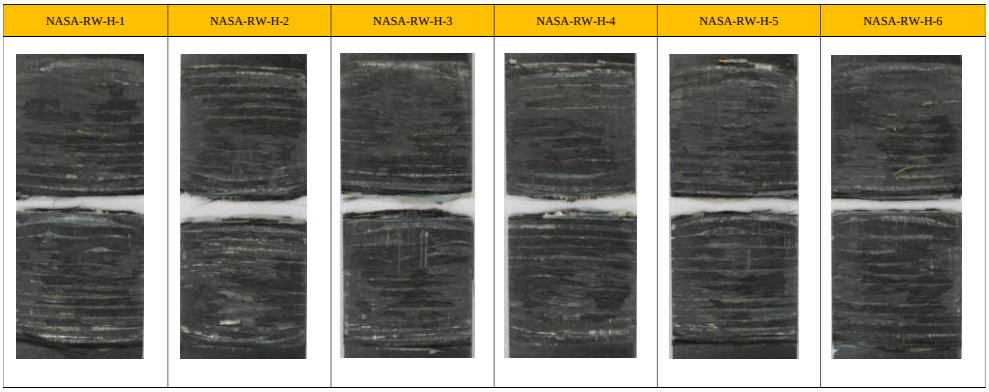

Figure 126 – Process H Failure Modes

NASA-RW-K-1	NASA-RW-K-2	NASA-RW-K-3
		

Figure 127 – Process K Failure Modes

15.3 Load vs. Displacement Data

NASA-RW-B1 Load vs. Displacement Data

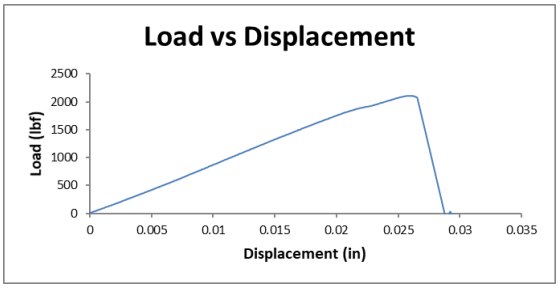

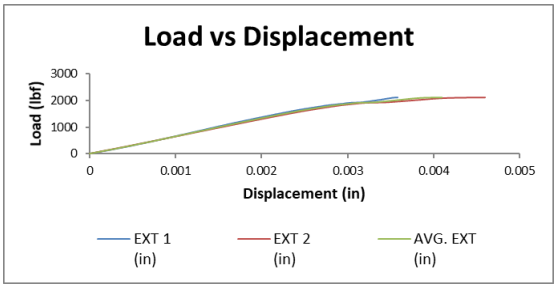

NASA-RW-B2 Load vs. Displacement Data

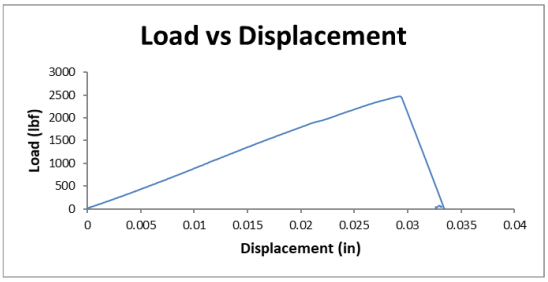

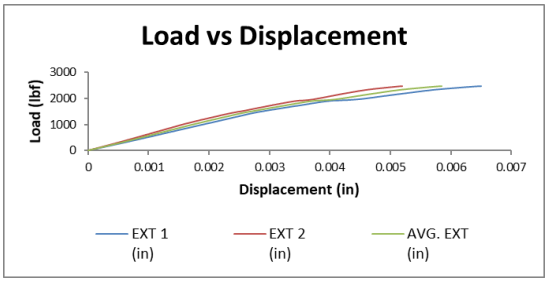

NASA-RW-B3 Load vs. Displacement Data

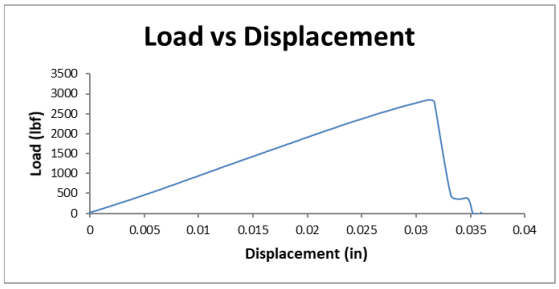

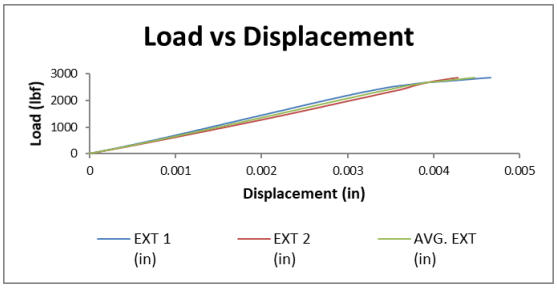

NASA-RW-B4 Load vs. Displacement Data

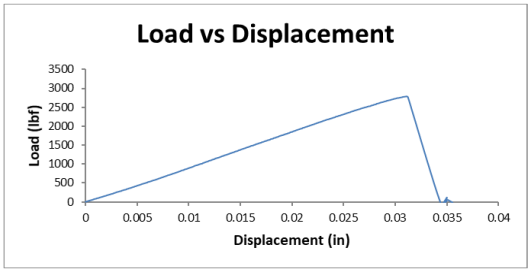

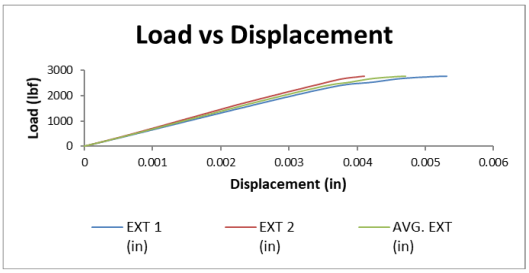

NASA-RW-B5 Load vs. Displacement Data

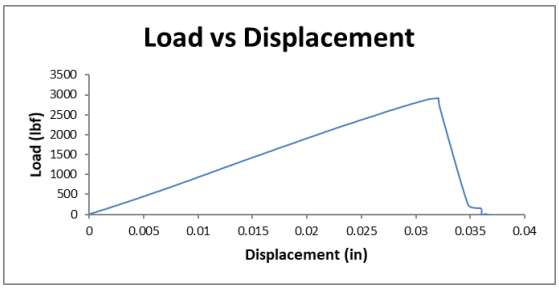

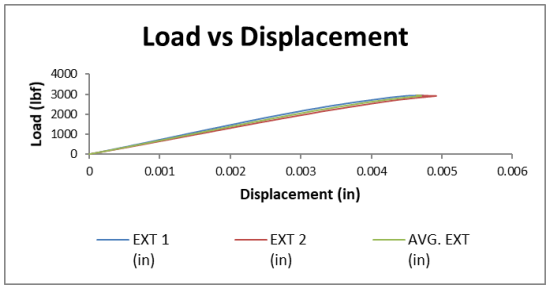

NASA-RW-C1 Load vs. Displacement Data

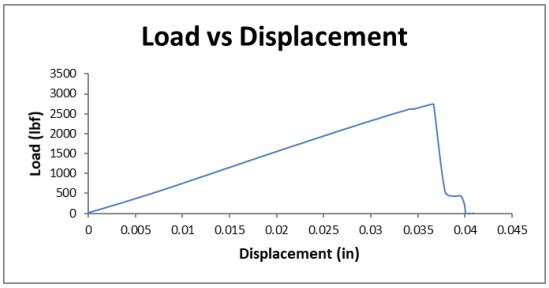

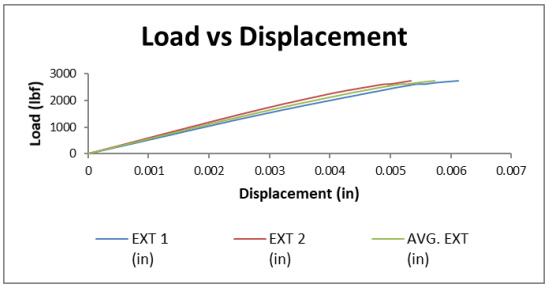

NASA-RW-C2 Load vs. Displacement Data

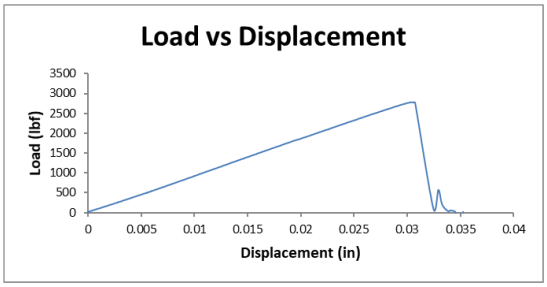

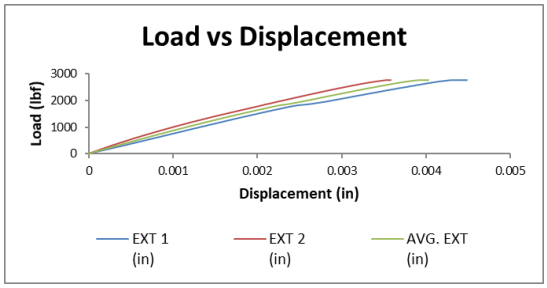

NASA-RW-C3 Load vs. Displacement Data

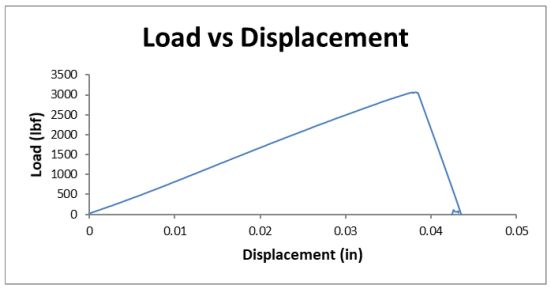

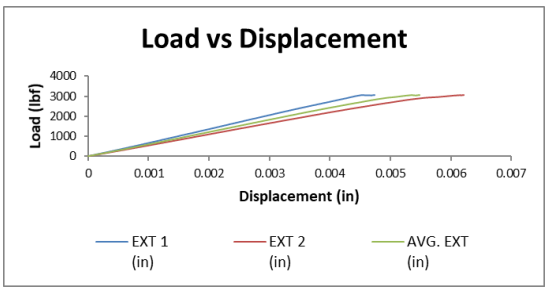

NASA-RW-C4 Load vs. Displacement Data

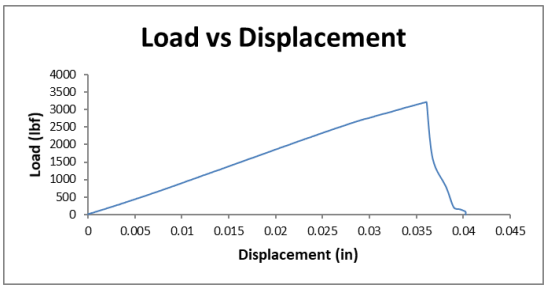

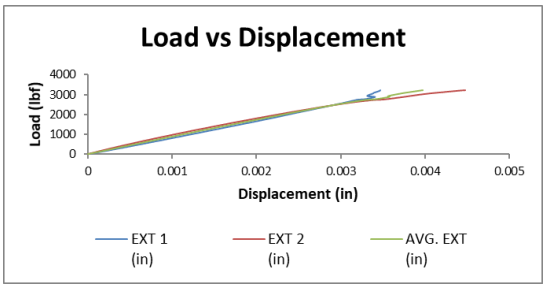

NASA-RW-C5 Load vs. Displacement Data

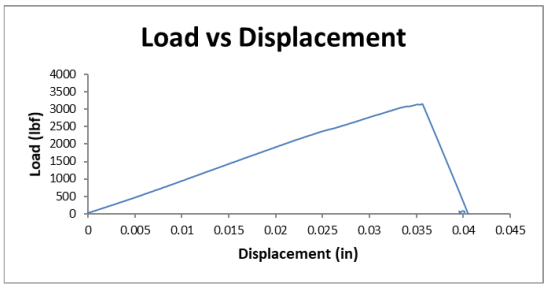

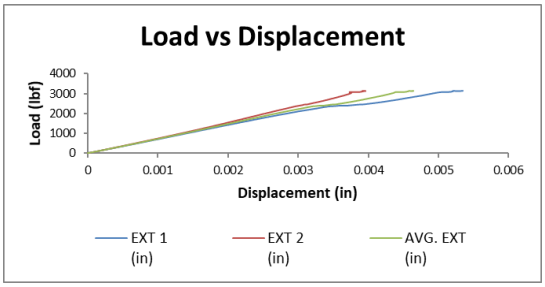

PEI (B&C) Single Lap Shear Load vs. Displacement Overall Summary

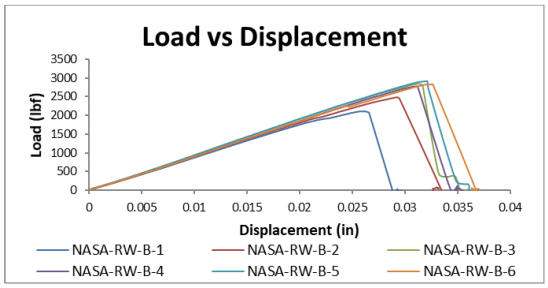

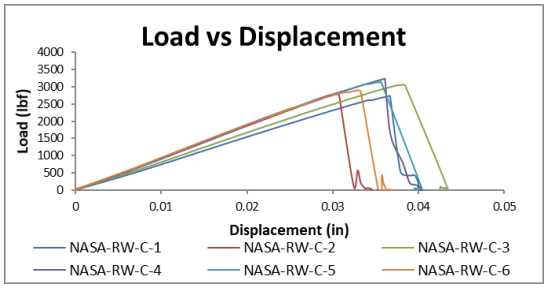

NASA-RW-G1 Load vs. Displacement Data

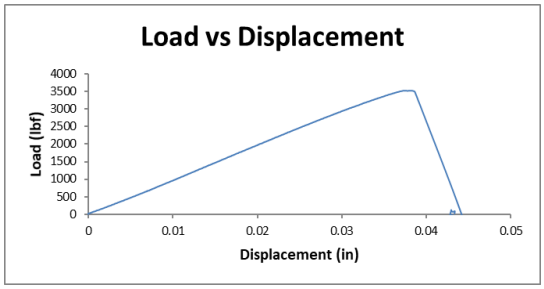

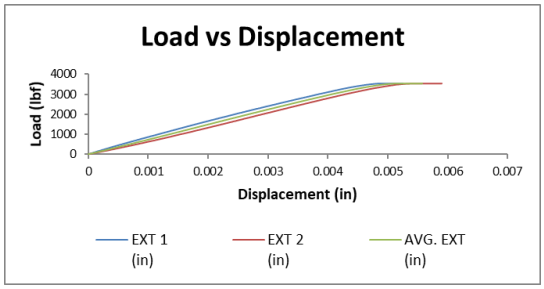

NASA-RW-G2 Load vs. Displacement Data

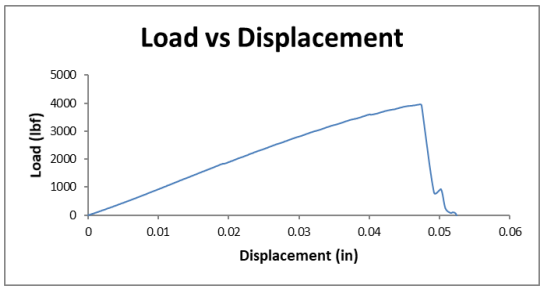

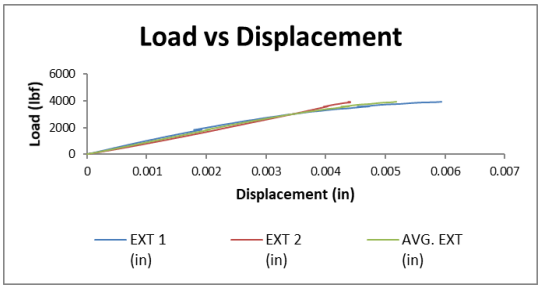

NASA-RW-G3 Load vs. Displacement Data

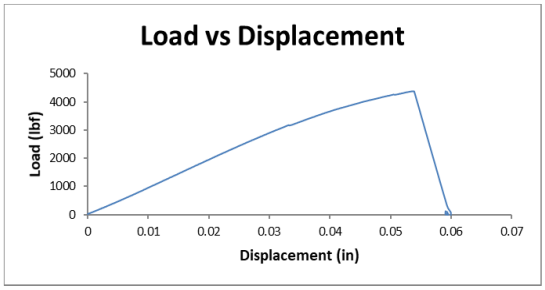

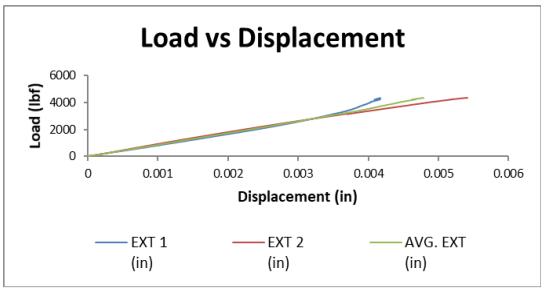

NASA-RW-G4 Load vs. Displacement Data

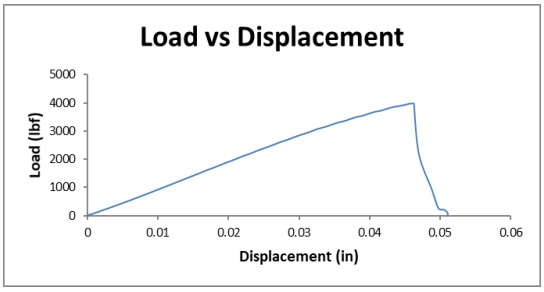

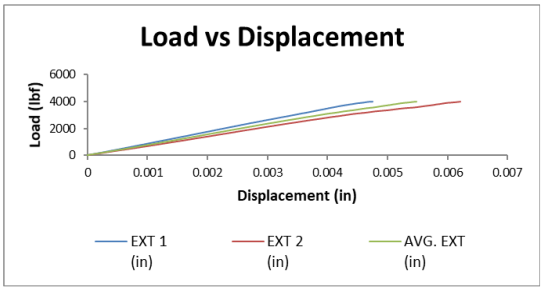

NASA-RW-G5 Load vs. Displacement Data

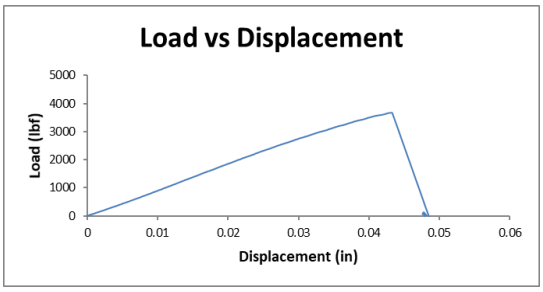

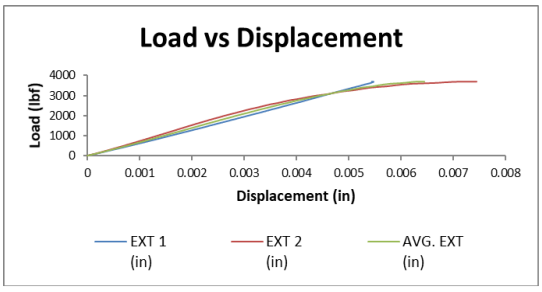

NASA-RW-H1 Load vs. Displacement Data

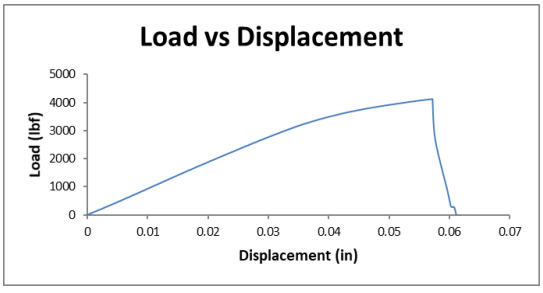

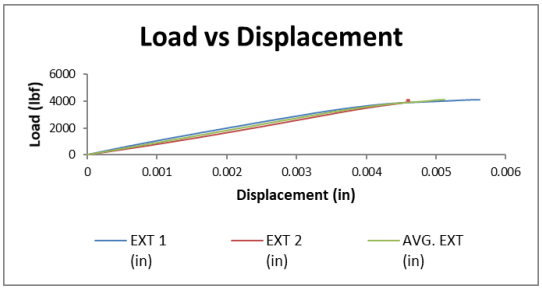

NASA-RW-H2 Load vs. Displacement Data

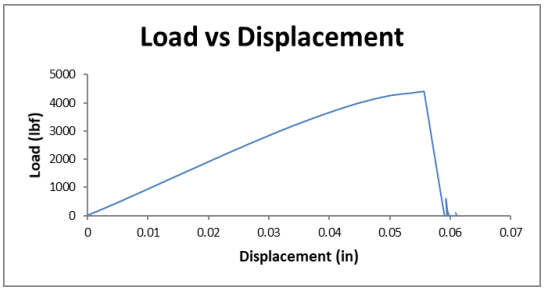

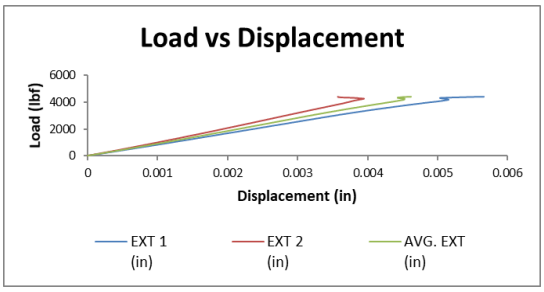

NASA-RW-H3 Load vs. Displacement Data

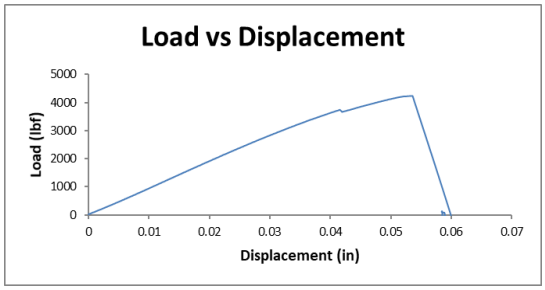

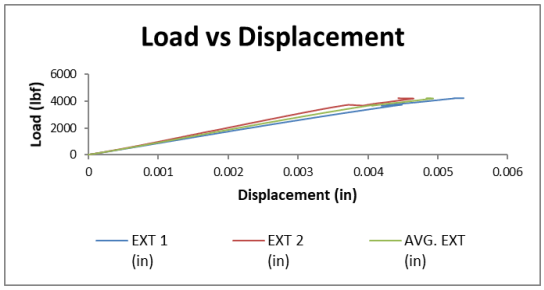

NASA-RW-H4 Load vs. Displacement Data

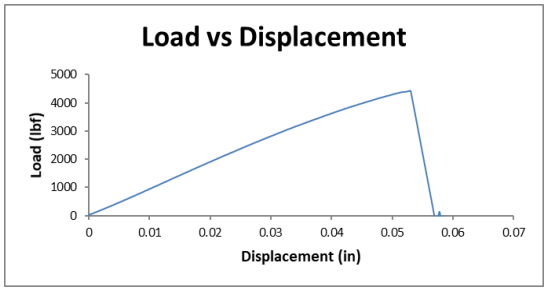

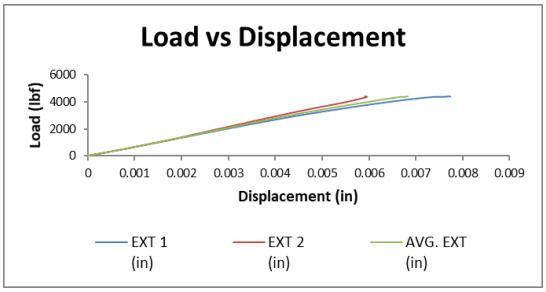

NASA-RW-H5 Load vs. Displacement Data

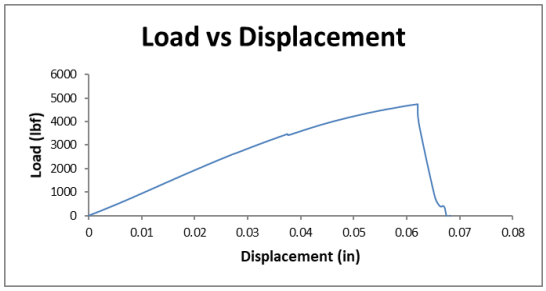

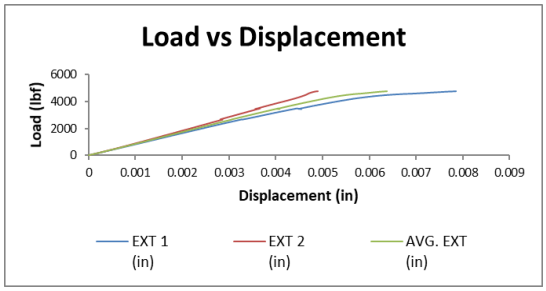

PEEK (G&H) Single Lap Shear Load vs. Displacement Overall Summary

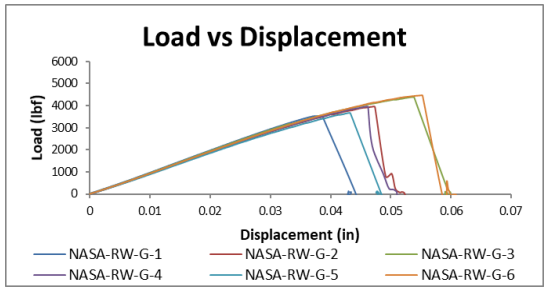

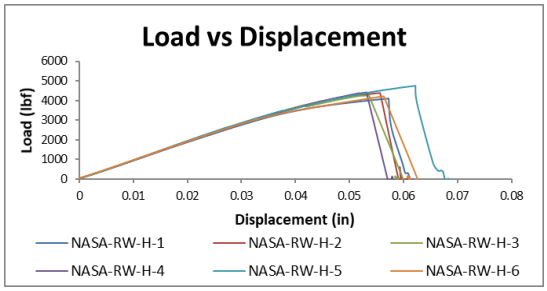

NASA-RW-K1 Load vs. Displacement Data

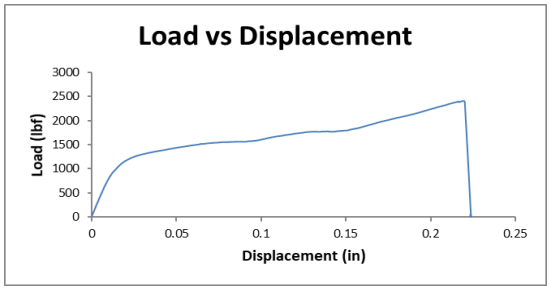

NASA-RW-K2 Load vs. Displacement Data

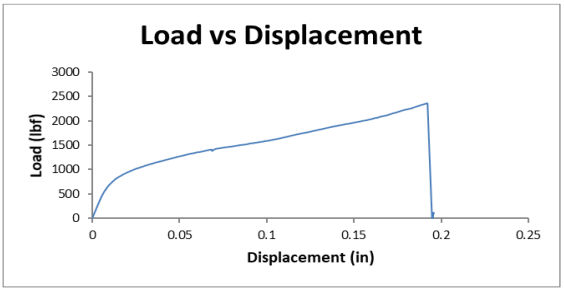

NASA-RW-K3 Load vs. Displacement Data

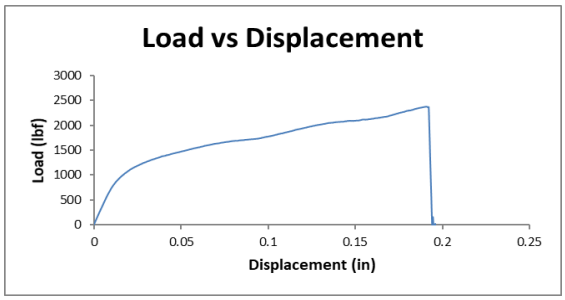

PEEK/PEI (K) Single Lap Shear Load vs. Displacement Overall Summary

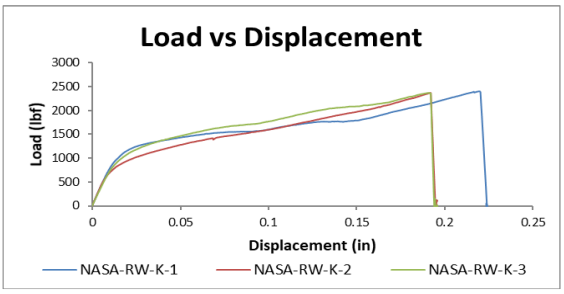

16.0 Appendix IV – Double Lap Shear Data

16.1 Double Lap Shear Data Failure Loads

Category	Specimen Name	Weld Area [in^2]	Failure Load [lbf]	Apparent Shear Strength [psi]	Apparent Shear Strength [MPa]
NASA-RW-A-X	NASA-RW-A-3	2.00	3925.50	1962.75	13.53
	NASA-RW-A-4	2.00	5357.43	2678.71	18.47
	NASA-RW-A-5	2.00	5979.35	2989.68	20.61
	NASA-RW-A-6	2.00	5715.53	2857.77	19.70
	NASA-RW-A-7	2.00	5593.99	2797.00	19.28
	NASA-RW-A-8	2.00	6088.48	3044.24	20.99
NASA-RW-F-X	NASA-RW-F-1	2.00	3723.80	1861.90	12.84
	NASA-RW-F-2	2.00	5956.12	2978.06	20.53
	NASA-RW-F-3	2.00	5939.46	2969.73	20.48
	NASA-RW-F-4	2.00	6324.53	3162.27	21.80
	NASA-RW-F-5	2.00	5213.15	2606.57	17.97
	NASA-RW-F-6	2.00	6641.18	3320.59	22.89

Figure 128 – Double Lap Shear Failure Loads

16.2 Double Lap Shear Data Failure Modes

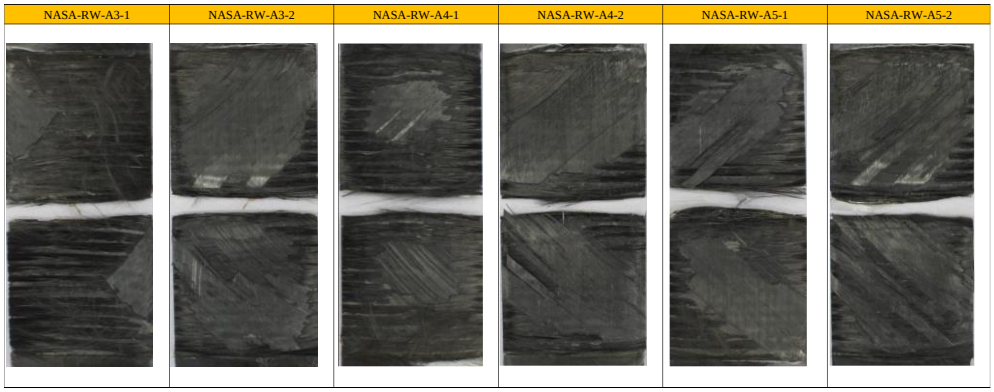

Figure 129 – Process A Failure Modes PT. 1

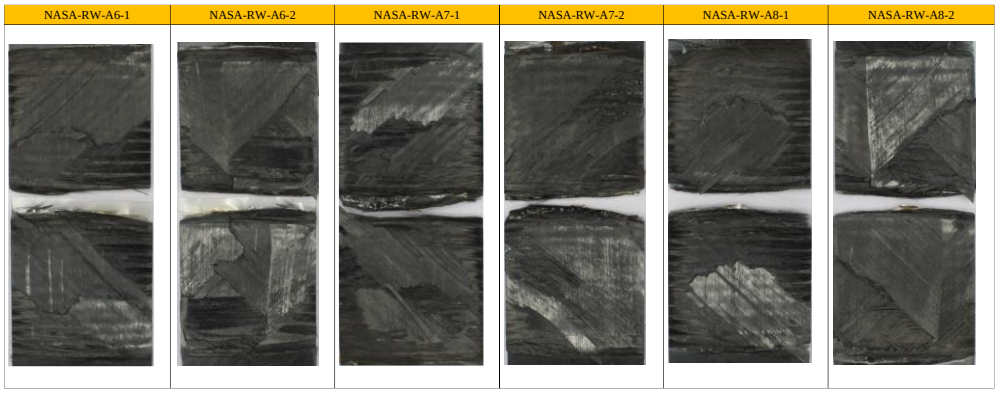

Figure 130 – Process A Failure Modes PT. 2

NASA-RW-F1-1	NASA-RW-F1-2	NASA-RW-F2-1	NASA-RW-F2-2	NASA-RW-F3-1	NASA-RW-F3-2
Weld Did Not Fail - No Failure Photo Available					Weld Did Not Fail - No Failure Photo Available

Figure 131 – Process F Failure Modes PT. 1

NASA-RW-F4-1	NASA-RW-F4-2	NASA-RW-F5-1	NASA-RW-F5-2	NASA-RW-F6-1	NASA-RW-F6-2
Weld Did Not Fail - No Failure Photo Available					

Figure 132 – Process F Failure Modes PT. 2

16.3 Load vs. Displacement Data

NASA-RW-A3 Load vs. Displacement Data

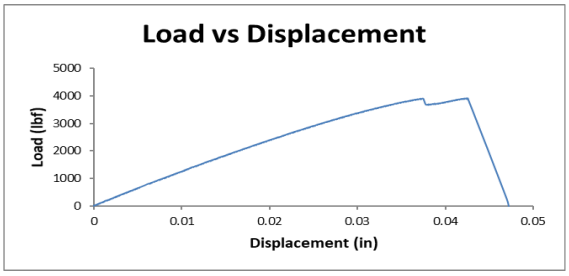

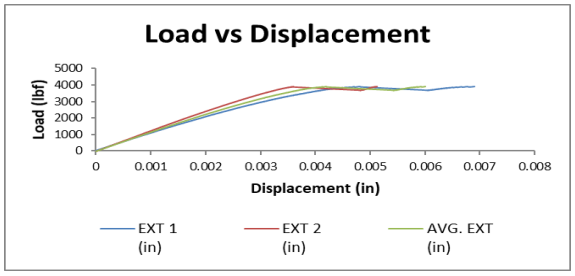

NASA-RW-A4 Load vs. Displacement Data

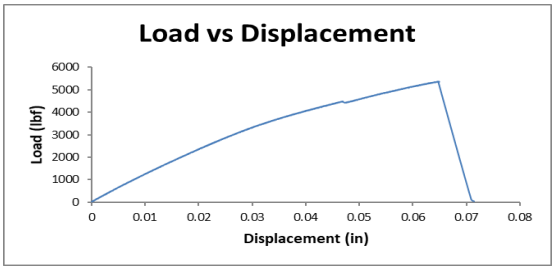

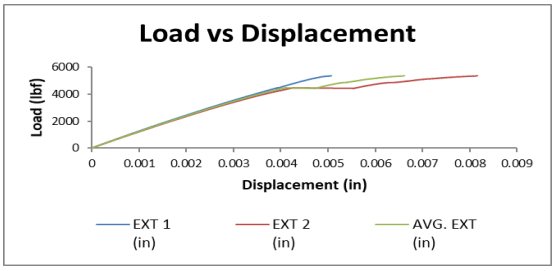

NASA-RW-A5 Load vs. Displacement Data

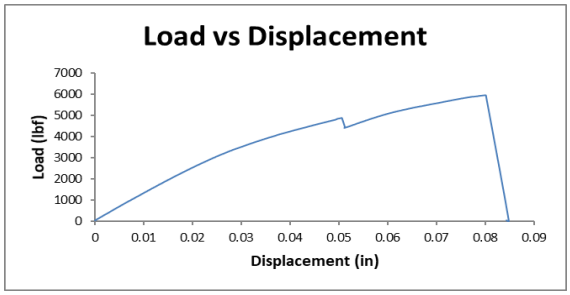

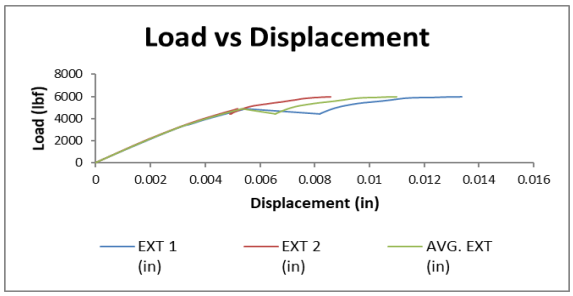

NASA-RW-A6 Load vs. Displacement Data

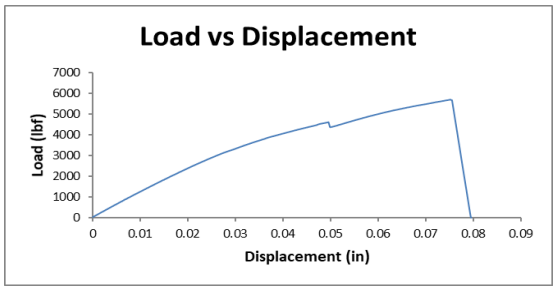

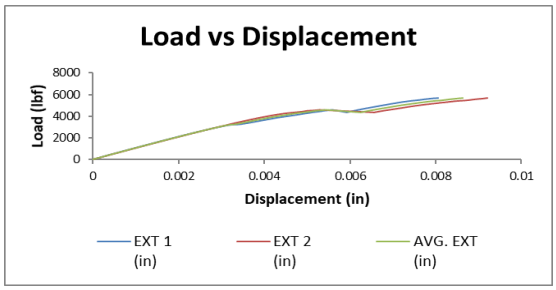

NASA-RW-A7 Load vs. Displacement Data

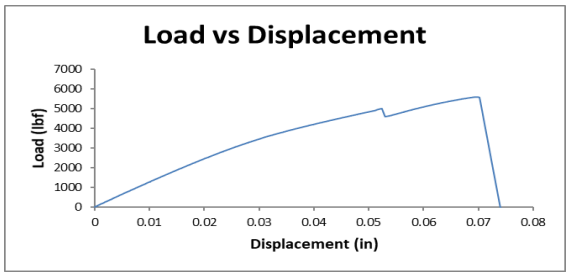

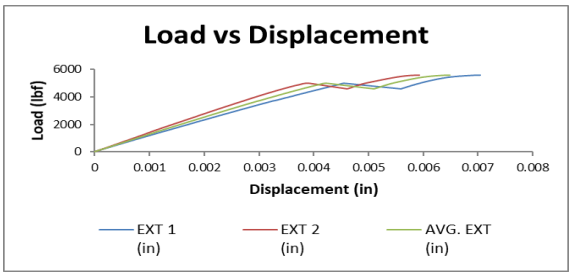

NASA-RW-F1 Load vs. Displacement Data

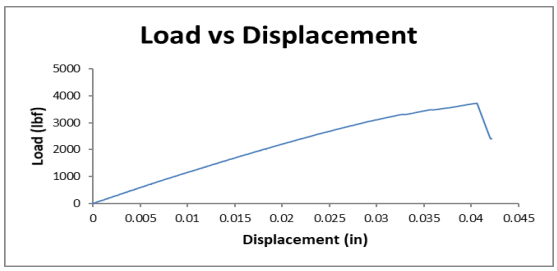

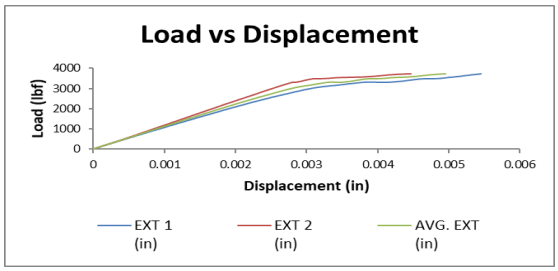

NASA-RW-F2 Load vs. Displacement Data

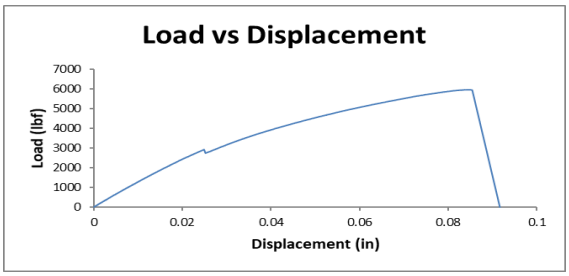

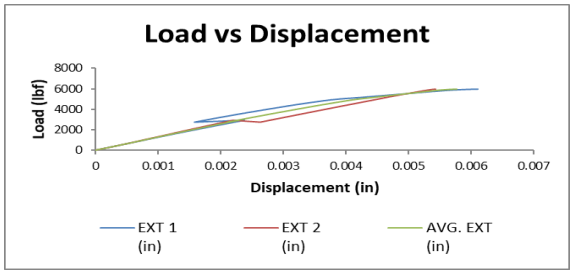

NASA-RW-F3 Load vs. Displacement Data

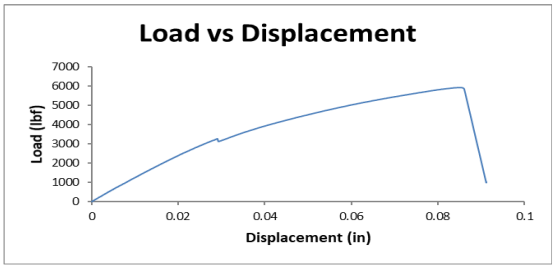

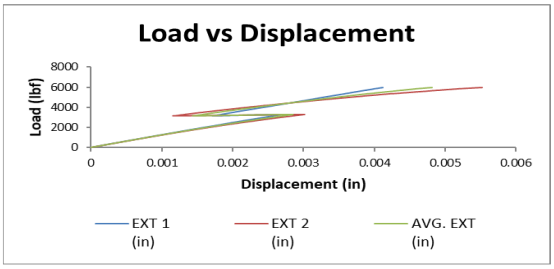

NASA-RW-F4 Load vs. Displacement Data

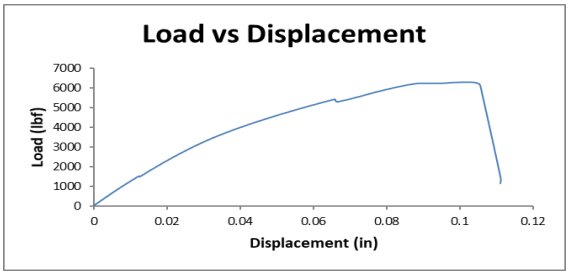

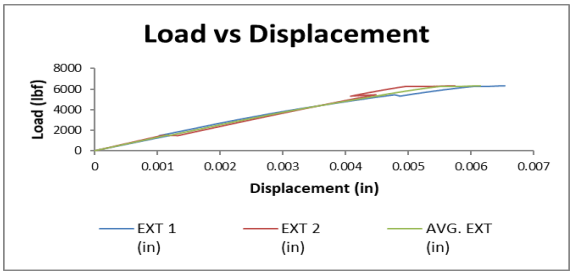

NASA-RW-F5 Load vs. Displacement Data

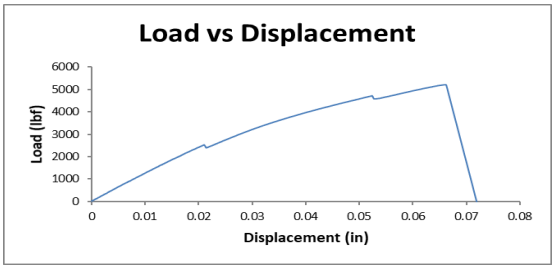

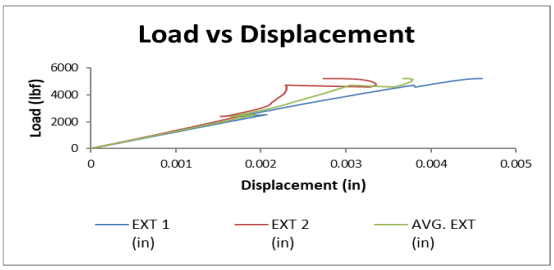

Double Lap Shear Load vs. Displacement Overall Summary

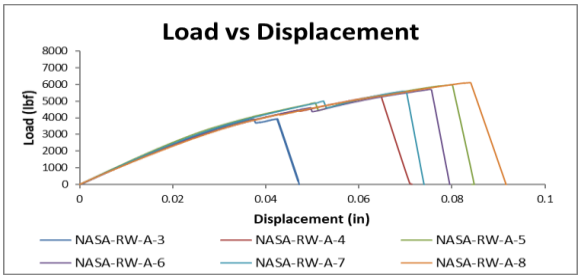

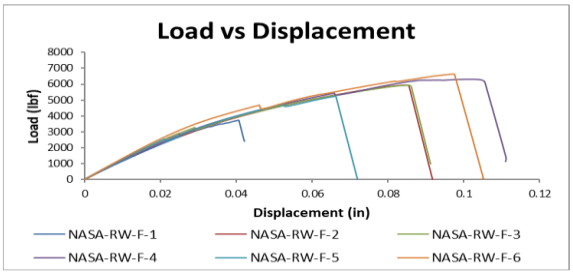

17.0 Appendix V – Mode I Data

17.1 Mode I Data Failure Loads

Category	Specimen Name	Weld Area [in^2]	Pre-Crack Length	PC Max Load [lbf]	PC G_{IC} Value	Actual Load [lbf]	Actual G_{IC} Value
NASA-RW-D-X	NASA-RW-D-1	7.00	3.00	30.34	1.11	41.66	1.07
	NASA-RW-D-2	7.00	3.00	1.58	0.00	16.54	0.20
	NASA-RW-D-3	7.00	3.00	25.34	0.81	33.70	0.72
	NASA-RW-D-4	7.00	3.00	23.75	0.60	24.39	0.45
	NASA-RW-D-5	7.00	3.00	14.79	0.25	24.91	0.08
	NASA-RW-D-6	7.00	3.00	27.09	0.67	27.47	0.65
NASA-RW-I-X	NASA-RW-I-1	7.00	3.00	30.02	0.35	48.72	0.94
	NASA-RW-I-2	7.00	3.00	30.25	0.72	46.53	1.01
	NASA-RW-I-3	7.00	3.00	27.74	0.47	46.03	0.76
	NASA-RW-I-4	7.00	3.00	38.80	0.48	42.52	1.67
	NASA-RW-I-5	7.00	3.00	28.82	0.49	40.80	1.20
	NASA-RW-I-6	7.00	3.00	26.94	0.57	45.97	0.83

Figure 133 – Mode I Max Loads

17.2 Mode I Data Failure Modes

NASA-RW-D-1

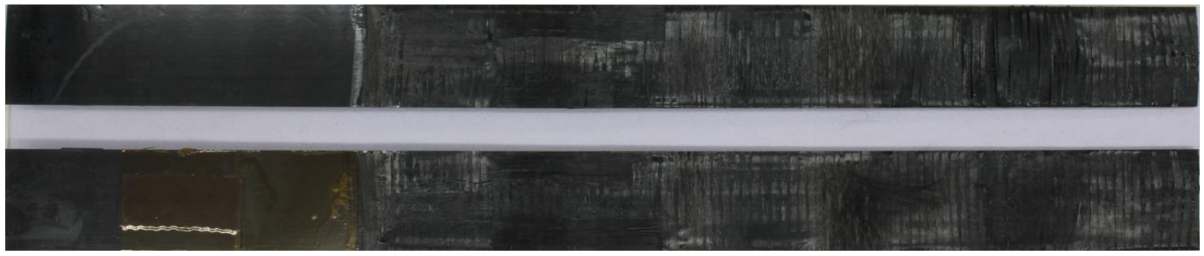

NASA-RW-D-2

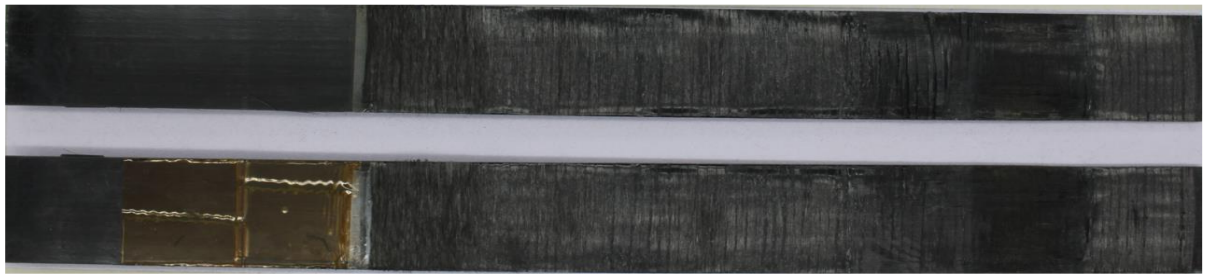

NASA-RW-D-3

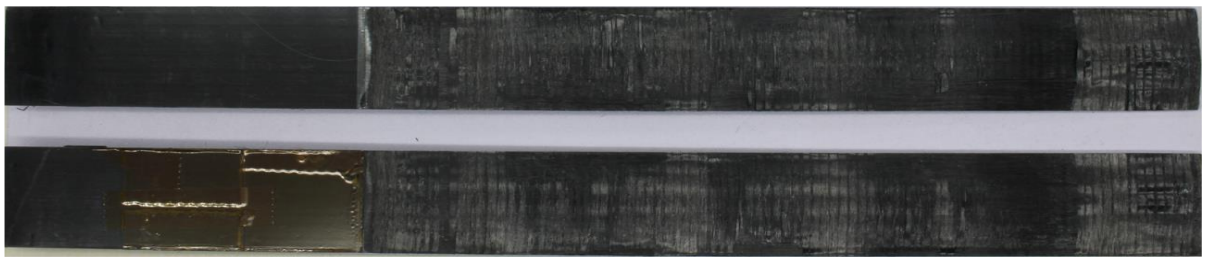

NASA-RW-D-4

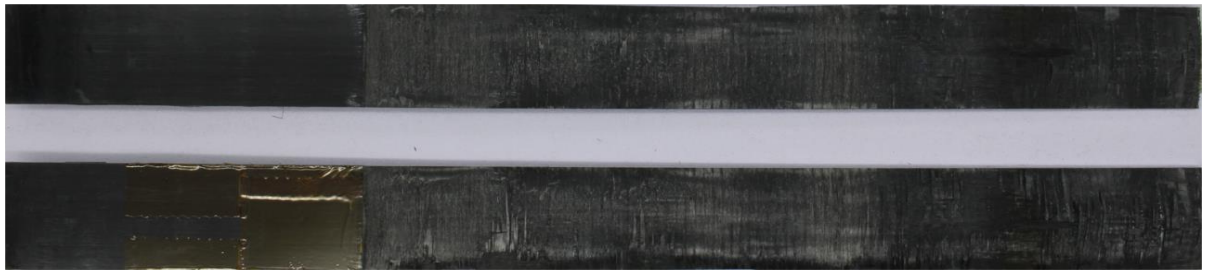

NASA-RW-D-5

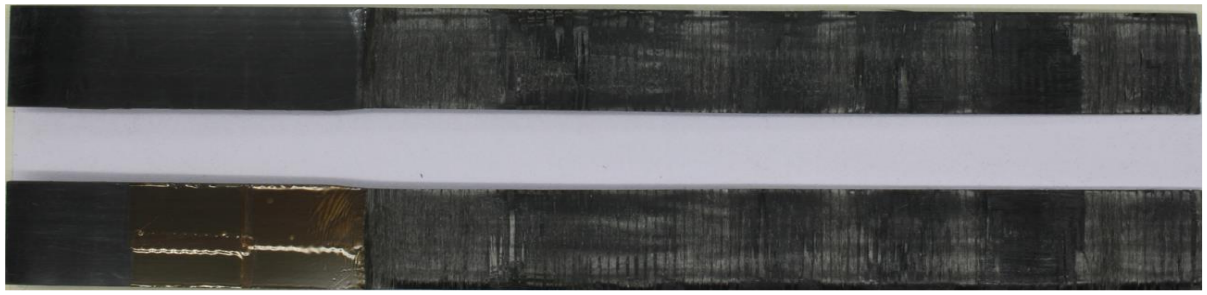

NASA-RW-D-6

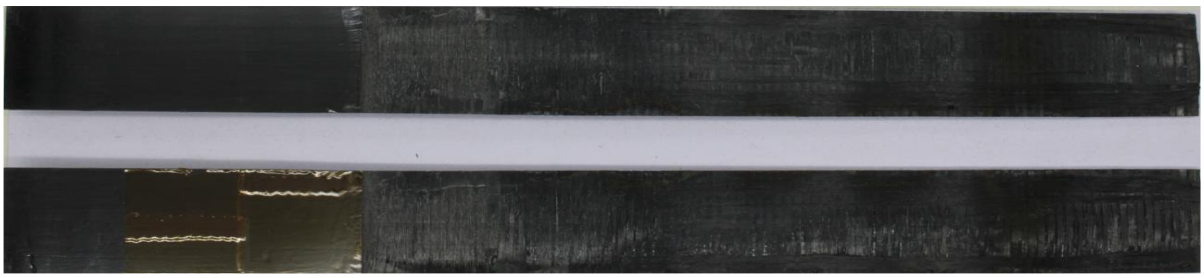

NASA-RW-I-1

NASA-RW-I-2

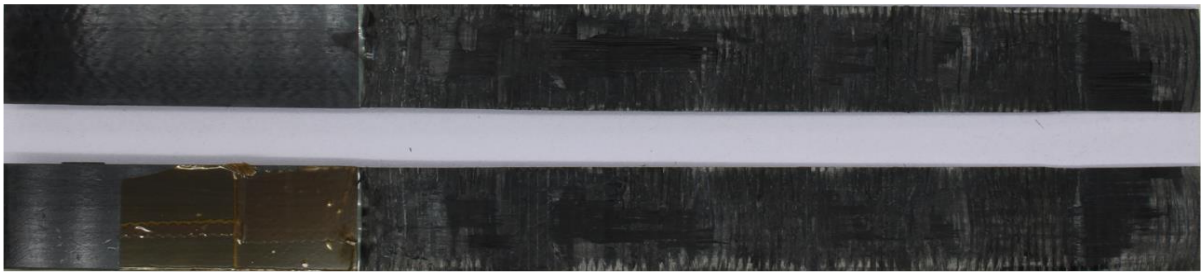

NASA-RW-I-3

NASA-RW-I-4

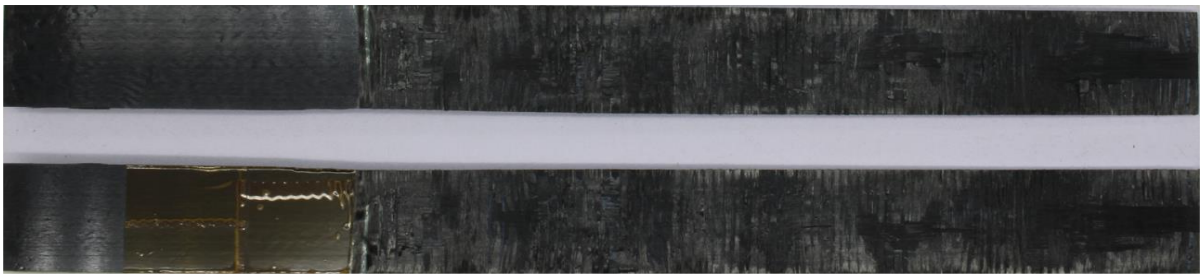

NASA-RW-I-5

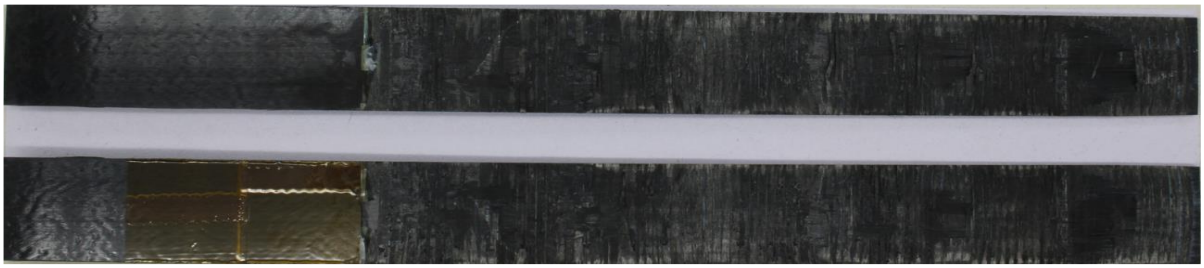

NASA-RW-I-6

17.3 Load vs. Displacement Data

NASA-RW-D-1 Load vs. Displacement Data

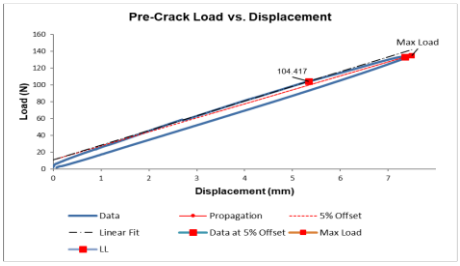

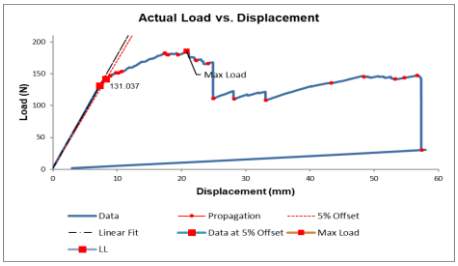

NASA-RW-D-2 Load vs. Displacement Data

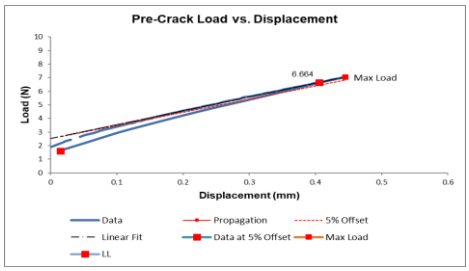

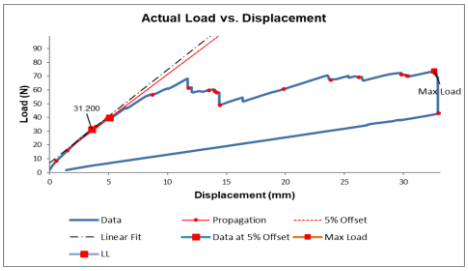

NASA-RW-D-3 Load vs. Displacement Data

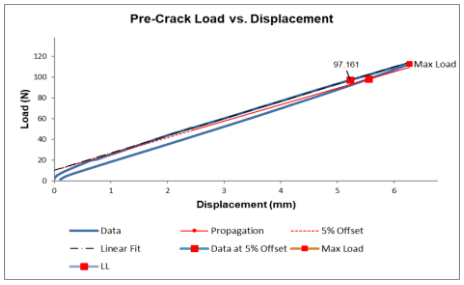

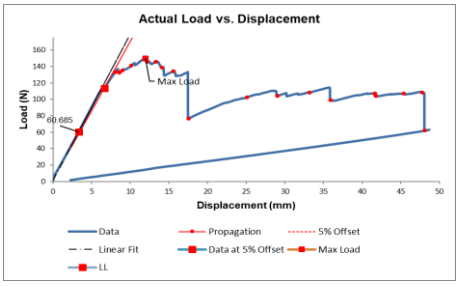

NASA-RW-D-4 Load vs. Displacement Data

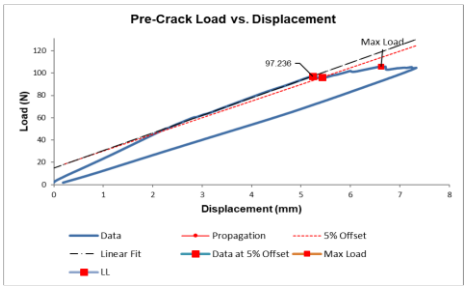

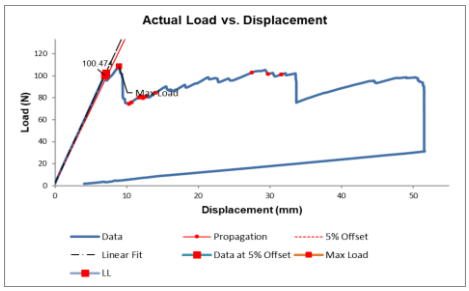

NASA-RW-D-5 Load vs. Displacement Data

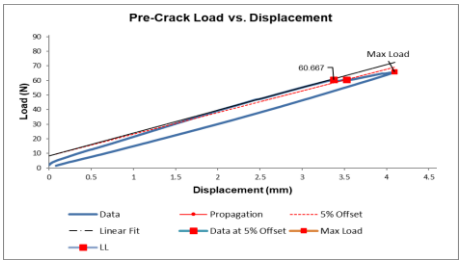

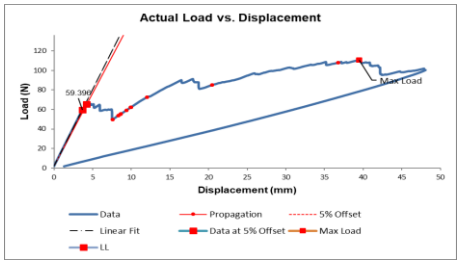

NASA-RW-D-6 Load vs. Displacement Data

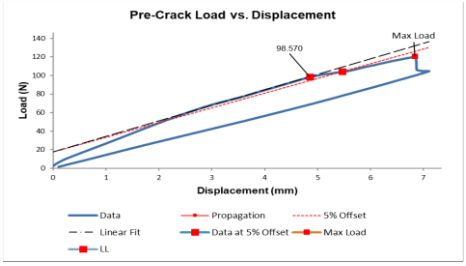

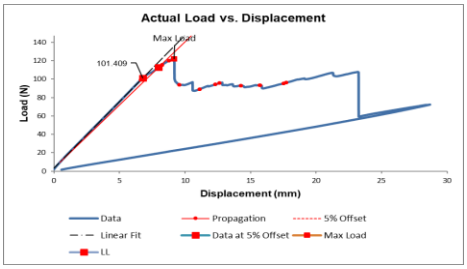

NASA-RW-I-1 Load vs. Displacement Data

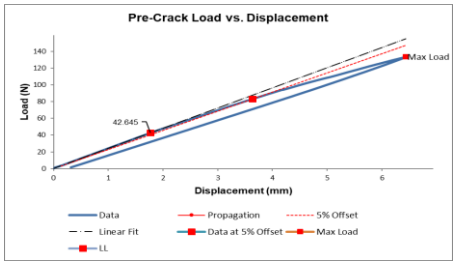

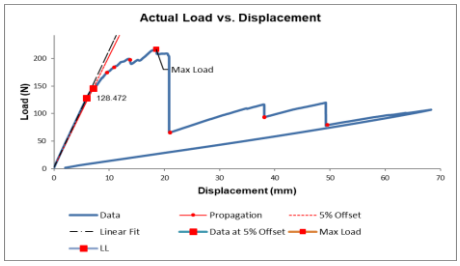

NASA-RW-I-2 Load vs. Displacement Data

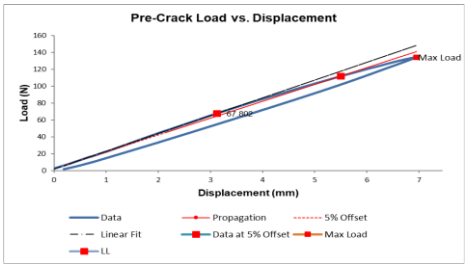

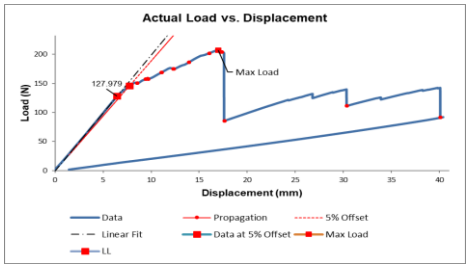

NASA-RW-I-3 Load vs. Displacement Data

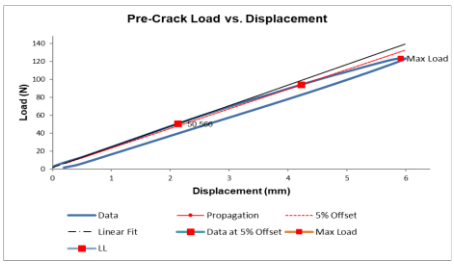

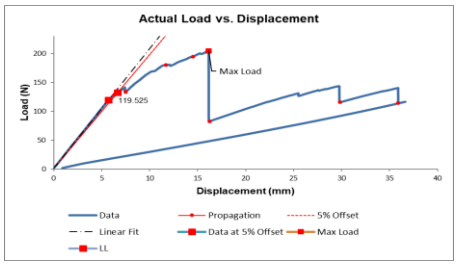

NASA-RW-I-4 Load vs. Displacement Data

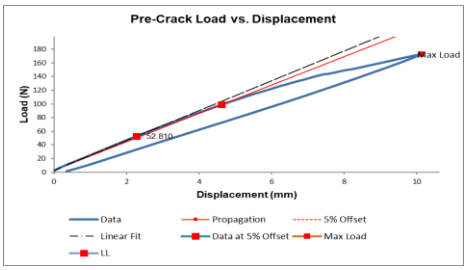

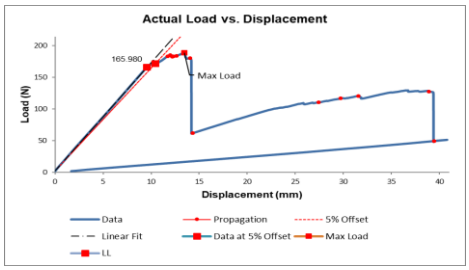

NASA-RW-I-5 Load vs. Displacement Data

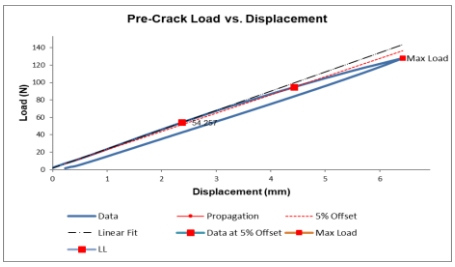

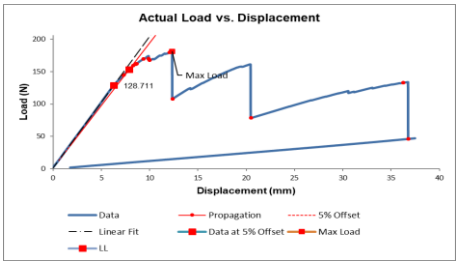

NASA-RW-I-6 Load vs. Displacement Data

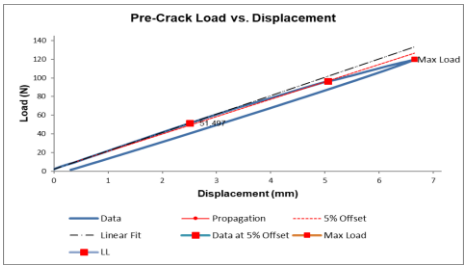

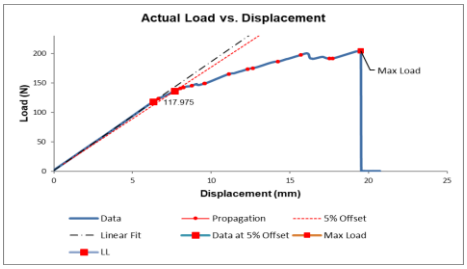

PEI Mode I Load vs. Displacement Overall Summary

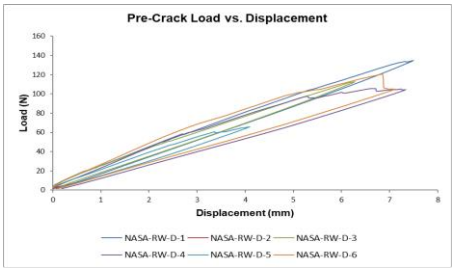

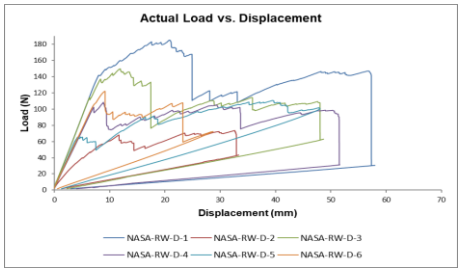

PEEK Mode I Load vs. Displacement Overall Summary

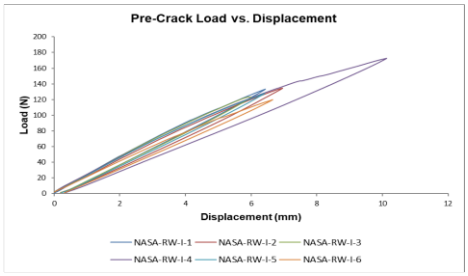

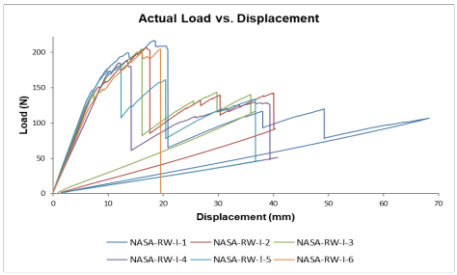

18.0 Appendix VI – Mode II Data

18.1 Mode II Data Failure Loads

Category	Specimen Name	Weld Area [in^2]	Pre-Crack Length	NPC Max Load [lbf]	NPC G_{IIC} Value	PC Max Load [lbf]	PC G_{IIC} Value
NASA-RW-E-X	NASA-RW-E-1	5.00	2.00	1090.41	-	1489.76	-
	NASA-RW-E-2	5.00	2.00	983.83	0.97	1104.11	-
	NASA-RW-E-3	5.00	2.00	438.34	-	1304.23	1.29
	NASA-RW-E-4	5.00	2.00	624.82	-	1215.19	0.77
	NASA-RW-E-5	5.00	2.00	850.98	-	966.88	-
	NASA-RW-E-6	5.00	2.00	792.99	0.49	1116.58	1.17
NASA-RW-J-X	NASA-RW-J-1	5.00	2.00	1102.74	-	1807.51	-
	NASA-RW-J-2	5.00	2.00	1122.01	1.27	1559.19	1.16
	NASA-RW-J-3	5.00	2.00	1076.09	1.28	1546.94	2.50
	NASA-RW-J-4	5.00	2.00	1163.57	0.85	1588.52	1.97
	NASA-RW-J-5	5.00	2.00	1232.34	-	1983.44	-
	NASA-RW-J-6	5.00	2.00	1182.43	0.97	1960.21	2.44

Figure 134 – Mode II Failure Loads

18.2 Mode I Data Failure Modes

NASA-RW-E-1

NASA-RW-E-2

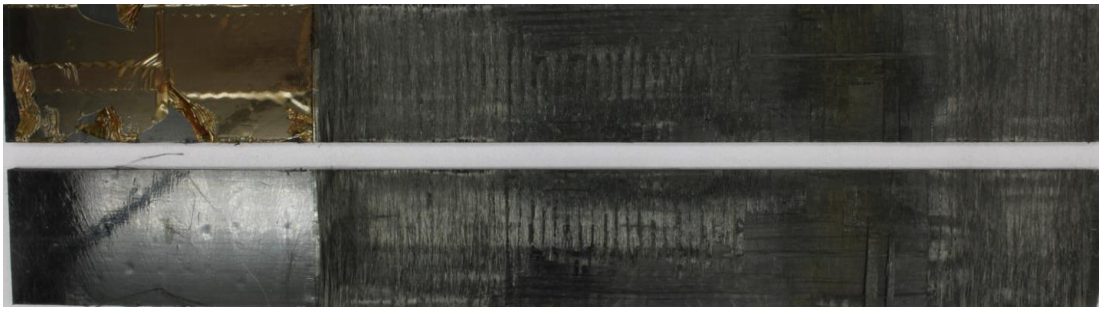

NASA-RW-E-3

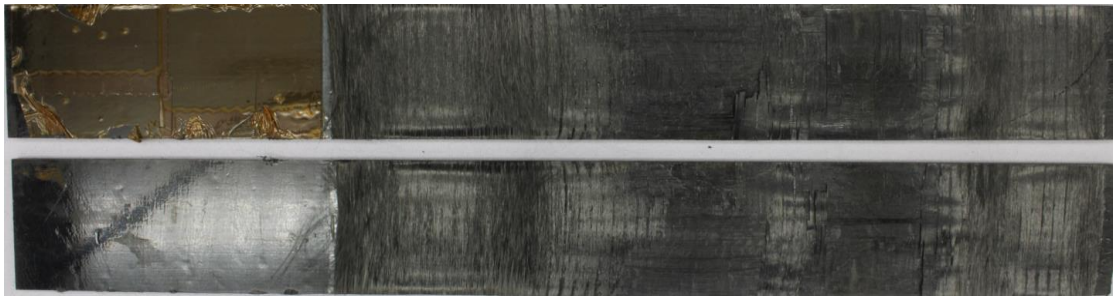

NASA-RW-E-4

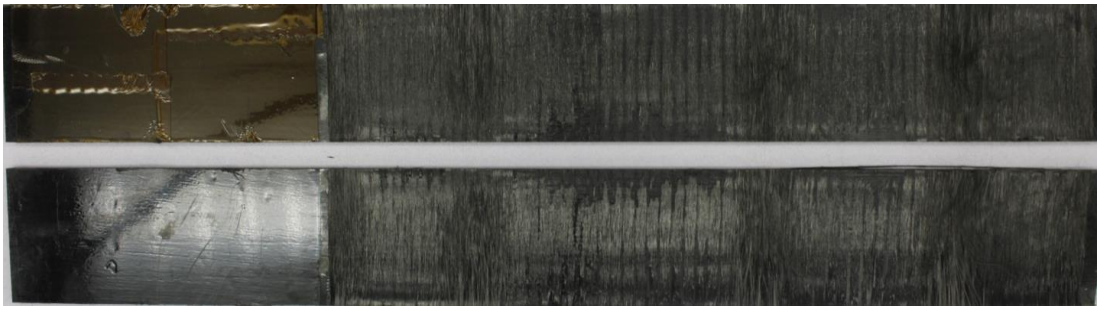

NASA-RW-E-5

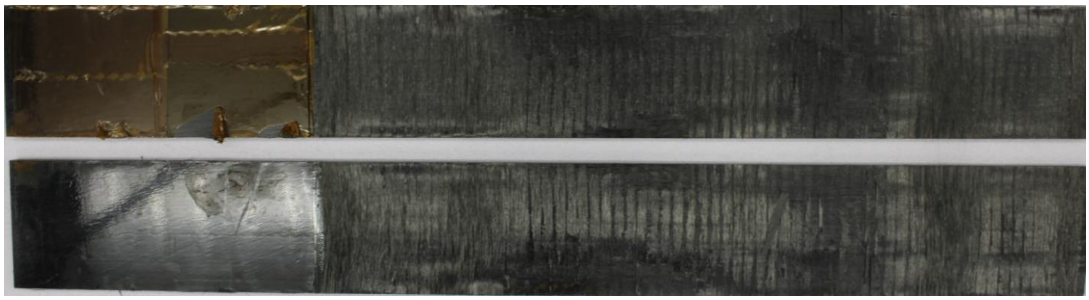

NASA-RW-E-6

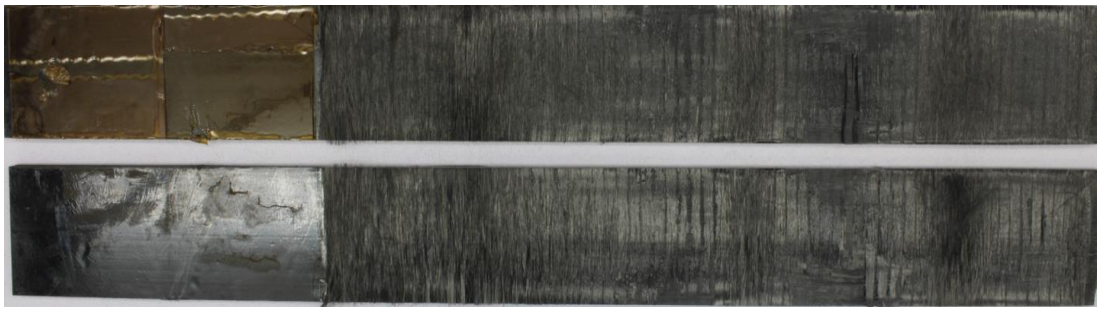

NASA-RW-J-1

NASA-RW-J-2

NASA-RW-J-3

NASA-RW-J-4

NASA-RW-J-5

NASA-RW-J-6

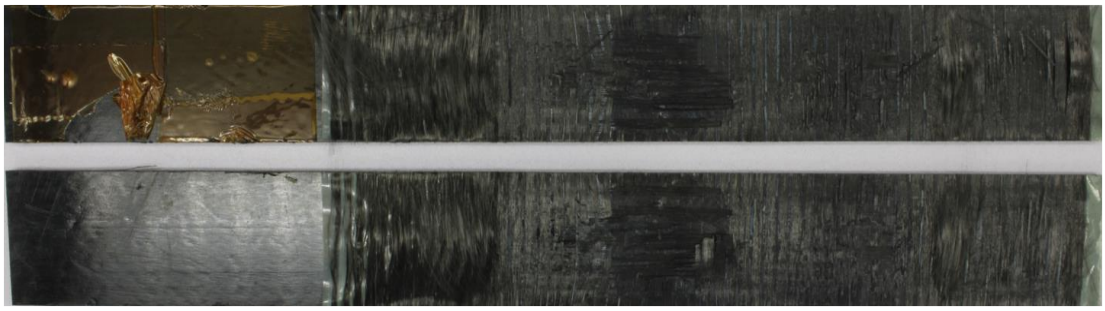

18.3 Load vs. Displacement Data

NASA-RW-E-1 Load vs. Displacement Data

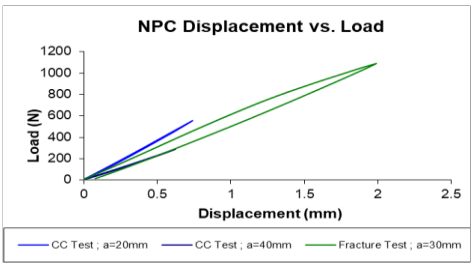

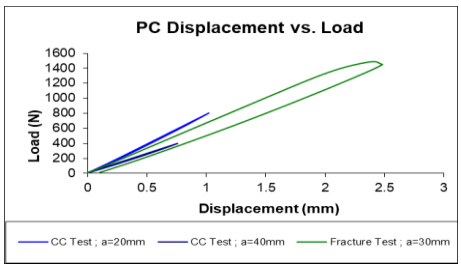

NASA-RW-E-2 Load vs. Displacement Data

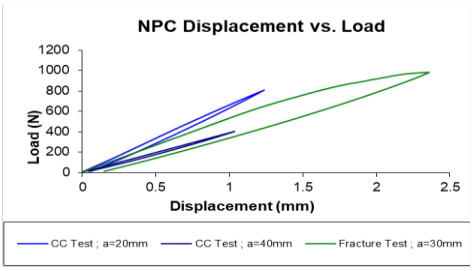

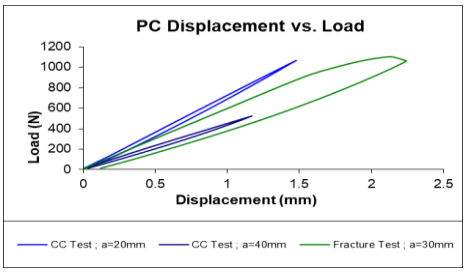

NASA-RW-E-3 Load vs. Displacement Data

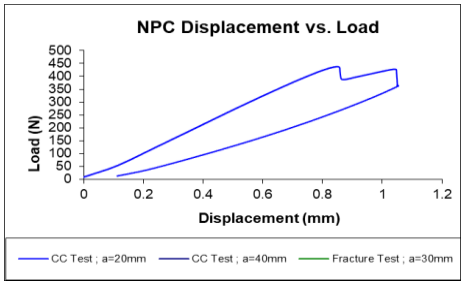

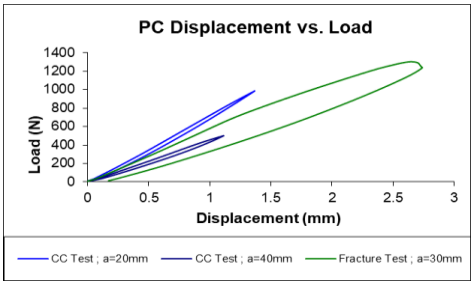

NASA-RW-E-4 Load vs. Displacement Data

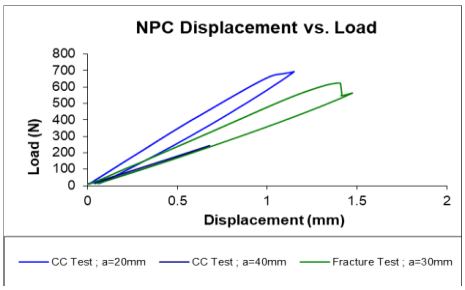

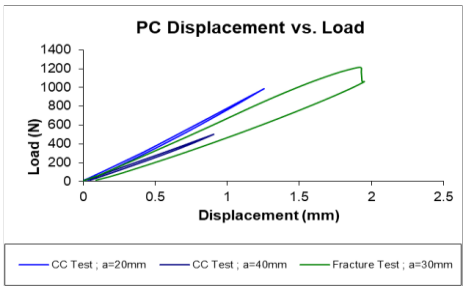

NASA-RW-E-5 Load vs. Displacement Data

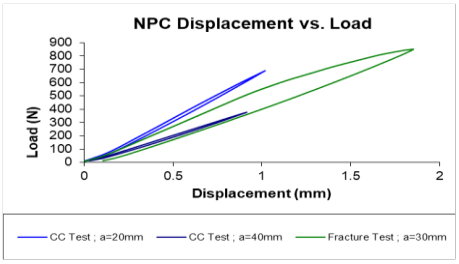

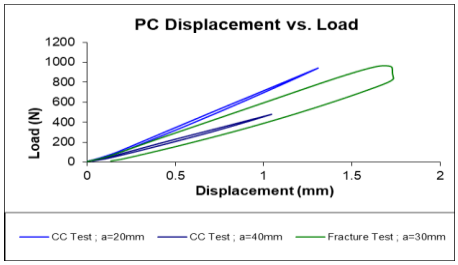

NASA-RW-E-6 Load vs. Displacement Data

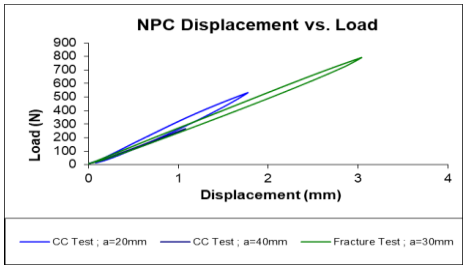

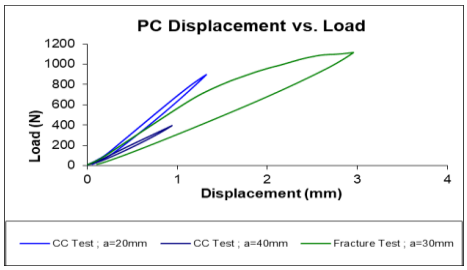

NASA-RW-J-1 Load vs. Displacement Data

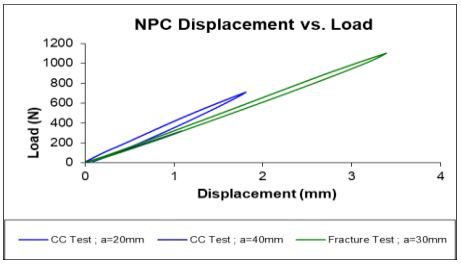

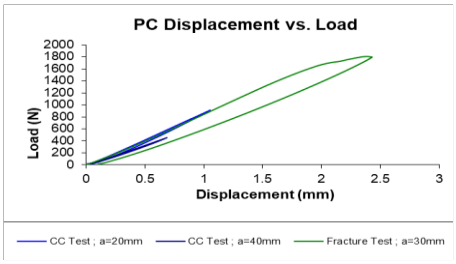

NASA-RW-J-2 Load vs. Displacement Data

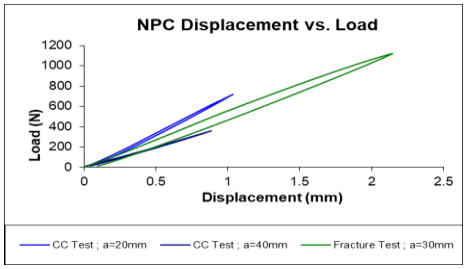

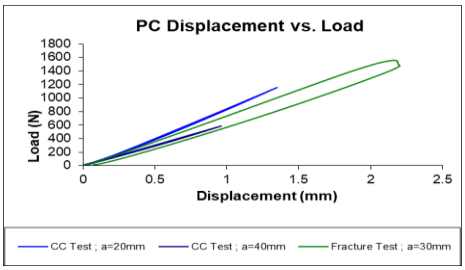

NASA-RW-J-3 Load vs. Displacement Data

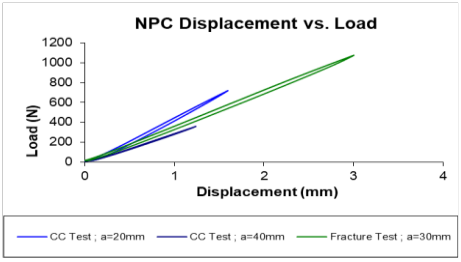

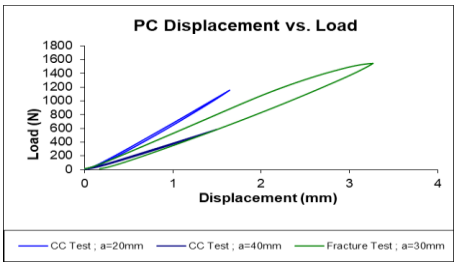

NASA-RW-J-4 Load vs. Displacement Data

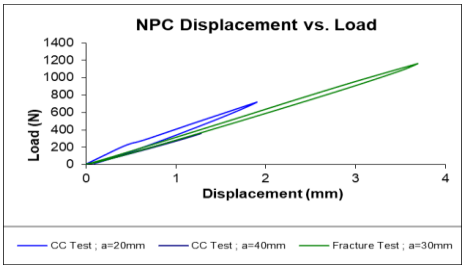

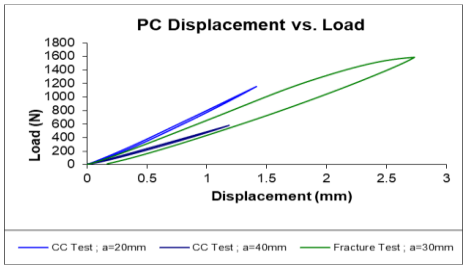

NASA-RW-J-5 Load vs. Displacement Data

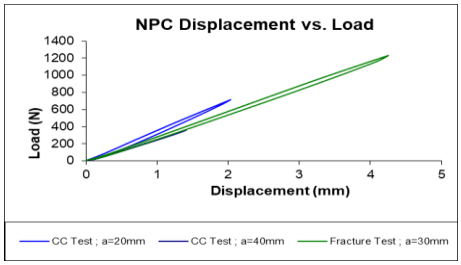

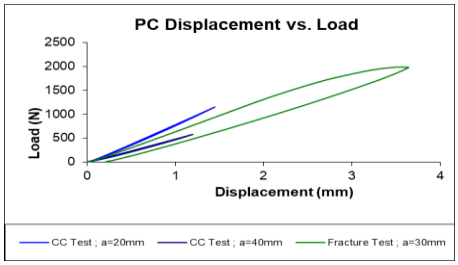

NASA-RW-J-6 Load vs. Displacement Data

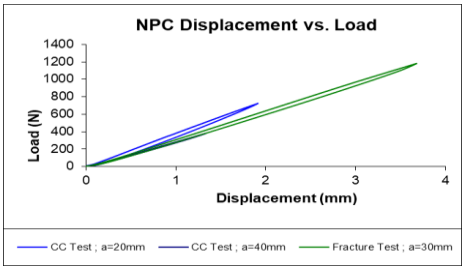

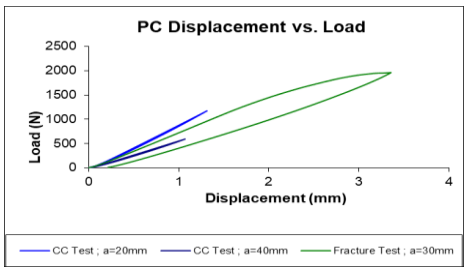

PEI Mode II Load vs. Displacement Overall Summary

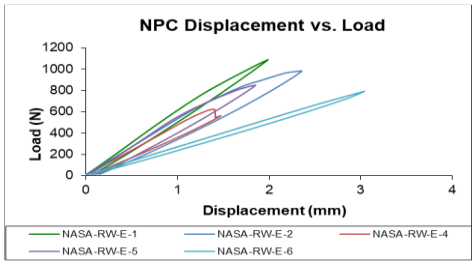

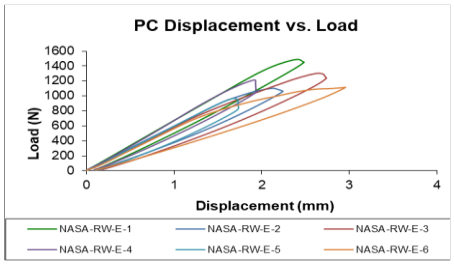

PEEK Mode II Load vs. Displacement Overall Summary